

Evaluation of Alternatives to Calcined Bauxite for Use in High Friction Surface Treatment (HFST) in Missouri



September 2021
Final Report

Project number TR202005
MoDOT Research Report number cmr 21-006

PREPARED BY:

Eslam Deef-Allah

Korrenn Broaddus

Magdy Abdelrahman, Ph.D.

Missouri University of Science and Technology

PREPARED FOR:

Missouri Department of Transportation

Construction and Materials Division, Research Section

TECHNICAL REPORT DOCUMENTATION PAGE

1. Report No. cmr21-006	2. Government Accession No.	3. Recipient's Catalog No.	
4. Title and Subtitle Evaluation of Alternatives to Calcined Bauxite for Use in High Friction Surface Treatment (HFST) in Missouri		5. Report Date Published: September 2021	
7. Author(s) Eslam Deef-Allah, https://orcid.org/0000-0003-1405-8257 Korrenn Broaddus Magdy Abdelrahman, Ph.D.		6. Performing Organization Code	
9. Performing Organization Name and Address Department of Civil, Architectural and Environmental Engineering Missouri University of Science and Technology 1401 N. Pine St., Rolla, MO 65409		8. Performing Organization Report No.	
12. Sponsoring Agency Name and Address Missouri Department of Transportation (SPR-B) Construction and Materials Division P.O. Box 270 Jefferson City, MO 65102		10. Work Unit No.	
15. Supplementary Notes Conducted in cooperation with the U.S. Department of Transportation, Federal Highway Administration. MoDOT research reports are available in the Innovation Library at https://www.modot.org/research-publications .		11. Contract or Grant No. MoDOT project # TR202005	
16. Abstract High Friction Surface Treatments (HFST) applications are used to reduce roadway crashes on risky locations and horizontal curves. Currently, Calcined Bauxite (CB) is the primary aggregate used for HFST in Missouri. Calcined Bauxite has very limited sources, which makes it more expensive than locally available aggregates. This research evaluated CB's feasible alternative aggregates through a comprehensive experimental program for use in HFST applications. The alternative aggregates were Earthworks, Meramec River, Steel Slag, Rhyolite, Black Diabase, Quartzite, Flint Chat, and Potosi Dolomite aggregate sources. Three categories of testing were followed in the experimental program: the first category was for the physical properties testing, the second category was for durability testing, and the third category was for performance testing. Two main conclusions related to aggregate sources in HFST applications were noted: the availability of alternative aggregate sources that compare to Calcine Bauxite quality and the applicability of performance testing to evaluate aggregate sources. A Life-Cycle-Cost simple program was developed to conduct cost analysis based on performance of the tested aggregate sources. The study recommended to construct HFST field sections using the selected alternative aggregates.		13. Type of Report and Period Covered Final Report November 2019-September 2021	
17. Key Words HFST; Calcined Bauxite; Aggregates; Friction tests; Skid resistance; Economic Analysis; Predictive models		18. Distribution Statement No restrictions. This document is available through the National Technical Information Service, Springfield, VA 22161.	
19. Security Classif. (of this report) Unclassified.	20. Security Classif. (of this page) Unclassified.	21. No. of Pages 128	22. Price
Form DOT F 1700.7 (8-72)		Reproduction of completed page authorized	

**Evaluation of Alternatives to Calcined Bauxite for Use in High Friction Surface Treatment (HFST)
in Missouri**

by

Eslam Deef-Allah
Ph.D. Candidate

Korrenn Broaddus
Ph.D. Student

and

Magdy Abdelrahman, Ph.D.
Missouri Asphalt Pavement Association (MAPA) Endowed Professor

Missouri University of Science and Technology

Missouri Department of Transportation Project # TR202005

September 2021

Copyright Permissions

Authors herein are responsible for the authenticity of their materials and for obtaining written permissions from publishers or individuals who own the copyright to any previously published or copyrighted material used herein.

Disclaimer

The opinions, findings, and conclusions expressed in this document are those of the investigators. They are not necessarily those of the Missouri Department of Transportation, U.S. Department of Transportation, or Federal Highway Administration. This information does not constitute a standard or specification.

Acknowledgments

The authors would like to express their great appreciation to the Missouri Department of Transportation for supporting them with the fund, instruments, and information.

Executive Summary

Maintaining the appropriate amount of pavement friction is critical for safe driving. High friction surface treatment (HFST) can enhance the ability of a road surface to provide pavement friction to vehicles in critical braking or cornering maneuvers. MoDOT has used HFST since 2013 to restore pavement surface friction where traffic has worn down pavement surface aggregates and to improve wet crash locations. Aggregates used in HFST have higher friction characteristics and Polished Stone Value (PSV) compared to other aggregates. Currently, Calcined Bauxite (CB) is the primary aggregate used for HFST in Missouri. Calcined Bauxite has very limited sources, which makes it more expensive than locally available aggregates. This research evaluated CB's feasible alternative aggregates through a comprehensive experimental program for use in HFST applications. The alternative aggregates were Earthworks, Meramec River, Steel Slag, Rhyolite, Black Diabase, Quartzite, Flint Chat, and Potosi Dolomite aggregate sources.

Three categories of testing were followed in the experimental program: the first category was for the physical properties testing, the second category was for durability testing, and the third category was for performance testing. Physical testing included aggregate gradation, specific gravity & absorption, and Uncompacted Void Content (UVC) of fine aggregates. Durability testing included Los Angeles Abrasion (LAA), Micro-Deval (MD) polishing; discussed under performance testing, sodium sulfate soundness, water-alcohol freeze thaw, and acid-insoluble residue. Physical properties and durability tests were run to classify the aggregates and identify the routine tests that investigate the performance of the proposed aggregates as HFST materials. Performance testing included Micro-Deval (MD) polishing, Aggregate Image Measurement System (AIMS), dynamic friction testing, and British Pendulum (BP) testing. The MD results reflected the aggregates' resistances to polishing and abrasion. The AIMS explored the changes that occurred to the Texture (TX) indices and Gradient Angularity (GA) indices, using the gradient method, for the coarse aggregates before, after 105-, and after 180-minutes polishing times in MD. The Dynamic Friction Tester (DFT) examined the Coefficient of Friction (COF) values before and after polishing cycles at different speeds. The polishing process was conducted using the Three-Wheel Polishing Device (TWPD). Finally, the BP evaluated the aggregates' surface frictional properties before and after 10-hr polishing time using the British Wheel.

The researchers developed a Life-Cycle-Cost (LCC) simple process using Excel to calculate the Net Present Value (NPV) for HFST applications based on AIMS, DFT, or BP results. The major input data for the LCC program were categorized into material and project specifics. Performance prediction models were used to convert the input data into Skid Number (SN) values. The predicted terminal SN was compared with the recommended terminal SN using rehabilitation matrix. This matrix was proposed based on the predicted and recommended terminal SN values. Finally, the output data were calculated; these data presented the NPVs for the HFST applications. Based on the lowest NPV, the best HFST application was selected.

Two main categories of conclusions related to aggregate sources in HFST applications were noted: the alternative aggregate sources to Calcine Bauxite and the use of performance testing to evaluate aggregate sources. 1) Alternative aggregate sources to Calcined Bauxite in HFST. The results of this study indicated that quality aggregate sources compare to calcined bauxite following the MoDOT HFST aggregate criteria. 2) The use of performance testing to evaluate aggregate sources for HFST applications. The conducted performance systems including Micro-Deval (MD) and Aggregate Image Measurement System (AIMS), dynamic friction testing, and British Pendulum (BP) testing, and the Dynamic Friction Testing (DFT) seem applicable to HFST aggregates. There are no strong correlations between the three systems; mainly because they are based on different mechanisms of measuring the aggregate friction properties.

The study recommended to construct High Friction Surface Treatment (HFST) field sections using the selected alternative aggregates. This will evaluate the field performance of the selected aggregates. The DFT and BP results in the field could be compared to the results conducted in the lab. It is also recommended to update current MoDOT specifications on aggregate requirements for HFST following the findings of this research. Micro-Deval testing can be used for preliminary screening of HFST aggregate selection. It is recommended to extend the use of high friction aggregate sources, with larger sizes, in HMA applications particularly in mixes with high recycled aggregate contents; for example, mixes with high RAP contents that have been subjected to weathering and abrasion for years.

Table of Contents

1	CHAPTER 1: INTRODUCTION	1
1.1	Research Objectives	1
1.2	Research Management	1
2	CHAPTER 2: LITERATURE REVIEW	3
2.1	Introduction.....	3
2.2	Application of High Friction Surface Treatment	4
2.2.1	The Construction Process of High Friction Surface Treatment	4
2.2.1.1	Field Inspection.....	4
2.2.1.2	Constrains, Identification, and Removal	4
2.2.1.3	Materials Mixing Precautions and Conditions	5
2.3	Service Life of High Friction Surface Treatment	5
2.4	Cost of High Friction Surface Treatment.....	5
2.5	High Friction Surface Treatment Standards.....	7
2.5.1	MoDOT Requirements for HFST (NJSP-15-13B)	7
2.5.2	AASHTO MP 41-19	8
2.5.3	Other state Standards	8
2.5.3.1	Aggregate Gradation Standards	9
2.5.3.2	Physical Properties and Abrasion Testing Standards	9
2.5.3.3	Performance and Durability Testing Standards	12
2.5.4	High Friction Surface Treatment Performance Testing	13
2.5.5	Performance Tests.....	13
2.5.5.1	British Pendulum Test.....	13
2.5.5.2	Accelerated Friction Testing	14
2.5.5.3	Micro-Deval and Aggregate Image Measurement System	14
2.5.6	Previous Relevant Research.....	14
2.5.7	Skid Resistance Prediction Models.....	16
3	CHAPTER 3: EXPERIMENTAL CONSIDERATIONS	18
3.1	Introduction.....	18
3.2	Experimental Design.....	18
3.2.1	Aggregate Physical Properties Testing	18
3.2.1.1	Aggregate Gradation	23
3.2.1.2	Specific Gravity and Absorption of Aggregates	23
3.2.1.3	Uncompacted Void Content of Fine Aggregate.....	24
3.2.2	Aggregate Durability Testing.....	24
3.2.2.1	Los Angeles Abrasion Test	24
3.2.2.2	The Soundness of Aggregate Using Sodium Sulfate	24
3.2.2.3	Water-Alcohol Freeze Thaw	24
3.2.2.4	Acid Insoluble Residue	24
3.2.3	Aggregate Performance Testing.....	24
3.2.3.1	Micro-Deval and Aggregate Image Measurement System	24
3.2.3.2	Accelerated Friction Testing	25
I	Preparing High Friction Surface Treatment Applications on Hot Mix Asphalt Slabs	25
II	Sand Patch Test (Measuring Pavement Macrotexture Using a Volumetric Technique)	25
III	Dynamic Friction Test.....	25
3.2.3.3	Measuring Aggregate Coupons' Surface Friction Using the British Pendulum Tester	26
I	Preparing Aggregate Coupons.....	26
II	British Pendulum Test	26
III	Accelerated Polishing of Aggregates Using the British Wheel.....	26

3.3	Physical Properties, Durability, and Performance Testing Comparative Studies	26
3.4	Economic Study	26
4	CHAPTER 4: AGGREGATE PHYSICAL PROPERTIES AND DURABILITY TESTING	28
4.1	Introduction.....	28
4.2	Part-I Testing	28
4.2.1	Physical Properties Testing Results	28
4.2.1.1	Aggregate Gradation	28
4.2.1.2	Specific Gravity and Absorption.....	29
4.2.1.3	Uncompacted Void Content.....	29
4.2.2	Durability Testing Results	29
4.2.2.1	Los Angeles Abrasion.....	29
4.2.2.2	Sodium Sulfate Soundness.....	30
4.2.2.3	Water-Alcohol Freeze Thaw	31
4.2.2.4	Acid Insoluble Residue	31
4.3	Part-II Testing	32
4.3.1	Aggregate Gradation	32
4.3.2	Specific Gravity and Absorption.....	32
4.3.3	Uncompacted Void Content.....	32
4.3.4	Los Angeles Abrasion.....	33
4.4	Summary.....	33
5	CHAPTER 5: AGGREGATE PERFORMANCE TESTING.....	36
5.1	Introduction.....	36
5.2	Micro-Deval Results	36
5.2.1	Coarse Aggregate.....	36
5.2.2	Fine Aggregate.....	37
5.3	Aggregate Image Measurement System.....	38
5.3.1	Effect of Aggregate Size on Texture and Angularity Indices	39
5.3.2	Analysis of Average Texture and Angularity Indices.....	41
5.3.3	Relationship between Texture and Angularity Indices	43
5.4	Accelerated Friction Testing Results	45
5.4.1	Sand Patch Test.....	46
5.4.2	Dynamic Friction Test	46
5.4.3	Relationship between Dynamic Friction Test Results and Number of Polishing Cycles ...	48
5.4.4	Estimated Skid Number and International Friction Index	51
5.5	British Pendulum Test Results	53
5.5.1	Effect of Aggregate Size on the British Pendulum Number Values	53
5.5.2	Average British Pendulum Number Values	54
5.6	Summary.....	55
6	CHAPTER 6: PHYSICAL PROPERTIES, DURABILITY, AND PERFORMANCE TESTING COMPARATIVE STUDIES	57
6.1	Introduction.....	57
6.2	Relationships between Micro-Deval and Aggregate Image Measurement System Results	57
6.2.1	Relationships between Micro-Deval Mass Losses and Texture or Angularity Indices	57
6.2.2	Relationships between Micro-Deval Polishing Times and Texture or Angularity Indices	60
6.3	Relationships between Micro-Deval and Los Angeles Mass Losses.....	61
6.3.1	Micro-Deval Mass Losses for Coarse Gradation Versus Los Angeles Abrasion for Grading D	61
6.3.2	Micro-Deval Mass Losses for Fine Gradation Versus Los Angeles Abrasion for Grading D	61
6.4	Relationship between Uncompacted Void Content, Micro-Deval, Sand Patch, and Aggregate Image Measurement System Results	63

6.4.1	Effect of Micro-Deval Polishing Time on the Uncompacted Void Content Percentages...	63
6.4.2	Relationship between Percentages of Uncompacted Void Content and Angularity Indices	66
6.4.3	Relationship between Percentages of Uncompacted Void Content and Mean Texture Depth Values	68
6.4.4	Relationship between Mean Texture Depth Values and Angularity Indices	69
6.5	Comparing Aggregate Image Measurement System and British Pendulum Test Results	70
6.6	Comparing Aggregate Image Measurement System and Dynamic Friction Test Results	71
6.7	Comparing British Pendulum Test and Dynamic Friction Test Results	72
6.8	Comparing the Predicted Initial and Terminal Skid Number Values for Alternatives	74
6.9	Relating Physical Properties and Durability Testing to Performance Testing	76
6.9.1	Relating Uncompacted Void Content Percentages to Angularity Indices and Mean Texture Depth	76
6.9.2	Relating Durability Testing to Performance Testing	77
6.9.3	Relating Micro-Deval Mass Losses and Los Angeles Abrasion to the British Pendulum Number	77
6.10	Summary	78
7	CHAPTER 7: ECONOMIC STUDY	79
7.1	Introduction	79
7.2	Calculation Process of LCCA	79
7.3	Performance Prediction	79
7.4	LCCA Results	80
7.4.1	Skid Number	81
7.4.2	Net Present Value	81
7.5	A Comparative Economic Study	85
7.6	Summary	85
8	SUMMARY, CONCLUSIONS, AND RECOMMENDATIONS	86
8.1	Summary	86
8.2	Conclusions	86
8.2.1	Alternative Aggregate Sources to Calcined Bauxite in HFST	86
8.2.2	The Use of Performance Testing to Evaluate Aggregate Sources for HFST Applications	87
8.3	Recommendations	88
	REFERENCES	89
A	APPENDIX A: STATE HFST AGGREGATES SPECIFICATION	A-1
A.1	State Standards	A-1
A.1.1	Alabama	A-1
A.1.2	Alaska	A-1
A.1.3	California	A-1
A.1.4	Florida	A-2
A.1.5	Illinois	A-2
A.1.6	Indiana	A-2
A.1.7	Iowa	A-2
A.1.8	Michigan	A-3
A.1.9	Pennsylvania	A-3
A.1.10	South Carolina	A-3
A.1.11	South Dakota	A-3
A.1.12	Tennessee	A-4
A.1.13	Texas	A-4
A.1.14	Virginia	A-5
A.1.15	Wisconsin	A-5
B	APPENDIX B: SKID PERFORMANCE MODELING	B-1

B.1	Skid Resistance Prediction Models Based on Aggregate Image Measurement System Results...	B-1
	B-1
B.1.1	Skid Resistance Prediction Models for Hot Mix Asphalt	B-1
B.1.2	Skid Resistance Prediction Model for Seal Coats	B-5
B.2	Skid Number Prediction Model Based on Dynamic Friction Test Results.....	B-6
B.3	Skid Number Prediction Model Based on British Pendulum Test Results	B-7
C	APPENDIX C: PHYSICAL PROPERTIES, DURABILITY, AND PERFORMANCE	
	TESTING.....	C-1
C.1	Physical Properties Testing.....	C-1
C.1.1	Procedures of Estimating the Uncompacted Void Content Percentages of Fine Aggregates	
	C-1
C.2	Durability Testing	C-1
C.2.1	Los Angeles Abrasion Test Conditions.....	C-1
C.3	Performance Testing	C-2
C.3.1	Accelerated Friction Testing.....	C-2
C.3.1.1	Preparation of Hot Mix Asphalt Test Slabs	C-2
C.3.1.2	Installation of High Friction Surface Treatment Application on Hot Mix Asphalt Slab	
	C-2
C.3.1.3	Procedures of Sand Patch Test.....	C-2
C.3.1.4	Three-Wheel Polishing Machine and Dynamic Friction Tester.....	C-3
C.3.2	Measuring Aggregate Coupons' Surface Frictional Properties Using the British Pendulum	
	C-3
C.3.2.1	Preparing Aggregate Coupons	C-3
C.3.2.2	British Pendulum Tester and the British Wheel.....	C-6
D	APPENDIX D: LIFE CYCLE COST ANALYSIS CALCULATION PROCESS.....	D-1
D.1	Input Data.....	D-1
D.1.1	Material Specifics	D-1
D.1.1.1	Aggregate Image Measurement System Results.....	D-1
D.1.1.2	Dynamic Friction Test Results.....	D-1
D.1.1.3	British Pendulum Test Results	D-1
D.1.1.4	Other Specifics.....	D-1
D.1.2	Project Specifics.....	D-2
D.2	Skid Performance Prediction Results.....	D-2
D.3	Output Data.....	D-2

List of Figures

Figure 2-1 Number of states requiring different HFST tests.	9
Figure 3-1 Experimental design.	20
Figure 4-1 Particles' size distribution, Part-I.	28
Figure 4-2 Percentages of UVC using two aggregates' sizes.	30
Figure 4-3 Percentages of LAA.	30
Figure 4-4 Water-alcohol freeze thaw test results.	31
Figure 4-5 Acid insoluble residue percentages.	32
Figure 5-1 Micro-Deval mass losses' percentages with (3/8" - #4) gradation.	37
Figure 5-2 Micro-Deval mass losses' percentages with (#6 - #16) gradation.	38
Figure 5-3 Texture and angularity indices.	40
Figure 5-4 Percentages of increase or decrease in the texture and angularity indices.	41
Figure 5-5 Average texture and average angularity indices.	42
Figure 5-6 Percentages of increase or decrease in average texture and average angularity indices.	43
Figure 5-7 Relationships between average texture and average angularity indices.	44
Figure 5-8 Relationship between average texture and average angularity indices.	45
Figure 5-9 Mean texture depth values for the HFST applications.	46
Figure 5-10 Coefficient of friction values using DFT at 20 km/hr.	47
Figure 5-11 Coefficient of friction values using DFT at 40 km/hr.	47
Figure 5-12 Coefficient of friction values using DFT at 60 km/hr.	48
Figure 5-13 Initial and terminal COF values using DFT.	49
Figure 5-14 Percentages of losses in COF values after polishing.	50
Figure 5-15 Relationship between COF values and the number of polishing cycles.	50
Figure 5-16 Measured versus predicted COF values.	51
Figure 5-17 Estimated SN40R values for HFST applications.	52
Figure 5-18 Estimated initial IFI values, based on DFT ₂₀ and MTD measurements, for the HFST applications.	52
Figure 5-19 Estimated initial SN(50) values, based on DFT ₂₀ and MTD measurements, for the HFST applications.	53
Figure 5-20 Average BPNs with two sizes.	54
Figure 5-21 Percentages of decrease or increase in the average BPNs after the polishing process with two sizes.	54
Figure 5-22 Average BPNs.	55
Figure 5-23 Percentages of decrease in the average BPNs after the polishing process.	55
Figure 6-1 Relationships between MD percentages of mass losses and texture or angularity indices.	58
Figure 6-2 Relationships between MD percentages of mass losses and average TX indices or average GA indices.	59
Figure 6-3 Relationships between the MD mass losses and LAA.	62
Figure 6-4 Effect of MD polishing times on the UVC percentages with two sizes.	64
Figure 6-5 Relationship between the MD polishing times and the UVC percentages for Rhyolite.	65
Figure 6-6 Predicted versus measured UVC percentages for Rhyolite.	65
Figure 6-7 Relationship between UVC percentages for two sizes.	66
Figure 6-8 Relationship between UVC percentages with (#8 - #100) gradation and the GA indices.	67
Figure 6-9 Relationship between UVC percentages with (#6 - #8) size and the GA indices.	67
Figure 6-10 Relationship between UVC percentages with (#6 - #16) gradation and the GA indices.	68
Figure 6-11 Relationship between UVC percentages with (#8 - #100) gradation and the MTD values.	68
Figure 6-12 Relationship between UVC percentages with (#6 - #8) size and the MTD values.	69
Figure 6-13 Relationship between UVC percentages with (#6 - #16) gradation and the MTD values.	69
Figure 6-14 Relationship between GA indices and the MTD values.	70
Figure 6-15 Relationships between AIMS and BP results.	71

Figure 6-16 Relationships between AIMS and DFT results.	72
Figure 6-17 Relationships between BP and DFT results.	73
Figure 6-18 Predicted initial SN values for HFST applications.	75
Figure 6-19 Predicted terminal SN values for HFST applications.	76
Figure 6-20 Relationships between MD mass losses' percentages or LAA percentages and BPN values.	78
Figure 7-1 LCCA calculation process.....	80
Figure 7-2 Predicted initial and terminal SN values for HFST applications.	83
Figure 7-3 Net present values for HFST applications.....	84
Figure C-1 Funnel and cylindrical measure.	C-1
Figure C-2 Three-wheel polishing device and DFT.	C-3
Figure C-3 Plaster used in metal molds.	C-4
Figure C-4 Plaster and epoxy cast.....	C-4
Figure C-5 Silicone molds.	C-5
Figure C-6 Prepared aggregate coupons.	C-5
Figure C-7 British pendulum tester.....	C-6
Figure C-8 The British wheel and the road wheel with aggregate coupons (before polishing).....	C-6
Figure D-1 LCC program input data (material specifics) based on AIMS.	D-3
Figure D-2 LCC program input data (project specifics).	D-4
Figure D-3 LCC program output data based on AIMS.....	D-4

List of Tables

Table 2-1 Typical properties of CB.	4
Table 2-2 The construction methods of the HFST.....	6
Table 2-3 Required testing for resin binder systems.....	7
Table 2-4 MoDOT’s requirements for CB.....	7
Table 2-5 Testing conditions for epoxy, MMA, or polyester resins.....	8
Table 2-6 Calcined Bauxite’s testing conditions according to AASHTO MP 41-19.....	8
Table 2-7 High friction aggregate gradation requirements by state.....	10
Table 2-8 Requirements of high friction aggregates’ physical properties by state.....	11
Table 2-9 Other high friction aggregates’ physical properties by state.....	11
Table 2-10 As delivered high friction aggregates’ moisture content threshold by state.....	12
Table 2-11 High friction aggregates’ Polished Stone Value and Micro-Deval requirements by state.....	12
Table 2-12 High friction aggregates’ additional durability and performance requirements by state.....	13
Table 2-13 Natural/synthetic aggregates’ requirements in Wisconsin.....	13
Table 2-14 The main results of Heitzman et al.’s study.....	15
Table 3-1 Received aggregate sizes and sources information.....	19
Table 3-2 Used epoxy binder information.....	19
Table 3-3 Aggregate testing matrix.....	21
Table 3-4 Specific aggregates’ percentages/weights used in Micro-Deval and Uncompacted Void Content testing.....	23
Table 3-5 Minimum aggregates’ weight used in specific gravity and absorption test.....	23
Table 4-1 The absorption and specific gravity results.....	29
Table 4-2 Sodium sulfate soundness test results.....	31
Table 4-3 Part-II physical properties and LAA results.....	35
Table 5-1 Micro-Deval mass losses’ percentages with two gradations.....	38
Table 5-2 Fitting parameters for (DFT _{20-N}) model.....	50
Table 6-1 Ranking of aggregates based on AIMS and MD results.....	59
Table 6-2 Fitting parameters for (TX-MD t) model.....	60
Table 6-3 Fitting parameters for (GA-MD t) model.....	60
Table 6-4 Fitting parameters for (UVC-MD t) model.....	65
Table 6-5 Ranking of aggregates based on DFT and BP results.....	74
Table 6-6 Ranking of aggregates based on predicted SN values.....	76
Table 7-1 Rehabilitation matrix for HFST applications.....	80
Table 7-2 Ranking of HFST applications based on the NPV.....	85
Table A-1 Physical characteristics of high friction aggregates in Alabama State.....	A-1
Table A-2 The high friction Aggregate Gradation in Alaska State.....	A-1
Table A-3 Physical characteristics of high friction aggregates in California State.....	A-1
Table A-4 Physical characteristics of high friction aggregates in Florida State.....	A-2
Table A-5 Physical characteristics of high friction aggregates in Illinois State.....	A-2
Table A-6 Physical characteristics of high friction aggregates in Indiana State.....	A-2
Table A-7 Physical characteristics of high friction aggregates in Iowa State.....	A-3
Table A-8 Physical characteristics of high friction aggregates in Michigan State.....	A-3
Table A-9 Physical characteristics of high friction aggregates in Pennsylvania State.....	A-3
Table A-10 Physical characteristics of high friction aggregates in South Carolina State.....	A-4
Table A-11 Physical characteristics of high friction aggregates in South Dakota State.....	A-4
Table A-12 Physical characteristics of high friction aggregates in Tennessee State.....	A-4
Table A-13 Physical characteristics of high friction aggregates in Texas State.....	A-4
Table A-14 Physical characteristics of high friction aggregates in Virginia State.....	A-5
Table A-15 Physical characteristics of high friction aggregates in Wisconsin State.....	A-5
Table B-1 SN threshold values after 5 years of service.....	B-3

Table B-2 Traffic groups based on TMF for HMA.	B-5
Table B-3 Design lane factors of AADT and trucks.	B-5
Table B-4 Traffic groups based on TMF for seal coats.	B-6
Table B-5 Friction Limits for states based on SN40R.	B-6
Table C-1 Charge weight and the number of revolutions for the LAA test.	C-1
Table C-2 Grading of test samples used in LAA test.	C-2

List of Abbreviations

AADT	Average Annual Daily Traffic
AIMS	Aggregate Image Measurement System
AMD 5	After 5-minutes of Micro-Deval polishing time
AMD 15	After 15-minutes of Micro-Deval polishing time
AMD 30	After 30-minutes of Micro-Deval polishing time
AMD 105	After 105-minutes of Micro-Deval polishing time
AMD 180	After 180-minutes Micro-Deval polishing time
BMD	Before Micro-Deval polishing
BP	British Pendulum
BPN	British Pendulum Number
CB	Calcined Bauxite
COF	Coefficient of Friction
CTM	Circular Texture Meter
DFT	Dynamic Friction Tester
DFT ₂₀	COF value measured by DFT at 20 km/hr
DFT ₄₀	COF value measured by DFT at 40 km/hr
EFST	Enhanced Friction Surface Treatment
FN	Friction Number
GA	Gradient Angularity
HFST	High Friction Surface Treatment
HMA	Hot Mix Asphalt
IFI	International Friction Index
LAA	Los Angeles Abrasion
LCCA	Life Cycle Cost Analysis
MAS	Maximum Aggregate Size
MD	Micro-Deval
MPD	Mean Profile Depth
MTD	Mean Texture Depth
NMAS	Nominal Maximum Aggregate Size
NPV	Net Present Value
PSV	Polished Stone Value
SN	Skid Number
SN40R	Skid Number measured at 40 mi/hr by a skid trailer with Ribbed tires
SN(50)	Skid Number measured at 50 mi/hr by a skid trailer with smooth tires
TWPD	Three-Wheel Polishing Device
TX	Texture
UVC	Uncompacted Void Content

CHAPTER 1: INTRODUCTION

Maintaining the appropriate amount of pavement friction is critical for safe driving. High friction surface treatment (HFST) can enhance the ability of a road surface to provide pavement friction to vehicles in critical braking or cornering maneuvers. MoDOT has used HFST since 2013 to restore pavement surface friction where traffic has worn down pavement surface aggregates and to improve wet crash locations. Aggregates used in HFST have higher friction characteristics and Polished Stone Value (PSV) compared to other aggregates. Currently, Calcined Bauxite (CB) is the primary aggregate used for HFST in Missouri. Calcined Bauxite has very limited sources, which makes it more expensive than locally available aggregates.

The presented research includes physical testing, durability testing, and aggregate performance testing. Experimental considerations are presented in Chapter 3. Physical properties testing and durability testing results are presented in Chapter 4. The aggregate performance testing includes the Aggregate Image Measurement System (AIMS) along with the Micro-Deval (MD) testing, the British Wheel along with the British Pendulum (BP), and the Dynamic Friction Testing. The aggregate performance testing results are discussed in Chapter 5. Testing results were analyzed and used to predict and compare the friction performance of the collected aggregate sources. Comparative studies on the physical and performance testing of aggregate sources are presented in Chapter 6. Cost analysis is presented in Chapter 7; a Life-Cycle-Cost (LCC) simple program has been developed based on the performance of the tested aggregate sources. Conclusions and recommendations are presented in Chapter 8.

Appendix A presents lists of the state HFST aggregate specifications. Appendix B presents skid resistance performance modeling that are related to this study. Appendix C presents details on the testing procedures and sample preparation as used in this research. Appendix D provides details on the LCC analysis and calculations as used in this study.

1.1 Research Objectives

The main objective of this study is to identify and compare alternatives to Calcined Bauxite through a comprehensive laboratory testing evaluation including measuring the aggregates' properties and their surfaces' friction. Research is extended to include advanced characterization of aggregate shape properties using AIMS and accelerated friction testing using a Three-Wheel Polishing Device (TWPD) and Dynamic Friction Tester (DFT).

1.2 Research Management

The presented research has been conducted at the facilities of Missouri University of Science and Technology (Missouri S&T) with part of the testing conducted at the University of Idaho. Dr. Magdy Abdelrahman serves as the principal investigator of this contract, Dr. John Myers serves as co-investigator, and Dr. Mike Lusher serves as technical personnel and consultant to the project. Ms. Korrenn Broaddus, Ph.D. Student at Missouri S&T, led the team of students who conducted the aggregate testing at Missouri S&T. Mr. Eslam Deef, Ph.D. Candidate at Missouri S&T, led the report writing and data analysis effort with contribution from Ms. Korrenn Broaddus.

The University of Idaho (U Idaho) is sub-contracted to assist with the testing program. Dr. Emad Kassem led the U Idaho effort and was assisted by Mr. Juan Pinto Ortiz. The U Idaho team conducted the Part-II aggregate testing that is presented in section 4.4 and the dynamic friction testing that is presented in Chapter 5. The AIMS testing was conducted at Texas A&M University.

The presented data and conclusions of this study will assist MoDOT to enhance road safety by using the appropriate HFST at a reduced cost. The outcomes of this study shall assist MoDOT to identify possible

alternative aggregates that provide comparable frictional characteristics to those of Calcined Bauxite and provide comparable performance.

This research provides recommendations for future screening and testing of potential HFST aggregates and future specifications, if needed.

CHAPTER 2: LITERATURE REVIEW

2.1 Introduction

This chapter presented a comprehensive review of the High Friction Surface Treatment (HFST) application and its impact on reducing the percentage of crashes. In addition, the standard specification of HFST aggregates and their threshold values for the states were also discussed. Eventually, the well-known performance tests for evaluating the friction property of aggregates and the previous research efforts on evaluating several HFST aggregates compared to Calcined Bauxite were outlined and reviewed.

Maintaining an appropriate amount of pavement friction is critical for safe driving and reducing crashes. Surface treatments are used primarily to extend the pavement life as well as improve the skid resistance (FHWA-CAI-14-019 n.d.). Among surface treatment applications, HFST provides better skid resistance. HFST is used to reduce roadway crashes on the horizontal curves or other risky locations (e.g., high-speed deceleration ramps, steep grades, intersections with high-speed approaches, transition lanes, and pedestrian crossings) (FHWA 2020; Heitzman, Turner, and Greer 2015; Heitzman, Michael; Moore 2017; Wilson and Mukhopadhyay 2016; FHWA-CAI-14-019 n.d.).

Generally, HFST was used to compensate for the deficiencies of geometric designs tight curves with small radii, small superelevation rates (Wilson and Mukhopadhyay 2016; FHWA-CAI-14-019 n.d.), or locations where moving fixed objects to clear the sightline was impossible (FHWA-CAI-14-019 n.d.; “High Friction Surface Treatments in Pennsylvania” n.d.). The tires of vehicles cause more polishing on the horizontal curved sections compared to the tangent sections as a result of generated shear forces on the pavement surfaces (Wilson and Mukhopadhyay 2016; Li et al. 2017). Crashes on the horizontal curves occur generally due to excess polishing and losing the safety skid friction (Li et al. 2017). Therefore, it was recommended to apply the HFST on horizontal and ramp curves with radii of curvatures less than 1500 ft (FHWA 2020) and apply at the beginning of the horizontal curves (point of curve) till the point of tangency (FHWA-CAI-14-019 n.d.).

Many studies concluded that using HFST had a considerable impact on reducing the rate of crashes at curves and intersections and wet surface conditions (Heitzman, Turner, and Greer 2015; FHWA-CAI-14-019 n.d.; Milstead et al. 2011; Heitzman, Michael; Moore 2017; Harkey et al. 2008; FHWA 2019). It was concluded that using HFST on curves dropped the crashes by 60 to 90% (Milstead et al. 2011; Harkey et al. 2008). Moreover, before/after total crash reduction of 100, 90, and 57% were reported by the Pennsylvania, Kentucky, and South Carolina DOT, respectively (FHWA-CAI-14-019 n.d.). It was reported that HFST decreased wet condition crash rates by 30% (Milstead et al. 2011; FHWA 2019). In 1976, the use of Calcined Bauxite (CB) in HFST showed significant crash reductions of 31% for 800 intersections in London (Heitzman, Turner, and Greer 2015; Heitzman, Michael; Moore 2017).

Performance is the primary goal in considering the friction of HFST application, which is identified through the microtextures of aggregates and the macrotextures of the surfaces (FHWA 2020; Kassem et al. 2013). The macrotexture depends on the aggregate gradation, compaction level, and mixture design, while aggregate microtexture is affected by the shape and Texture (TX) of the aggregates (Kassem et al. 2013; Kandhal and Parker 1998; Crouch et al. 1995). Moreover, resisting aggregate to the wear and polishing of traffic depends on the physical and mineralogical properties of the aggregates (FHWA-CAI-14-019 n.d.).

High Friction Surface Treatment (HFST) was determined to be a cost-effective safety treatment that consists of a polymer resin layer, which is used to bond the pavement with a 3–4 mm maximum size, and high abrasion, high angularity and texture, and polish resistant aggregates (e.g., CB, flint/chert, slags, or granite) (FHWA 2020; Merritt, Moravec, and Heitzman 2014; Milstead et al. 2011; Wilson and Mukhopadhyay 2016; Bloem 1971; FHWA-CAI-14-019 n.d.). The resin binder, like epoxy resin,

polyester resin, polyurethane resin, acrylic resin, or methyl methacrylate (MMA), is spread over the pavement surface to bond this surface with the aggregate layer (FHWA 2020; Merritt, Moravec, and Heitzman 2014; Wilson and Mukhopadhyay 2016). The most common resin binder that used in the High Friction Surface Treatment (HFST) is an epoxy resin: a two-part binder that consists of a resin (extender) and an epoxy (hardener) (Wilson and Mukhopadhyay 2016).

Among the high-friction aggregates, Calcined Bauxite (CB) is considered commonly used in the HFST. The leaders in bauxite production are Australia, China, Brazil, India, Guinea, and Jamaica (Wilson and Mukhopadhyay 2016). Calcined Bauxite is a synthetic aggregate that is produced from heating raw bauxite (aluminum ore) to 1000 and 1500 °C. Such a process produces dense, stable, and high-purity aggregates (Wilson and Mukhopadhyay 2016; FHWA-CAI-14-019 n.d.). Table 2-1 summarizes the physical and chemical properties of the CB.

Table 2-1 Typical properties of CB (FHWA-CAI-14-019 n.d.).

Property	Value
Alumina (Al ₂ O ₃), %	≥ 82
Bulk density, gm/cm ³	3
Alkali, %	≤ 0.4

2.2 Application of High Friction Surface Treatment

This section illustrates the precautions that should be considered before and during applying the HFST. Furthermore, the HFST application methods are summarized and demonstrated based on the distinct binder mixing method, binder and aggregate applications, pros, cons, and application rate.

2.2.1 The Construction Process of High Friction Surface Treatment

The construction stages of HFST may be classified into three main stages, which are field inspection, constraints, identification, and removal, and precautions and conditions of material mixing. The following subsections describe each of these stages.

2.2.1.1 Field Inspection

First of all, the pavement surface should be checked before applying the HFST materials. As it is not recommended to apply HFST on the highly distressed pavement with fatigue cracking, rutting, raveling, debonded surface layers, or surface bleeding (FHWA 2020; Wilson and Mukhopadhyay 2016). HFST should not be applied on shattered concrete slabs with more than three pieces; these areas should be removed and replaced before applying the HFST (Wilson and Mukhopadhyay 2016).

2.2.1.2 Constrains, Identification, and Removal

Many considerations should be followed before applying the HFST. Firstly, in case of the presence of severe pavement distresses like cracking. Sealing cracks with rubberized asphalt is recommended for pavement cracks greater than 0.25 inches in width and depth, and this should be applied 30 days before the HFST application (FHWA-CAI-14-019 n.d.; Missouri DOT 2015). Sealing cracks with mixed polymer resin makes the HFST installation faster because the HFST can be installed once the polymer has gelled (FHWA-CAI-14-019 n.d.). After that, asphalt pavement surfaces should be cleaned, using mechanical sweepers and high-pressure air was with sufficient oil traps, before HFST application (Heitzman, Michael; Moore 2017; Missouri DOT 2015). It is also recommended to use proper shot-blasting to remove debris, dust, dirt, paste, and other surface contaminants from the rigid pavement. In addition, all utilities, curbs, and drainage structures should be protected against the HFST. Additionally, pavement markings adjacent to the HFST application should be covered or removed because HFST does

not fully adhere to thermoplastic markings (FHWA-CAI-14-019 n.d.). HFST shall not be applied to newly placed asphalt pavement surfaces that are less than 30 days old (Missouri DOT 2015).

2.2.1.3 Materials Mixing Precautions and Conditions

The improper mixing of resin binders causes premature loss of aggregates and wear in the wheel path (FHWA-CAI-14-019 n.d.). Generally, the resin binder layer takes two to four hours to set (Wilson and Mukhopadhyay 2016). The resin binder's thickness is recommended to be 50% of the nominal maximum aggregate size (FHWA 2020; Wilson and Mukhopadhyay 2016; FHWA-CAI-14-019 n.d.), which is approximately 50 to 65 mils (Wilson and Mukhopadhyay 2016; Vandel n.d.). This enables the aggregates to be held firmly in place by the resin binder. If the resin binder layer is too thin or too thick, it will cause problems. A resin layer that is too thin cannot retain the aggregates for long-term durability. If the resin layer is too thick, it encapsulates the aggregates, which decreases the friction due to the resin's glassy surface (FHWA-CAI-14-019 n.d.). It is recommended that the aggregate layer be deposited on the resin binder's surface before the resin's gel time (FHWA 2020; Wilson and Mukhopadhyay 2016). If aggregates are applied to the resin layer after the gel started, the binder will resist the embedding of the aggregates. The fully automated installation method does not face this problem because it broadcasts the aggregates within seconds after placement of the binder resin (FHWA-CAI-14-019 n.d.). Therefore, many state agencies recommend using a fully automated method, which is described in Table 2-2, for constructing the High Friction Surface Treatment (HFST) (Heitzman, Michael; Moore 2017). HFST is applied to new asphalt pavement 30-days after the completion of the asphalt layer. While, for new rigid pavement, the waiting period is 28 days ("High Friction Surface Treatments in Pennsylvania" n.d.; FHWA-CAI-14-019 n.d.). Table 2-2 summarizes the construction methods of HFST (FHWA-CAI-14-019 n.d.; Wilson and Mukhopadhyay 2016).

Furthermore, it was reported that coarser and open-graded asphalt surface layers require double-layer HFST because the resin binder percolates down, which leaves the friction aggregate layer without bonding (Wilson and Mukhopadhyay 2016; FHWA-CAI-14-019 n.d.). Double-layer HFST provides longer service and a more durable surface in aggressive environments—places where vehicles are equipped with snow chains or studded tires—and on roadways with high traffic volumes. Double-layer HFST is less flexible than single layer; therefore, care should be taken when considering a double-layer HFST (FHWA-CAI-14-019 n.d.).

2.3 Service Life of High Friction Surface Treatment

The service life of the HFST varies based on climate and roadway characteristics such as traffic volume, mix types, nature of traffic movement, and roadway geometry. For correctly applied HFST, the service life of HFST ranges from 7 to 12 years. Vendors reported 5 years of service life for HFST applied on roadways with traffic volumes of approximately 50,000 vehicles per day and 5 to 8 years for traffic volumes of around 15,000 vehicles per day (FHWA-CAI-14-019 n.d.).

2.4 Cost of High Friction Surface Treatment

The HFST cost—including the materials, labor, equipment, and traffic control—ranges from \$21/yd² to \$26/yd², as reported in 2017, which would decrease in larger projects. HFST projects should be stand-alone, and not be added to paving or other related work through prime contracts, because the unit price of the HFST increases when additional percentages are added by the general contractors. It was reported that the cost of the epoxy resin binder, equipment, and labor are the significant driver of the project bid, not the cost of the aggregate (FHWA-CAI-14-019 n.d.).

Table 2-2 The construction methods of the HFST (FHWA-CAI-14-019 n.d.; Wilson and Mukhopadhyay 2016).

Installation Method	Manual	Machine-Aided Manual (Semi-Automated)	Fully Automated
Applicability	Small spot locations (≤ 200 sq. yd.)	-	-
Binder Mixing	Manually mixed in buckets on site. A Jiffy mixer should be used (a more efficient mixing process and no air-entrainment occurred).	Trucks are equipped with any combination of a mixing machine, binder spreader, and aggregate spreaders.	A truck is mounted with a mechanical system to meter, mix, and apply a binder.
Binder Application	The mixed binder is poured onto the prepared surface and spread using the squeegees to the proper mil thickness.	<ul style="list-style-type: none"> • The machine pumps the binder out a spigot, behind the truck. • Workers spread the binder using squeegees. 	<ul style="list-style-type: none"> • The binder is applied uniformly and automatically across the pavement surface. • The binder thickness is controlled by adjusting the vehicle speed.
Aggregate Application	<ul style="list-style-type: none"> • The aggregate is broadcast, by hand or a blower, on the top of the binder. • The binder must be completely covered. 	<ul style="list-style-type: none"> • The aggregate is broadcast, by hand or a blower, on the top of the binder. • The binder must be completely covered. 	The aggregate is dropped uniformly on the binder layer. This process is similar to the chip spreader.
Benefits	Low cost for small locations.	The roadway is covered more quickly than the manual installation.	<ul style="list-style-type: none"> • Minimize the lane closure due to the quick installation time and the low number of workers on the roadway. • High-quality application. • Lower overall project costs on large systemic installations. • More sensitive to delayed drain-down into open Textures (TXs) or surface TX variation.
Drawbacks	<ul style="list-style-type: none"> • Safety risks by prolonging workers' exposure to traffic. • Human error and inconsistency. • Quality and uniformity are a concern. 	<ul style="list-style-type: none"> • Human errors. • Inconsistency in the resin application. 	Expensive equipment's price reaches \$600,000.
Other	The application rate is 200 to 300 yd ² /hr.	The application rate is 300 yd ² /hr.	Application rate is 1,500 to 2,300 yd ² /hr.

2.5 High Friction Surface Treatment Standards

States have their own standards for High Friction Surface Treatment (HFST) applications. These standards were used as the basis for most of the tests that were performed during this project. The goal is that the new Enhanced Friction Surface Treatment (EFST) standard for MoDOT would follow their current HFST requirements, but also reflect upcoming changes to the requirements that will follow the AASHTO MP 41-19 specification. The EFST proposed a friction repair and improvement strategy that uses an epoxy binder topped with an aggregate, other than Calcined Bauxite (CB). This section compares the current state standards about HFST applications and discusses their role in the recommendations for the new MoDOT EFST standard.

2.5.1 MoDOT Requirements for HFST (NJSP-15-13B)

The NJSP-15-13B (Missouri DOT 2015) is the current MoDOT requirement for HFST applications and is the base work for the development of the EFST specification. The tests of resin binder (polymeric and MMA) systems are summarized in Table 2-3.

Table 2-3 Required testing for resin binder systems (Missouri DOT 2015).

Testing	Specifications
Adhesive Strength at 24 hours	ASTM D4541
Compressive Strength	ASTM C579
Cure Rater (Dry through time)	ASTM D1640
Durometer Hardness (Shore D)	ASTM D2240
Elongation at Break Point	AASHTO M 235
Gel Time	AASHTO M 235 Class C
Ultimate Tensile Strength	AASHTO M 235
Viscosity	ASTM D2556 Class C
Water Absorption	AASHTO M 235

The requirements for the polymeric binder are not the same as the requirements for the MMA for four of the nine requirements. The four different requirements are stricter (with less allowable variance) for the polymeric resin, except for the viscosity requirement. The viscosity is required to be between 7–30 poises for the polymeric and 12–20 poises for the MMA resin system. The specification requires that the aggregate provided be CB. The requirements for the CB are illustrated in Table 2-4.

Table 2-4 MoDOT’s requirements for CB (Missouri DOT 2015).

Tests	Threshold Values	Specifications
Degradation Resistance (LAA) ^a	20% Loss Max.	AASHTO T 96
Moisture Content	0.2% Max.	AASHTO T 255
Aluminum Oxide Content	87% Min.	ASTM C25
Gradation (% passing)	#4	100% Min.
	#6	95% Min.
	#16	5% Max.

^a LAA: Los Angeles Abrasion.

It should be noted that DOTs, including MoDOT, may be adjusting this specification to align closely to the new AASHTO MP 41-19 specification. While the Los Angeles Abrasion (LAA) degradation resistance was used as a preliminary disqualifier for the aggregates, the other requirements here are not as helpful in this aspect. The moisture content is important when delivering the aggregate to make sure that the aggregate can securely bind to the resin binder. The gradation is important but is being controlled in

this study. Aluminum oxide content is important for ensuring the quality of Calcined Bauxite (CB) being supplied but does not apply to the alternative aggregates.

2.5.2 AASHTO MP 41-19

The AASHTO MP 41-19 is the standard replacing the provisional standard AASHTO PP 79-14, which is used in the MoDOT requirements document (NJSP-15-13B) (Missouri DOT 2015). The required testing for the resins and the specifications are demonstrated in Table 2-5. While the required tests besides the refractory grade of CB, specifications and their threshold for the CB are presented in Table 2-6.

Table 2-5 Testing conditions for epoxy, MMA, or polyester resins.

Tests	Specifications
Absorption	ASTM C881/AASHTO M 235
Compressive Modulus 7days	ASTM D695
Compressive Strength 3h and 24 hr	ASTM C579 Test Method B
Tensile Elongation	ASTM C881/AASHTO M 235
Flash Point	ASTM D3278
Gel Time	ASTM C881/AASHTO M 235
Type D Hardness cured for 7d±6hr	ASTM D2240
Tensile Strength	ASTM C881/AASHTO M 235
Thermal Compatibility	ASTM C884
Infrared Spectrum	ASTM E573
Viscosity	ASTM D2256-11

^a Note: the thermal compatibility test is not required for the polyester resin system.

Table 2-6 Calcined Bauxite’s testing conditions according to AASHTO MP 41-19.

Tests	Threshold	Specifications
Fine Aggregate MD ^a	3% Max. loss	ASTM D7428
Modified LAA (Backup)	20% Max. loss	AASHTO T 96
Moisture Content	0.2% Max.	AASHTO T 255
Aluminum Oxide Content	87±2%	ASTM E1621
Gradation (% Passing)	#4	100% Min.
	#6	95% Min.
	#16	5% Max.
	#30	0.2% Max.

^a MD: Micro-Deval.

Notable changes between this standard and MoDOT’s NJSP-15-13B are the change to the fine aggregate Micro-Deval (MD) from the Los Angeles Abrasion (LAA), the upper limit and lower limit on the aluminum oxide content, and the restriction on the amount of the aggregate, which passes the #30. Out of these requirements, only the 3% max loss on the fine aggregate MD was taken into consideration for the alternative aggregate study. MoDOT is expected to follow the move from the LAA to the MD in their new HFST standard, and it is recommended that the Enhanced Friction Surface Treatment (EFST) standard matches the HFST standard as much as reasonably possible.

2.5.3 Other state Standards

In addition to the MoDOT requirements and AASHTO standard, HFST standards for 14 other states and an EFST standard for Wisconsin were analyzed to guide MoDOT’s EFST standard. The requirements that each standard has regarding the aggregate topping for the High Friction Surface Treatment (HFST) and Enhanced Friction Surface Treatment (EFST) are briefly discussed in the following subsections. More

details are discussed in Appendix A. It is worth noting that while there are significant differences between states on which tests, they require, the required values for each of these tests are largely consistent when present. Figure 2-1 shows the number of states requiring different HFST tests. As seen in Figure 2-1, the two most common tests for the HFST applications are the Los Angeles Abrasion (LAA) and the aluminum oxide content. In the most recent AASHTO specification, the LAA test was replaced by the fine aggregate Micro-Deval (MD) test. If using an aggregate other than Calcined Bauxite (CB), the aluminum oxide content is not important.

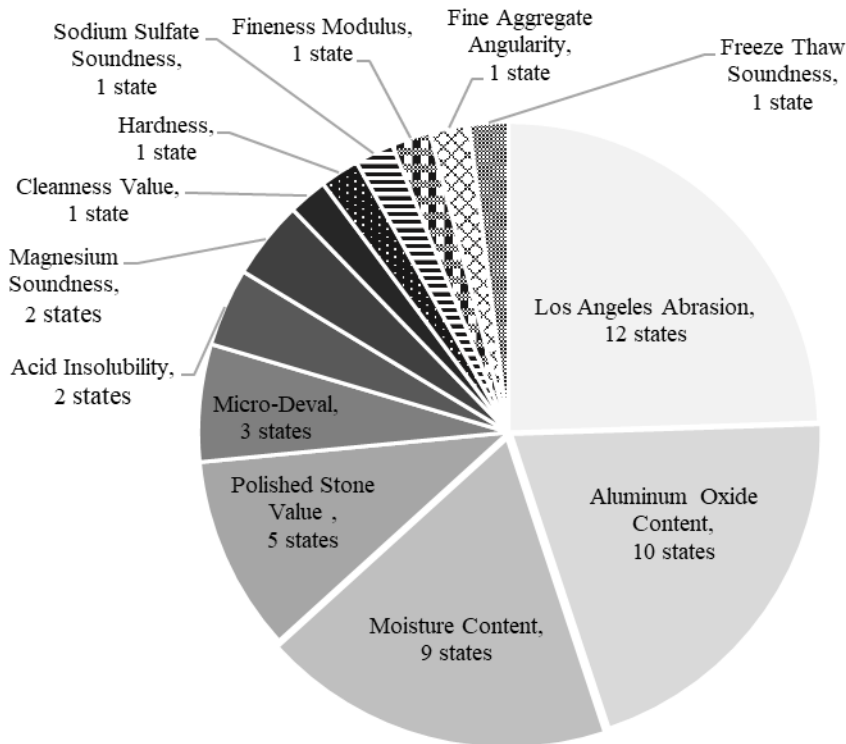


Figure 2-1 Number of states requiring different HFST tests.

2.5.3.1 Aggregate Gradation Standards

High Friction Surface Treatment (HFST) applications consist of a small size aggregate topping on an epoxy base. The gradation requirements for the aggregate topping are demonstrated in Table 2-7. These requirements were fairly consistent, with most states requiring the #4 to be analyzed and a few states requiring the #30 to be analyzed. Only Michigan replaced the #6 with the #8.

2.5.3.2 Physical Properties and Abrasion Testing Standards

The physical properties of the aggregates were specified in every state. The most common requirements are listed in Table 2-8 by state. Alaska was the most flexible state for its HFST requirements according to the retrieved specifications. Table 2-9 lists some other requirements that were not common among the states. Wisconsin was the only state that had an EFST specification instead of an HFST specification, and it was also the only state to require the fine aggregate angularity to be measured.

Table 2-7 High friction aggregate gradation requirements by state.

States	% Passing					Gradation Test Method	References
	#4	#6	#8	#16	#30		
Alabama	100% Min.	95% Min.	-	5% Max.	-	AASHTO T 27	(Alabama DOT 2014)
Alaska	-	95% Min.	-	5% Max.	-	AASHTO T 27	(Alaska DOT 2004)
California	-	95% Min.	-	5% Max.	-	AASHTO T 27	(California DOT, n.d.)
Florida	100% Min.	95% Min.	-	5% Max.	-	AASHTO T 27	(Florida DOT 2014)
Georgia	100% Min.	95% Min.	-	5% Max.	-	AASHTO T 27	(Georgia DOT 2017)
Illinois	100% Min.	95% Min.	-	5% Max.	-	AASHTO T 27	(Illinois DOT 2014)
Indiana	100% Min.	95% Min.	-	5% Max.	1% Max.	AASHTO T 27	(Indiana DOT 2017)
Iowa	100% Min.	95% Min.	-	5% Max.	-	AASHTO T 27	(Iowa DOT 2011)
Kentucky	100% Min.	95% Min.	-	5% Max.	-	AASHTO T 27	(Kentucky DOT, n.d.)
Michigan	98% Min.	-	30–70%	5% Max.	1% Max.	AASHTO T 27	(Michigan DOT 2016)
Pennsylvania	100% Min.	95% Min.	-	5% Max.	-	AASHTO T 27	(Pennsylvania DOT 2014)
South Carolina	100% Min.	95% Min.	-	5% Max.	-	AASHTO T 27	(South Carolina DOT 2015)
South Dakota	100% Min.	95% Min.	-	5% Max.	-	AASHTO T 27	(South Dakota DOT 2015)
Tennessee	100% Min.	95% Min.	-	5% Max.	-	AASHTO T 27	(Tennessee DOT 2017)
Texas	-	95% Min.	-	5% Max.	-	AASHTO T 27	(Texas DOT 2004)
Virginia	-	95% Min.	-	5% Max.	-	AASHTO T 27	(Virginia DOT 2012)
Wisconsin	100% Min.	95% Min.	-	5% Max.	1% Max.	AASHTO T 27	(Wisconsin DOT, n.d.)

In addition to the physical properties of the aggregates, many states required additional physical properties for the delivered aggregate. Maximum moisture content was the most common of these requirements. Table 2-10 shows the moisture content requirements by state for the delivered aggregate. Moreover, California state required additional physical property, which was cleanness value following AASHTO CT-227. The threshold value for this property was 75 Min. (California DOT, n.d.).

Table 2-8 Requirements of high friction aggregates' physical properties by state.

States	Aggregates	Los Angeles Abrasion (LAA) Threshold	LAA Specification	Aluminum Oxide Content Threshold	Aluminum Oxide Content Specification	References
Alabama	Calcined Bauxite (CB)	20% Max.	AASHTO T 96	87% Min.	ASTM C25	(Alabama DOT 2014)
Alaska	Blend of CB					(Alaska DOT 2004)
California	Blend of CB	10% Max.	CT 211			(California DOT, n.d.)
Florida	CB	10% Max.	AASHTO T 96	87% Min.	ASTM C25	(Florida DOT 2014)
Illinois	CB	20% Max.	AASHTO T 96	87% Min.	ASTM C25	(Illinois DOT 2014)
Indiana	CB	10% Max.	AASHTO T 96	87% Min.	ASTM C25	(Indiana DOT 2017)
Iowa	CB	20% Max.	AASHTO T 96			(Iowa DOT 2011)
Michigan	CB			87% Min.	ASTM C25	(Michigan DOT 2016)
Pennsylvania	CB	20% Max.	AASHTO T 96	87% Min.	ASTM C25	(Pennsylvania DOT 2014)
South Carolina	CB	20% Max.	AASHTO T 96	87% Min.	ASTM C25	(South Carolina DOT 2015)
South Dakota	CB	20% Max.	AASHTO T 96	87% Min.	ASTM C25	(South Dakota DOT 2015)
Tennessee	CB			87% Min.	ASTM C25	(Tennessee DOT 2017)
Texas	CB	10% Max.	ASTM C131	87% Min.	ASTM C25	(Texas DOT 2004)
Virginia	CB	20% Max.	AASHTO T 96			(Virginia DOT 2012)
Wisconsin	Natural or Synthetic	25% Max. & 10% Max.	AASHTO T 96			(Wisconsin DOT, n.d.)

Table 2-9 Other high friction aggregates' physical properties by state.

States	Fineness Modulus	Fine Aggregate Angularity (FAA) Threshold	FAA Specification	Hardness Test Threshold	Hardness Test Specification	References
Indiana	-	-	-	8 Min	Mohs Scale	(Indiana DOT 2017)
Michigan	2.28–22.81	-	-	-	-	(Michigan DOT 2016)
Wisconsin	-	45% Min	AASHTO T 304	-	-	(Wisconsin DOT, n.d.)

Table 2-10 As delivered high friction aggregates' moisture content threshold by state.

States	Moisture Content Threshold	Moisture Content Specification	References
Alabama	0.2% Max.	AASHTO T 255	(Alabama DOT 2014)
Florida	0.2% Max.	AASHTO T 255	(Florida DOT 2014)
Illinois	0.2% Max.	AASHTO T 255	(Illinois DOT 2014)
Indiana	0.2% Max.	AASHTO T 255	(Indiana DOT 2017)
Pennsylvania	0.2% Max.	AASHTO T 255	(Pennsylvania DOT 2014)
South Carolina	0.2% Max.	AASHTO T 255	(South Carolina DOT 2015)
South Dakota	0.2% Max.	AASHTO T 255	(South Dakota DOT 2015)
Tennessee	0.2% Max.	AASHTO T 255	(Tennessee DOT 2017)
Wisconsin	0.2% Max.	AASHTO T 255	(Wisconsin DOT, n.d.)

2.5.3.3 Performance and Durability Testing Standards

High Friction Surface Treatment (HFST) applications are used to enhance the friction property on special roadways locations, so the aggregates' durability used in these applications is important. Without high durability aggregates, the HFST application would not be able to be in place for a long period. Table 2-11 demonstrates the Polished Stone Value (PSV) and Micro-Deval (MD) requirements by state, and Table 2-12 shows some additional durability requirements by state. It is worth noting that there was significantly less agreement between states on which durability tests are important for the aggregates than the required physical properties. Wisconsin is the only state that was found to have an Enhanced Friction Surface Treatment (EFST) standard rather than an HFST standard as outlined in Table 2-13. Due to this, their specifications were of higher importance to this study than the other states.

Table 2-11 High friction aggregates' Polished Stone Value and Micro-Deval requirements by state.

States	Polished Stone Value (PSV) Threshold	PSV Specification	Micro-Deval (MD) Threshold	MD Specification	References
Alabama	38 Min.	AASHTO T 279			(Alabama DOT 2014)
Indiana	38–44	AASHTO T 279			(Indiana DOT 2017)
Iowa	70.0 BPN ^a Min.	ASTM E660			(Iowa DOT 2011)
Pennsylvania	38 Min.	AASHTO T 279			(Pennsylvania DOT 2014)
South Carolina	38 Min.	AASHTO T 279			(South Carolina DOT 2015)
Tennessee			5% Max.	ASTM D7428	(Tennessee DOT 2017)
Virginia			5% Max.	AASHTO T-327	(Virginia DOT 2012)
Wisconsin			15% Max.	ASTM D7428	(Wisconsin DOT, n.d.)

^a BPN: British Pendulum Number.

Table 2-12 High friction aggregates’ additional durability and performance requirements by state.

States	Acid Insolubility Threshold	Acid Insolubility Specification	Magnesium/Sodium Sulfate Soundness Threshold	Magnesium/Sodium Sulfate Soundness Specification	References
California	90% Min.	ASTM D-3042	30% Max.	ASTM C88	(California DOT, n.d.)
Indiana	-	-	12% Max.	AASHTO T 104	(Indiana DOT 2017)
Texas	90% Min.	Tex-512-J	30% Max.	Tex-411-A	(Texas DOT 2004)
Wisconsin	-	-	-	-	(Wisconsin DOT, n.d.)

Table 2-13 Natural/synthetic aggregates’ requirements in Wisconsin (Wisconsin DOT, n.d.).

Tests	Threshold Values	Specification
Fine Aggregate Micro-Deval (MD)	15% Max. loss	ASTM D7428
Los Angeles Abrasion (LAA)	10% Max. loss at 100 revolutions & 20% Max. loss at 500 revolutions	AASHTO T 96
Moisture Content	0.2% Max.	AASHTO T 255
Water-Alcohol Freeze Thaw Soundness	9% Max. loss	AASHTO T 103

2.5.4 High Friction Surface Treatment Performance Testing

This section outlines two points, which are the available performance tests for assessing the friction property of aggregates/mixes and the previous research efforts that were devoted to evaluating several High Friction Surface Treatment (HFST) aggregates when compared to Calcined Bauxite (CB). These performance tests were typically used to evaluate the proposed aggregates/mixes before and after polishing conditions. The most common performance tests and the associated polishing devices were British pendulum tester & British accelerated polishing machine, dynamic friction tester & National Center for Asphalt Technology’s (NCAT) Three-Wheel Polishing Device (TWPD), and Aggregate Image Measurement System (AIMS) & Micro-Deval (MD) device. These tests aimed to identify the friction characteristic of aggregates and/or mixes.

2.5.5 Performance Tests

2.5.5.1 British Pendulum Test

The British Pendulum (BP) measures the resistance of the coarse aggregates to polishing before and after the 10-hr polishing process by the British accelerated polishing machine (British wheel). In the ASTM D3319-11, the initial polishing value (PV-i) and 10-hrs polishing value (PV-10) were recorded for the curved aggregate coupons using the BP on the F-scale, as illustrated in Figure C-7. The F-scale was used for the slider that was 1.25-inches wide; however, the main scale was used for the 3-inches wide slider, which was used for flat surfaces. The polished stone value was used to evaluate the coarse aggregates’ resistances to polishing, and it was calculated using Equation 2.1 (Li et al. 2017). Li et al. (Li et al. 2017) concluded that the Polished Stone Value (PSV)—calculated according to BS EN 1097-8—and the PV-10—measured following ASTM D3319-11—were different. The difference was due to the various procedures and materials used in each specification: the abrasive material, the polishing time, and the abrasive feed rate. The researchers (Li et al. 2017) mentioned that there was no evidence to select the most accurate parameter (PSV or PV-10).

$$PSV = S - C + 52.5$$

Equation 2.1

where,

S is the average value of the four aggregate test samples, and
 C is the average value of the four control stone samples.

It was reported that the PV did not only depend on the aggregate Texture (TX), but also relied on the other experimental considerations: the coupons' curvatures, aggregates' sizes, and the arrangements of the aggregates (Kassem et al. 2013; Won and Fu 1996). Additionally, it was difficult to accurately differentiate between the polishing resistance for the aggregates because of the narrow range of PV (Kassem et al. 2013; Kandhal, Parker, and Bishara 1993; E. M. Mahmoud 2005).

2.5.5.2 Accelerated Friction Testing

Accelerated friction testing was used to evaluate the surface frictional characteristics of pavement surfaces. The accelerated testing included measuring the Mean Texture Depth (MTD) using the sand patch test or the Mean Profile Depth (MPD) using the Circular Texture Meter (CTM). The MPD or MTD was used to evaluate the macrotexture of surfaces. A Dynamic Friction Tester (DFT) was used to measure the Coefficient of Friction (COF) at different speeds (i.e., 20, 40, 60 km/hr) following ASTM E 1911 at different numbers of polishing cycles [i.e., 0 cycles (initial), 70k cycles, and 140k cycles (considered terminal)].

2.5.5.3 Micro-Deval and Aggregate Image Measurement System

The Micro-Deval (MD) device—developed in France in the 1960s—was used to characterize aggregates' durability and resistance to polishing, abrasion, and grinding in the existence of water (Li et al. 2017; Wilson and Mukhopadhyay 2016; Kassem et al. 2013). Water simulated environmental effects, which were considered better judgments of aggregate durability compared to the Los Angeles Abrasion (LAA) test (Li et al. 2017; Cuelho et al. 2007; Wu, Parker, and Kandhal 1998). The existence of the water and the use of smaller steel balls than the steel balls used in the LA test reduced the impact action. Contrarily, surface wear by grinding and abrasion was prevalent (Li et al. 2017).

An Aggregate Image Measurement System (AIMS)—developed at Texas A&M University—was used to measure the aggregates' form (shape), Gradient Angularity (GA), and surface Texture (TX) before and after polishing in the MD device (Kassem et al. 2013; E. Mahmoud and Masad 2007; Masad, Luce, and Mahmoud 2006; Masad et al. 2009). The aggregates' shape was determined by a two-dimensional form, the angularity was identified by the irregularity of a particle's surface using black and white images, and the surface TX was determined by analysis of grayscale images using the wavelet analysis method (Kassem et al. 2013).

2.5.6 Previous Relevant Research

Heitzman and Moore (Heitzman, Michael; Moore 2017) investigated the long-term friction loss trend (terminal friction) for eleven types of aggregates. The aggregate types were Basalt, Copper Slag, Flint 65-8, RK Bauxite 6×14C CB, 47 - 4×20 Calcined Kaolin, 60 - 4×20 Calcined Kaolin, 70 - 4×20 Calcined Kaolin, Best Sand 612 Quartz, Armor Stone Quartz, EP5-Mod Quartz, and Traction Control Feldspar Mineral. This was achieved by measuring the surface TXs using a CTM and the DFT. The CTM was used to evaluate the macrotexture by providing a MPD (Heitzman, Michael; Moore 2017; Heitzman, Turner, and Greer 2015). The DFT was utilized to measure the pavement surface frictions [Friction Number (FN)] at 20, 40, and 60 km/hr (Heitzman, Michael; Moore 2017; Heitzman, Turner, and Greer 2015). Using the DFT provided an estimation for the microtexture (Kassem et al. 2013). The FN and MPD were measured

for the aggregate before and after polishing by using the NCAT Three-Wheel Polishing Device (TWPD). There was no relationship found between the CTM and DFT results. The Calcined Bauxite (CB) had the highest friction when compared to other aggregates; it yielded the highest FN values (Heitzman, Michael; Moore 2017).

Heitzman et al. (Heitzman, Turner, and Greer 2015) investigated the friction performance of seven friction aggregates and explored their comparison with CB. The friction aggregates that were compared to the CB were Granite, Flint, Basalt, Silica, Emery, and Taconite. None of the seven friction aggregates showed friction comparable to the CB based on the DFT results. The researchers concluded that the friction aggregates had similar friction losses between 70k and 140k cycles. Table 2-14 summarizes the terminal FN and MPD results of this study. No relationship was recorded between the DFT and CTM measurements. Moreover, the effect of aggregate—CB, Slag, Taconite, and Flint—size on the friction performance was evaluated using the DFT and CTM before and after polishing using the NCAT TWPD, MD, and AIMS. It was reported that decreasing the particle size of the aggregate decreased the surface TX: changing the particle size from #6 to #16 caused a reduction in the CTM macrotexture from 2.3 mm to 1 mm. Aggregate particles with #8 size had the highest friction values. A relationship was found between the Micro-Deval (MD) mass losses and the friction ranking values for Calcined Bauxite (CB), Slag, and Taconite. The Flint aggregate was an exception to this relationship. No relationship was found between the Aggregate Image Measurement System (AIMS), particle shape, GA, and friction (Heitzman, Turner, and Greer 2015).

Table 2-14 The main results of Heitzman et al.’s study (Heitzman, Turner, and Greer 2015).

Aggregate Types	Terminal FN ^a	Terminal MPD ^b
Calcined Bauxite (CB)	> 0.8	≥ 1.4 mm
Basalt, Emery, Taconite, and Flint	> 0.6	
Granite	0.5:0.6	
Silica & Slag	≤ 0.5	

^a Terminal average Friction Number values were recorded at 70k and 140k polishing cycles.

^b Terminal Mean Profile Depth for conventional dense graded asphalt mixes was typically between 0.3 to 0.5 mm.

Wilson and Mukhopadhyay (Wilson and Mukhopadhyay 2016) investigated the friction performance of two sources of CB aggregate, one from China and the other from India, and a third unknown aggregate obtained from the UK. The first two CB aggregates contained 87% Al₂O₃ and the third one contained 60% SiO₂ and 20% Al₂O₃. The friction performances were evaluated using the Circular Texture Meter (CTM) and Dynamic Friction Tester (DFT) before and after the polishing using the NCAT Three-Wheel Polishing Device (TWPD). Additionally, the aggregates’ shapes, Textures (TXs), and angularities were examined before and after the MD device using the AIMS. The two CB aggregates showed the lowest mass loss (5.5% average) after 50 minutes, and the aggregate obtained from the UK yielded a higher mass loss (24.6%). The AIMS angularities for the three aggregates were moderate; however, the angularities decreased after polishing. Additionally, polishing lowered the TXs slightly. The CB aggregates showed the highest Friction Number (FN) and Mean Profile Depth (MPD). The aggregate obtained from the UK started with a lower initial FN, as compared to the CB aggregates, and it polished faster than the CB aggregates. Furthermore, the UK aggregate showed lower MPD than the CB aggregates (Wilson and Mukhopadhyay 2016).

Kassem et al. (Kassem et al. 2013) evaluated the friction performance of three aggregates—limestone 1 (soft aggregate), limestone 2 (intermediate hardness aggregate), and sandstone (hard aggregate)—using AIMS, CTM, and DFT. The DFT and CTM applied on slabs with different mix designs: a porous friction course (PFC), a stone matrix asphalt (SMA), a fine dense-graded mixture (Type F), and a coarse dense-graded mixture (Type C). One asphalt binder—with a true performance grade of 67–22—was used in

these mixtures. The DFT and CTM measurements were conducted before and after polishing using the TWPD at 5,000, 10,000, 30,000, 50,000, and 100,000 cycles. AIMS was performed on the aggregates before and after the MD polishing. The MD results showed that the sandstone aggregate had the highest resistance to degradation—the lowest mass loss after 105- and 180-minutes of polishing. On the Contrary, limestone 1 showed the lowest resistance to degradation. The AIMS results showed different TX and Gradient Angularity (GA) values for the same aggregate of different sizes. The sandstone aggregate showed the highest TX and GA indices, after the MD polishing when compared to the other two limestone aggregates. The GA and TX indices decreased—after the MD—because of abrasion and polishing that occurred in the MD apparatus. The macrotexture was evaluated from the MPD, and it depended on the mixtures' gradations. The slabs containing coarse aggregate gradation (PFC mixtures) showed the highest MPD values when compared to the other mixtures. After the polishing process using the TWPD, the MPD values increased slightly. This occurred because the fine aggregates and asphalt binder film around the aggregates were washed during the polishing process. The COF values measured by DFT at 20 km/hr (DFT₂₀)—the indicator of the pavement microtexture—reached the highest values for slabs that contained the sandstone aggregate indicating rough microtexture. The DFT₂₀ decreased with increasing polishing cycles due to the abrasion and polishing of aggregate particles on the slabs' surfaces (Kassem et al. 2013).

Mahmoud and Ortiz (E. Mahmoud and Ortiz 2014) explored the terminal polishing using the Micro-Deval (MD). The researchers tried different polishing times (e.g., 15, 30, 45, 60, 75, 90, 105, and 180 minutes), and they used t-test statistical analysis to compare the mean of aggregate Texture (TX) between two consecutive MD polishing times using a 95% confidence interval (CI). For instance, the CI limits at 180 minutes—the CI lower and upper limits—represented the difference in the TX mean between 105- and 180-minutes polishing times. However, the researchers deemed that the two aggregates reached the terminal TX values because the rate of TX loss with time reached a near-zero value at the 210-minutes polishing time. It was concluded that the terminal TX or GA, measured by Aggregate Image Measurement System (AIMS), was achieved at 210 minutes or less (E. Mahmoud and Ortiz 2014). Mahmoud (E. M. Mahmoud 2005) showed that implementing a fitting curve at three MD polishing times—0, 105, and 180 minutes—was sufficient to obtain the AIMS TX and Gradient Angularity (GA) parameters instead of using fitting at nine polishing times, note Equation B.8 and Equation B.9. Aldagari et al. (Aldagari et al. 2020) used equations to predict the TX and GA parameters using two points at 0- and 105-minutes polishing times, which was standard practice at TxDOT. However, fitting curves using three points—0, 105, and 180 minutes—can be conducted if the 180-minutes polishing time was implemented. At 105-minutes MD polishing time, the TX and GA losses' rate reduced significantly. Therefore, the 105-minutes time was considered the initial time when the aggregates approached the terminal values (Greer 2015; Aldagari et al. 2020).

Li et al. (Li et al. 2017) evaluated the abrasions for the Calcined Bauxite (CB) and Steel Slag, with a maximum nominal aggregate size of 9.5 mm, using the MD test. The average percentage of mass losses for the Steel Slag was 17% higher than the average percentage of mass losses for the CB. Moreover, they studied the PV for the CB and Steel Slag—with aggregate sizes of 6.3–9.5 mm and 1–3 mm—before and after the polishing process. Decreasing the aggregate size increased the PV-i and PV-10 values. The researchers related this observation to the preparation process: the 1–3 mm aggregate size was smaller and separately placed in a single layer when compared to the larger aggregate size (6.3–9.5 mm). The PV values for the CB were greater than the PV values for the Steel Slag. However, the researchers (Li et al. 2017) recommended that the Steel Slag be used as an aggregate alternative to CB.

2.5.7 Skid Resistance Prediction Models

Research attempts were conducted to investigate the relationships between Hot Mix Asphalt (HMA) properties and the friction performance [Skid Number (SN) and/or International Friction Index (IFI)]. It

was observed that the aggregate gradation, AIMS GA indices, and AIMS TX indices of the used aggregates had a significant effect on the friction performance. Kassem et al. (Kassem et al. 2013) conducted a study on a limited number of aggregates (soft limestone, intermediate hardness limestone, and hard sandstone) to investigate the impact of aggregate source and gradation on the skid resistance. It was found that the International Friction Index (IFI) reflected the skid resistance of the pavement (Kassem et al. 2013). Therefore, a regression model was developed to correlate the IFI with COF values measured by DFT at 20 km/hr (DFT_{20}) and Mean Profile Depth (MPD) values, as demonstrated in Equation 2.2 (Wambold et al. 1995). The methodology of the development of the regression model is comprehensively discussed in Appendix B. Moreover, it was observed that the sandstone had the highest IFI value. In addition, the mixtures with finer gradation (Type C and Type F) showed lower IFI values than mixtures with the coarser gradation (SMA and PFC) (Kassem et al. 2013).

$$IFI = 0.081 + 0.732DFT_{20} \left(\frac{-40}{(14.2+89.7 \times MPD)} \right) \quad \text{Equation 2.2}$$

The skid resistance prediction model was explored by other studies (Kassem et al. 2013; E. Mahmoud and Masad 2007; Masad, Luce, and Mahmoud 2006; Masad et al. 2009; Masad, Rezaei, and Chowdhury 2011), which is illustrated in Equation 2.3. The regression coefficients (a_{mix} , b_{mix} , and c_{mix}), see Equation 2.3, were correlated with the aggregate Texture (TX), aggregate GA, and Weibull distribution parameters that described the AGs as explained in Appendix B. Eventually, the Skid Number measured at 50 mi/hr by a skid trailer with smooth tires [SN(50)] was correlated with the International Friction Index (IFI) and Mean Profile Depth (MPD) as presented in Equation 2.4 (Rezaei and Masad 2013).

$$IFI(N) = a_{mix} + b_{mix} \times e^{(-c_{mix} \times N)} \quad \text{Equation 2.3}$$

$$SN(50) = 1.41 + 143.19 \times (IFI - 0.045) \times e^{\left(-\frac{20}{(14.2+89.7 \times MPD)} \right)} \quad \text{Equation 2.4}$$

Chowdhury et al. (2016) followed the same methodology of Kassem et al. (2013) to propose two skid resistance prediction models for Hot Mix Asphalt (HMA) and seal coat surfaces. These models were developed based on a wide range of aggregates used in Texas for the HMA, which were collected from 56 different sources: 35 HMA test sections and 35 seal coat test sections (Chowdhury et al. 2016; Aldagari et al. 2020). The regression coefficients of Equation 2.3 for HMA and seal coats were calculated using Equation B.14 through Equation B.16 and Equation B.26 through Equation B.28, respectively. Moreover, 16 aggregate sources for the HMA and 19 aggregate sources for the seal coats were analyzed. The researchers calculated the TX and Gradient Angularity (GA) coefficients using regression analysis from only two points before Micro-Deval polishing (BMD) and After 105-minutes of Micro-Deval polishing time (AMD 105), instead of three points, as was proposed by Kassem et al. (2013) (Chowdhury et al. 2016; Aldagari et al. 2020). These coefficients were estimated using Equation B.17 to Equation B.22 and Equation B.29 to Equation B.34 for the HMA and seal coats, respectively.

CHAPTER 3: EXPERIMENTAL CONSIDERATIONS

3.1 Introduction

Calcined Bauxite and eight alternative aggregates were selected for testing. These aggregates were selected as possible alternatives to Calcined Bauxite (CB). Table 3-1 presents the received sizes, Maximum Aggregate Sizes (MAS), Nominal Maximum Aggregate Size (NMAS), sources, and notes. All these aggregates were tested to determine whether they met the MoDOT requirements for High Friction Surface Treatment (HFST) (NJSP-15-13B) and expected future changes to the HFST standard. In addition, a two-component (A and B) epoxy binder with a (1:1) mixing ratio by volume or a (1.18:1.00) mixing ratio by weight was utilized in the preparation of the coupons and HFST applications on Hot Mix Asphalt (HMA) slabs. Epoxy binder information is presented in Table 3-2.

Table 3-3 illustrates the aggregate testing matrix that shows a summary of the experimental design that was detailed in the following sections. Three testing categories were explored: the first category was physical properties testing, the second category was durability testing, and the third category was performance testing. The aggregates' physical properties testing, and durability testing were conducted at Missouri S&T (Part-I) and U Idaho (Part-II). Both parts referred to standard testing, and each was focused on specific size/gradation of the standards. See Table 3-3 for more details. Each category of testing included testing subdivisions. Physical properties testing was divided into aggregate gradation, specific gravity & absorption, and Uncompacted Void Content (UVC) of fine aggregates. Physical properties testing was included in Part-I and Part-II testing. Durability testing included Los Angeles Abrasion (LAA), sodium sulfate soundness, water-alcohol freeze thaw, and acid-insoluble residue. The LAA testing was existed in Part-I and Part-II; however, the remaining durability testing were in Part-I. Part-II was implemented for physical properties and LAA testing to address additional options in the standards (Note Table 3-3). Performance testing included Micro-Deval (MD) polishing, Aggregate Image Measurement System (AIMS), accelerated friction testing (sand patch test and dynamic friction test), and British Pendulum (BP). Inside each cell, the size of the used aggregate was specified. However, the AIMS testing was conducted at Texas A&M University. Table 3-4 shows the specific aggregate percentages/weights used in testing.

3.2 Experimental Design

Figure 3-1 shows the experimental design, the test used, and the tests' primary purposes. Three categories of testing were followed in the experimental design: the first category was for the physical properties testing, the second category was for durability testing, and the third category was for performance testing.

3.2.1 Aggregate Physical Properties Testing

The aggregate physical properties were tested for each source of the aggregate to classify the aggregates. Aggregate physical property tests are normally quick and simple. They are also routinely performed on aggregates being used for a variety of purposes.

Table 3-1 Received aggregate sizes and sources information.

Aggregate Type	Commercial Names and Received Sizes	Source	Notes
Calcined Bauxite (CB)	3/8" × #3: Maximum Aggregate Size (MAS) (3/8"), #3 × 0: MAS (#3), and GRIP Grain: MAS (#4).	Great Lakes Minerals, LLC in Wurtland, Kentucky, U.S.A.	The GRIP grain CB is specifically produced for High Friction Surface Treatment (HFST). The typical aluminum oxide content for the CB was 87.5%, which was just above the 87% minimum found in most of the HFST specifications. The GRIP grain bauxite product had a certificate of analysis that guaranteed that the material provided to us had an 88.65% aluminum oxide content. This was inside the range for the AASHTO MP 41-19 (85–89%). The 3/8" × #3 bauxite product was retained on sieve 3/8" to #3. The #3 × 0 bauxite product was retained through #3 and less (3 Minus).
Earthwork Solution (Natural Calcined Bauxite)	#6 × #16: MAS (#6).	Earth Work Solutions in Gillette, Wyoming, U.S.A.	The Earthwork solution source is known as natural Calcined Bauxite. It was named as Earthworks in this study to avoid any confusion between it and the control CB. The #6 × #16 Earthworks aggregate was graded to meet HFST specifications; the particles were retained on #6 to #16.
Meramec River Aggregate	C Gravel: MAS (1 1/2"), 5/16" Crushed Gravel: MAS (5/16"), Torpedo Gravel: MAS (1/2"), and Coarse Manufactured Sand: MAS (3/8").	Winter Brothers Material Company in Sint Louis, Missouri, U.S.A.	Meramec River Aggregate comes from the Meramec river, and it is used in road construction as well as a concrete aggregate.
Steel Slag	1" × 0: MAS (1").	Harsco Inc in Muscatine, Iowa, U.S.A.	The Steel Slag is typically used in surface courses to enhance the strength, durability, and frictional characteristics of the road. The 1" × 0 Steel Slag product had sizes of less than or equal to 1" (1" Minus).
Rhyolite (Iron Mountain Trap Rock)	1/2" × 0: MAS (1/2"), and #6 × #16: MAS (#6).	Fred Weber in Maryland Heights Missouri, U.S.A.	This aggregate is typically used for road and railroad construction as well as a chip seal. The 1/2" × 0 Rhyolite product had sizes of less than or equal to 1/2" (1/2" Minus). The #6 × #16 Rhyolite product was specifically graded to meet HFST specifications; the particles were retained on #6 to #16.
Black Diabase	1": MAS (1"), 3/8": MAS (3/8"), 1/4": MAS (1/4"), and Sand: Nominal Maximum Aggregate Size (NMAS) (#4).	Central Stone Butler Hill Facility in Farmington, Missouri, U.S.A.	The Black Diabase is granite that is typically used in the construction of bridges, highways, and airport runways.
Quartzite	1" × 0: MAS (1").	L. G. Everist, Inc., in South Dakota, U.S.A.	The 1" × 0 Quartzite product meant that most of the particles had sizes of less than or equal to 1" (1" Minus or a dense-graded aggregate).
Flint Chat	#6 × #16: NMAS (#6).	Williams Diversified Materials in Baxter Springs, Kansas, U.S.A.	The Flint Chat is specifically produced for friction-enhancing surface treatments. This product (#6 × #16) was graded to meet HFST specifications; particles retained through #6 to #16.
Potosi Dolomite	9/16" Clean: MAS (9/16"), and 3/8" Clean: MAS of (3/8").	Capital Quarries, Sullivan, Missouri, U.S.A.	Two sizes of Potosi Dolomite were collected; however, the 9/16" Clean size was used in testing.

Table 3-2 Used epoxy binder information.

Epoxy Binder Name	Epoxy Binder Type	Epoxy Binder Source	Notes
FasTrac CE330 Epoxy Binder. Low Modulus Epoxy Polymer Binder	Two-component epoxy binder	Cornerstone Construction Material (Lee's Summit, Missouri, U.S.A)	The epoxy binder had a bond strength of 2 ksi after 2 days & 2.8 ksi after 14 days and a tensile elongation of 40%

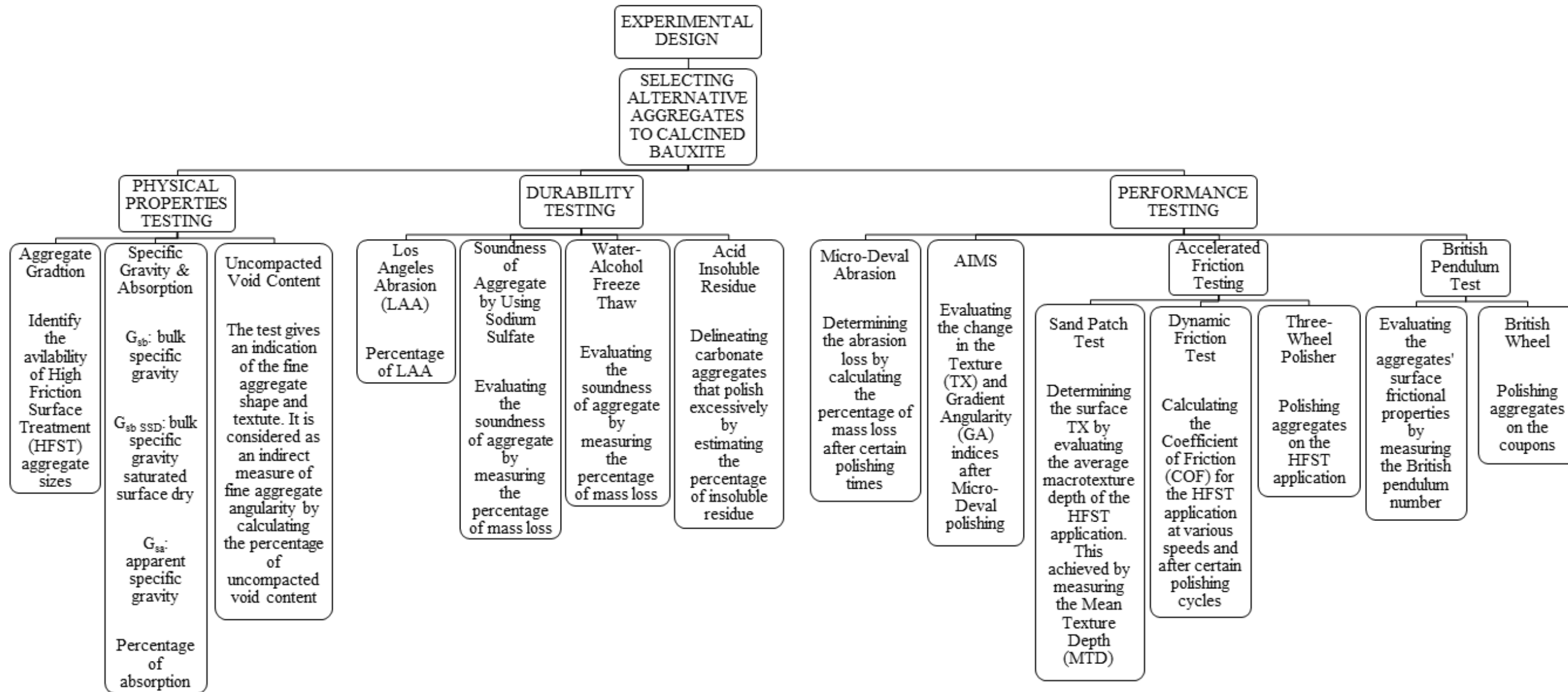


Figure 3-1 Experimental design.

Table 3-3 Aggregate testing matrix.

Aggregate Testing		Calcined Bauxite (CB) 3/8" x #3	CB #3 x 0	CB GRIP Grain	Earthworks #6 x #16	Meramec River Aggregate (MRA) C Gravel	MRA 5/16" Crushed Gravel	MRA Torpedo Gravel	MRA Coarse Man. Sand	Steel Slag 1" x 0	Rhyolite (Rh) 1/2" x 0	Rh #6 x #16	Black Diabase (BD) 1"	BD 3/8"	BD 1/4"	BD Sand	Quartzite 1" x 0	Flint Chat (FC) #6 x #16	FC Larger Particle Size	Potosi Dolomite (PD) 9/16" Clean	PD 3/8" Clean	
Physical Properties Testing	Aggregate Gradation	3/8" - #200 ^a	3/8" - #200	3/8" - #200	#4 - #200	1" - #4	3/8" - #200	3/8" - #8	3/8" - #200	1/2" - #200	3/4" - #200	3/8" - #200	1" - #4	1/2" - #200	3/8" - #200	#4 - #200	1" - #16	#4 - #200	1" - #16			
				#6 - #16	#6 - #16				#6 - #16	#6 - #16		#6 - #16			#6 - #16		#6 - #16	#6 - #16		#6 - #16		
	Specific Gravity & Absorption	- #4 ^b	- #4	- #4	- #4	- #4	- #4	- #4		- #4	- #4	- #4	- #4	- #4	- #4	- #4		- #4				
				#6 - #16	#6 - #16				#6 - #16	#6 - #16		#6 - #16			#6 - #16		#6 - #16	#6 - #16		#6 - #16		
	Uncompacted Void Content		#8 - #100 ^c				#8 - #100			#8 - #100	#8 - #100				#8 - #100							
				#6 - #8 ^d	#6 - #8				#6 - #8	#6 - #8		#6 - #8			#6 - #8		#6 - #8	#6 - #8		#6 - #8		
Durability Testing	Los Angeles Abrasion	C ^e	D	D	D	B	D	D	D	D	D	D	B	D	D		D	D				
				D ^f					D	D		D			D						D	
	Sodium Sulfate Soundness																					
				#4 - #6					#4 - #6	#4 - #6		#4 - #6									#4 - #6	
	Water-Alcohol Freeze-Thaw																					
				#6 - #8	#6 - #8				#6 - #8	#6 - #8		#6 - #8								#6 - #8		#6 - #8
Acid Insoluble Residue																						
			#6 - #8	#6 - #8				#6 - #8	#6 - #8		#6 - #8				#6 - #8		#6 - #8	#6 - #8		#6 - #8		
Performance Testing	Micro-Deval (MD)																					
				3/8" - #4 ^g	3/8" - #4					3/8" - #4	3/8" - #4		3/8" - #4		3/8" - #4		3/8" - #4	3/8" - #4		3/8" - #4		

			#6 - #16 ^g	#6 - #16				#6 - #16	#6 - #16		#6 - #16		#6 - #16		#6 - #16	#6 - #16		#6 - #16	
			#4 - #12 ^g					#4 - #12	#4 - #12									#4 - #12	
			1/4" - #10 ^g																
Aggregate Image Measurement System (AIMS)																			
			3/8" - 1/4"	3/8" - 1/4"				3/8" - 1/4"	3/8" - 1/4"		3/8" - 1/4"				3/8" - 1/4"	3/8" - 1/4"		3/8" - 1/4"	
			1/4" - #4	1/4" - #4				1/4" - #4	1/4" - #4		1/4" - #4				1/4" - #4	1/4" - #4		1/4" - #4	
Sand Patch Test			#6 - #8	#6 - #8				#6 - #8	#6 - #8	#6 - #8						#6 - #8			
Dynamic Friction Test			#6 - #8	#6 - #8				#6 - #8	#6 - #8	#6 - #8						#6 - #8			
British Pendulum Test																			
			#6 - #8	#6 - #8				#6 - #8	#6 - #8	#6 - #8						#6 - #8		#6 - #8	
			#4 - #6					#4 - #6	#4 - #6	#4 - #6								#4 - #6	

^aThe gradation was conducted from sieve 3/8" to #200.

^bIf the aggregates contained a substantial amount of materials finer than #4, materials retained up to #8 were used.

^c#8 - #100 according to test method A in ASTM C1252 – 17 (see Table 3-4).

^d#6 - #8 according to test method B & #6 - #16 (CB gradation, note Table 3-4) according to test method C in ASTM C1252 – 17.

^eC grading according to AASHTO T 96.

^fD grading according to ASTM C131/C131M – 20.

^gMore details about these gradations are presented in Table 3-4.

Part-I, conducted at Missouri S&T	
Part-II, conducted at the U Idaho	
Conducted at Texas A&M	

Table 3-4 Specific aggregates' percentages/weights used in Micro-Deval and Uncompacted Void Content testing.

Gradation	Testing	3/8" - 1/4" ^a	1/4" - #4	#4 - #6	#6 - #8	#8 - #10	#10 - #12	#12 - #16	#16 - #30	#30 - #50	#50 - #100
#8 - #100	Uncompacted Void Content (UVC)					44g			57 g	72 g	17 g
3/8" - #4	Micro-Deval (MD)	750 g	750 g								
#6 - #16	UVC & MD				53.0 %	21.1 %	13.7 %	11.9 %			
#4 - #12	MD			53.0 %	21.1 %	13.7 %	11.9 %				
1/4" - #10	MD		53.0 %	21.1 %	13.7 %	11.9 %					

^a 3/8" - 1/4": Passed from sieve 3/8" and retained on sieve 1/4".

3.2.1.1 Aggregate Gradation

The test was conducted following ASTM C136/C136M-19 [Part-I testing (#6 - #16)] and AASHTO T 27 [(Part-II testing (as-delivered gradation)]. The as-delivered gradations of these aggregates were needed to determine if the aggregates had comparable gradations in the size range specified in the MoDOT requirements file (NJSP-15-13B) for High Friction Surface Treatment (HFST). Note Table 3-3 shows details about the sieves used for aggregate gradation.

3.2.1.2 Specific Gravity and Absorption of Aggregates

This test was conducted following ASTM C128 – 15 for fine aggregates' gradations [Part-I testing (#6 - #16)] and AASHTO T 85 for coarse aggregates' gradations [Part-II testing (- #4)]. The aggregates' sizes used in this test are presented in Table 3-3. Specific gravity was expressed as bulk specific gravity (G_{sb}), bulk specific gravity saturated surface dry ($G_{sb SSD}$), or apparent specific gravity (G_{sa}).

According to AASHTO T 85, aggregates smaller than #4 were excluded; however, if the coarse aggregates contained a substantial amount of materials finer than #4, it was recommended to use the materials retained up to #8. See Table 3-3 for more details about this test's used aggregate sizes. Table 3-5 shows the minimum aggregates' mass according to the Nominal Maximum Aggregate Size (NMAS).

Table 3-5 Minimum aggregates' weight used in specific gravity and absorption test.

NMAS (inch)	Minimum Mass of Test Sample (g)
1/2	2000
3/4	3000
1	4000
1 1/2	5000
2	8000
2 1/2	12000
3	18000

3.2.1.3 *Uncompacted Void Content of Fine Aggregate*

The Uncompacted Void Content (UVC) was conducted following ASTM C1252 – 17. See Section C.1.1 for more details. The test was used as an indirect measure of fine aggregate angularity. Test method A (#8 - #100), as discussed in the ASTM C1252 – 17, was used in Part-II testing; however, test method B (#6 - #8) and test method C (#6 - #16) were used in Part-I testing. For more details, see Table 3-3.

3.2.2 *Aggregate Durability Testing*

The aggregates used in the High Friction Surface Treatment (HFST) applications are exposed to outside weather, de-icing, and snowplowing, so the durability of the aggregates is important to be tested.

3.2.2.1 *Los Angeles Abrasion Test*

The test was conducted following ASTM C131/C131M – 20 [Part-I testing (grading D)] and AASHTO T 96 [Part-II testing (gradings B, C, or D were used)] to evaluate the quality, hardness, and durability of tested aggregates subjected to impact and abrasion. The test provided information about aggregate toughness and degradation characteristics because the aggregates were subjected to heavyweights during compaction and after construction under traffic. Gradings B, C, or D were used (see Table 3-3). The number of steel spheres (charges) and the number of revolutions were selected based on the selected grading according to the ASTM specification (note Table C-1 and Table C-2).

3.2.2.2 *The Soundness of Aggregate Using Sodium Sulfate*

The soundness of the aggregates using sodium sulfate was tested according to AASHTO T 104-99 (2011). Aggregates with a size (#4 - #6) were tested (note Table 3-3). The aggregate samples were put through 3 cycles of immersion and drying, then washed over #8 in running water for 30 minutes. The samples were then oven-dried at a temperature of 110 °C overnight and sieved over #8 for 15 minutes. Finally, the percentages of mass loss were calculated for aggregates.

3.2.2.3 *Water-Alcohol Freeze Thaw*

The water-alcohol freeze thaw resistance of the aggregates was tested following MoDOT standard 106.3.2.14 TM-14. The test aimed to evaluate the soundness of the aggregates. Aggregates with size (#6 - #8) were tested (see Table 3-3). The tested aggregate samples were put through 10 cycles of freezing and thawing, then they were oven-dried at a temperature of 110 °C. The samples were sieved over #8 for 15 minutes. To evaluate the aggregates' soundness, the percentages of mass losses were calculated.

3.2.2.4 *Acid Insoluble Residue*

The Aggregates were tested for their acid-insoluble residues. The test was run following ASTM D3042 – 17 on aggregates with (#6 - #8) size (see Table 3-3). The test estimated the percentages of insoluble residues in carbonate aggregates using a hydrochloric acid solution to investigate the carbonates' reactions. Calculating percentages of insoluble residues aimed to delineate the carbonate aggregates that polish excessively.

3.2.3 *Aggregate Performance Testing*

3.2.3.1 *Micro-Deval and Aggregate Image Measurement System*

The aggregates were tested for their degradation/polish resistances in the Micro-Deval (MD) apparatus. The MD test was utilized to explore aggregates' durability and resistance to polishing, abrasion, and grinding in the existence of water (Li et al. 2017; Wilson and Mukhopadhyay 2016; Kassem et al. 2013). Coarse aggregate and fine aggregate samples were tested. The coarse aggregate MD test was run following ASTM D6928 – 17 on aggregate size (3/8" - #4), as seen in Table 3-3. The test was run for 105

and 180 minutes. Each aggregate had one sample tested for each run time. After the samples were tested using the MD test (105- and 180-minutes abrasion times), samples of all of the aggregates, except Black Diabase and Quartzite, were tested in the Aggregate Image Measurement System (AIMS) along with aggregate samples before MD abrasion. Two sizes [(3/8" – 1/4") & (1/4" - #4)] for each aggregate were explored using AIMS. For more details, see Table 3-3. The AIMS analysis was conducted to explore the changing occurred to the Texture (TX) indices and Gradient Angularity (GA) indices after Micro-Deval (MD) polishing. The GA indices were identified by the irregularity of a particle’s surface using black and white images, and the surface TX indices were determined by analysis of grayscale images using the wavelet analysis method (Kassem et al. 2013)

The fine aggregate MD test was run following ASTM D7428 – 15. It was run on the Calcined Bauxite (CB) gradation (#6 - #16) for all nine aggregates for 5-, 15-, and 30-minutes run times. For each run time, two samples were tested, and the percentages of mass losses were calculated. The fine aggregate MD test was also run on the (#4 - #12) gradation for four aggregates (note Table 3-3). The run time for these samples was 15 minutes. The CB was also run for 15 minutes on the (1/4" - #10) gradation, and it had 2 samples tested. All of the weights for this test were reflected oven-dried aggregates.

3.2.3.2 Accelerated Friction Testing

I Preparing High Friction Surface Treatment Applications on Hot Mix Asphalt Slabs

Loose asphalt mixtures were acquired from an asphalt plant in Pullman, WA, U.S.A. They were dense-graded asphalt mixture with a 12.5-mm Nominal Maximum Aggregate Size (NMAS). The plant mixtures were reheated, and the Hot Mix Asphalt (HMA) slabs (20 in × 20 in × 2 in) were prepared and compacted in the laboratory using a small plate compactor. The HMA slabs were prepared as discussed in Section C.3.1.1.

Two-component (A and B) epoxy binder was applied to the surface of the HMA slabs before the aggregates—with a size (#6 - #8) (see Table 3-3)—were spread. The ratio of component A to component B of the epoxy was 1:18 to 1.00 by weight per the instructions from the supplier. The steps used to install High Friction Surface Treatment (HFST) applications on the HMA slabs were discussed in Section C.3.2.

II Sand Patch Test (Measuring Pavement Macrotexture Using a Volumetric Technique)

The Mean Texture Depth (MTD) of the prepared test slabs was measured using the sand patch test following ASTM E965 – 15. The average MTD was calculated for each surface using Equation 3.1. The results were based on the average of two replicates (two test slabs). The test procedures were explained in Section C.3.3.

$$MTD = 4V/(\pi D^2) \tag{Equation 3.1}$$

where,

MTD is mean texture depth (mm),
V is the sand volume (mm³), and
D is the average diameter of the sand patch circle (mm).

III Dynamic Friction Test

A Three-Wheel Polishing Device (TWPD) was used to polish the test slabs [see Figure C-2a and Figure C-2b]. The TWPD had three pneumatic rubber wheels attached to a turntable, and it had a water spray system to simulate wet conditions, thus reducing the wear of the rubber wheels and washing away the fines at the surface allowing more polishing. The total weight on the wheel including the metal plates

(total of six plates) and wheel cluster was 149 lb. The researchers measured the Coefficient of Friction (COF) at different polishing cycle numbers [i.e., 0 cycles (initial), 70k cycles, and 140k cycles (terminal)]. The COF was measured using a Dynamic Friction Tester (DFT)—note Figure C-2c and Figure C-2d—at different speeds (20, 40, and 60 km/hr) following ASTM E1911 - 19. This device consisted of a circular disk with three rubber pads attached to the disk. The circular disk rotated up to 100 km/hr. Once the disk reached the specified speed, the disk was lowered to the pavement surface, and the COF was measured as the speed of the rotating disk when it gradually decreased. The friction was measured in wet conditions. The results were based on the average of two replicates (two test slabs).

3.2.3.3 Measuring Aggregate Coupons' Surface Friction Using the British Pendulum Tester

I Preparing Aggregate Coupons

The aggregate coupons were prepared as discussed in Appendix C (Section C.3.2.1). See the prepared aggregate coupons in Figure C-6. The used aggregates had sizes of (#6 - #8) and (#4 - #6); see Table 3-3. The coupons made were tested for their initial British Pendulum Number (BPN), run through the polishing process in the British wheel for 10 hours, and then tested for their BPN after 10-hours polishing time.

II British Pendulum Test

This test was run following AASHTO T 278-90 (2017). The test aimed to measure the surfaces' frictional properties using the British Pendulum (BP). The tester presented in Figure C-7 was prepared according to the AASHTO specification with zero adjustments (Section 7.2) and slide length adjustments (Section 7.3). A slider with 1/4- × 1- × 1 1/4-inch dimension was used. Each coupon was tested a minimum of 5 times. The BPN values were recorded on the F-scale (see Figure C-7) as pre-polish BPN values. Then, the aggregates on the coupons were polished using the British wheel, and the BPN values were recorded using the BP device after polishing (post-polish BPN values).

III Accelerated Polishing of Aggregates Using the British Wheel

The aggregates on the coupons were polished—after they were tested in the BP—following AASHTO T 279-18 using the British wheel (see Figure C-8a). The test simulated the polishing action that occurs to aggregates in the field. For each run, 14 aggregate coupons were clamped around the periphery of the road wheel (see Figure C-8b). The speed of the road wheel was set to 320 ± 5 rpm, and the pneumatic-tired wheel was lowered to bear on the surface of the aggregate coupons with a total load of 391.44 ± 4.45 N. The aggregates were subjected to polishing action for 10 hours with the presence of water and polishing agent (#150 silicon carbide grit).

3.3 Physical Properties, Durability, and Performance Testing Comparative Studies

The physical properties, durability, and performance testing results of aggregates were compared. The relationships between MD mass losses and AIMS TX or GA indices were explored, and the relationships between MD polishing times and AIMS TX or GA indices were confirmed. The percentages of mass losses through Los Angeles Abrasion (LAA) and MD testing were compared for the aggregates. The relationships between the UVC percentages for the aggregates and the MD polishing time, AIMS GA indices, or MTD values were investigated. The AIMS TX and GA indices were compared to the BPN values, and the AIMS TX or GA indices were compared to the COF values measured by the DFT. Additionally, the BPN values were compared to the COF values measured by the DFT.

3.4 Economic Study

Life Cycle Cost Analysis (LCCA) was performed on High Friction Surface Treatment (HFST) alternatives. The researchers developed a LCC simple program using Excel for this purpose. The main

input data for this program were material and project specifics. The material specifics included Aggregate Image Measurement System (AIMS) Texture (TX) indices and Gradient Angularity (GA) indices, DFT results, or BPN values. Other inputs were involved in the material specifics (e.g., costs). These inputs included costs for aggregates and epoxy binder (materials and shipping costs). The project specifics were Average Annual Daily Traffic (AADT), percentages of trucks (%T), highway classification, lane width, length of HFST application, recommended terminal Skid Number (SN) value, interest rate, and inflation rate. The input data were converted to predicted SN values using prediction models. The rehabilitation matrix was set to finalize the rehabilitation decision of the HFST applications based on the predicted terminal and recommended terminal SN values. Finally, the Net Present Values (NPVs) were estimated of HFST applications. Based on the NPVs, the best HFST application was selected. The major purpose of this LCC program was to present a rational method for converting different input data (material and project specifics) into comparable output data (NPV) that facilitated comparison between different alternatives.

CHAPTER 4: AGGREGATE PHYSICAL PROPERTIES AND DURABILITY TESTING

4.1 Introduction

This chapter was focused on the physical properties and durability testing of aggregates. These tests were run to classify the aggregates and identify the routine tests that investigate the performance of the proposed aggregates as High Friction Surface Treatment (HFST) materials. Therefore, physical properties [e.g., aggregate gradation, specific gravity and absorption, and Uncompacted Void Content (UVC)] and durability tests [e.g., Los Angeles Abrasion (LAA), sodium sulfate soundness, water-alcohol freeze thaw, and acid-insoluble residue] were conducted in Part-I testing. Part-II testing included physical properties testing and durability testing (LAA) following standards with different sizes. Comparisons between aggregates were achieved through analyzing the physical properties and durability testing results.

4.2 Part-I Testing

In this section, the results of the physical properties testing, and durability testing conducted in Part-I testing were discussed.

4.2.1 Physical Properties Testing Results

The investigated aggregates in this study were comprehensively defined in Chapter 3 (see Table 3-3). These aggregates included Calcined Bauxite (CB) and eight alternative high friction aggregates. The following tests were conducted to evaluate and differentiate between the proposed aggregates.

4.2.1.1 Aggregate Gradation

The proposed aggregates were sieved as delivered from their respective sources into different sizes (i.e., #6 - #16, note Table 3-3) and then remixed in controlled manners to prepare specimens for the other physical, durability, and performance tests. The combination of aggregate sizes was made based on available gradations from the manufacturer. An average of two replicated samples was computed and plotted in Figure 4-1. The main purpose of the gradation test was to check if the aggregates matched the current MoDOT requirements for HFST (NJSP-15-13B).

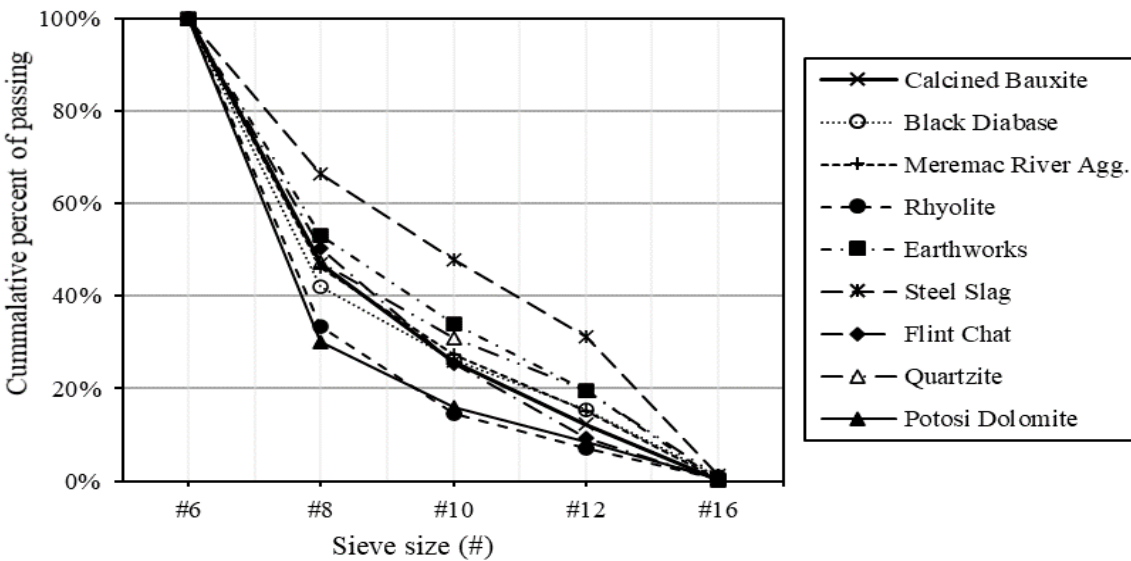


Figure 4-1 Particles' size distribution, Part-I.

4.2.1.2 Specific Gravity and Absorption

The specific gravity of the investigated aggregates was tested on aggregates with (#6 - #16) size, as mentioned in Table 3-3. The specific gravity values were the highest for Calcined Bauxite (CB). Therefore, the researchers thought that specific gravity was a good filter for the investigated aggregates. Steel Slag had the highest specific gravity values among the alternative aggregates. Moreover, the values of the specific gravities and water absorption percentages of the investigated materials are demonstrated in Table 4-1. Slight slumping of a molded fine aggregate indicated that it had reached a surface dry condition.

Table 4-1 The absorption and specific gravity results.

Aggregate Type	G_{sb}^a	$G_{sb\ SSD}^b$	Absorption (%)
Calcined Bauxite (CB)	3.271	3.354	0.187
Black Diabase	2.912	2.934	0.168
Meramec River Agg.	2.414	2.502	0.197
Potosi Dolomite	2.658	2.706	0.180
Rhyolite	2.544	2.573	0.167
Steel Slag	2.944	3.056	0.206
Earthworks	2.452	2.495	0.179
Flint Chat	2.522	2.569	0.179
Quartzite	2.598	2.569	0.170

^a G_{sb} : Bulk specific gravity.

^b $G_{sb\ SSD}$: Bulk specific gravity saturated surface dry.

4.2.1.3 Uncompacted Void Content

The Uncompacted Void Content (UVC) of fine aggregates was used as an indirect measure of the fine aggregates' angularities. The UVC percentages were calculated for the aggregates (mentioned in Table 3-3) using the as-received grading [CB gradation: (#6 - #16)] and the individual fraction size (#6 - #8), see Table 3-3. The test was conducted on two different gradations to assess the impacts of aggregates' gradations on the uncompacted void percentages. Figure 4-2 shows the UVC percentages. No meaningful difference was observed among the UVC percentages for #6 - #8 size and those observed for CB gradation (#6 - #16 size). For the two sizes, #6 - #8 and #6 - #16 sizes, CB had the lowest UVC difference percentage (0%) and Steel Slag had the highest UVC difference percentage (1.68%). Flint Chat had the highest uncompacted void percentages ($\approx 48\%$), followed by Black Diabase ($\approx 45.8\%$), Potosi Dolomite ($\approx 45.4\%$), and Steel Slag ($\approx 44.7\%$). Flint Chat yielded the highest UVC percentages, which agreed with the Mean Texture Depth (MTD) results discussed in Chapter 5. Flint Chat had the highest MTD. Meramec River Aggregate had the lowest UVC percentages. The relationships between the UVC percentages and MTD or GA indices were discussed in Chapter 6.

4.2.2 Durability Testing Results

The High Friction Surface Treatment (HFST) aggregates experience direct exposure to outside weather, like repetitive cycles of being wet and dry, de-icing, and snowplowing. Therefore, investigating the durability of the aggregates is essential. The test specimens were prepared and mixed with different gradations based on the tests' specifications.

4.2.2.1 Los Angeles Abrasion

The aggregate samples were tested for their degradation resistances using the Los Angeles machine with grading D (see Table 3-3). The LAA percentages represented the quality of various aggregates. Figure 4-3 presents the results of the Los Angeles test. Potosi Dolomite had the highest LAA (33.27%), followed by

Black Diabase (23.26%) and then Rhyolite (17.87%). By contrast, Meramec River Aggregate had the lowest Los Angeles Abrasion (LAA) (14.06%). The LAA percentages for Potosi Dolomite and Black Diabase exceeded the acceptable level (20%). Meramec River Aggregate and Steel Slag sources are the best types to replace the Calcined Bauxite (CB), based on the LAA percentages.

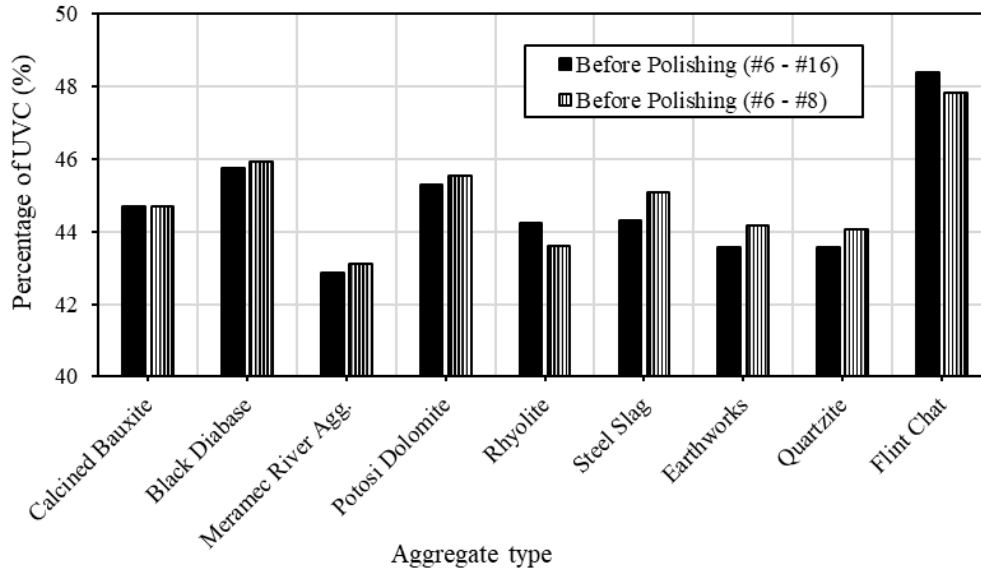


Figure 4-2 Percentages of UVC using two aggregates' sizes.

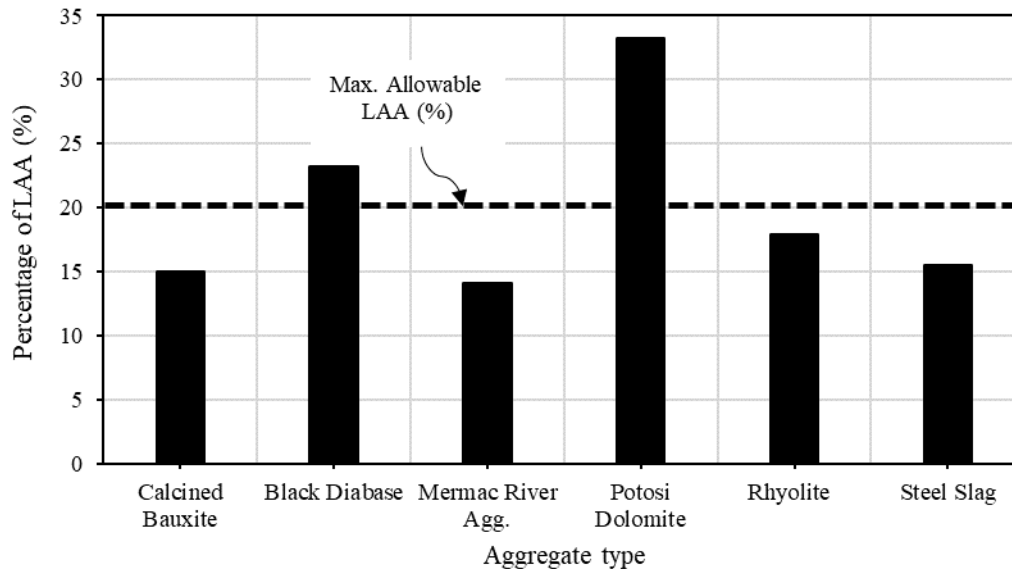


Figure 4-3 Percentages of LAA.

4.2.2.2 Sodium Sulfate Soundness

The sodium sulfate soundness test was conducted to evaluate the aggregates' resistances to disintegration through repeated immersion in sodium sulfate solutions, followed by oven drying. The tests were conducted on (#4 - #6) sized aggregates, as mentioned in Table 3-3. Two replicates' results were demonstrated in Table 4-2. Calcined Bauxite had the lowest percentage lost, followed by Meramec River Aggregate, Rhyolite, and then Steel Slag. The highest percentage lost was noted for Potosi Dolomite.

Table 4-2 Sodium sulfate soundness test results.

Aggregate Type	Initial Weight (g)	Final Weight (g)	% Loss
Calcined Bauxite (CB)	200.1	199.6	0.25
	200.4	200.3	0.05
Meramec River Agg.	200.2	199.5	0.35
	200.2	199.7	0.25
Steel Slag	200.0	196	2.00
Potosi Dolomite	200.1	198.7	0.70
	200.0	190.9	4.55
Rhyolite	200.0	197.2	1.40

4.2.2.3 Water-Alcohol Freeze Thaw

The water-alcohol freeze thaw resistances of the aggregates were tested on (#6 - #8) size, as explained in Table 3-3. The tests were conducted to assess the soundness of coarse aggregates. The results shown in Figure 4-4 demonstrated that CB had the highest percentage of loss (7.24%), followed by Meramec River Aggregate (6.7%). Contrarily, Earthworks had the lowest percentage of loss (2.56%). All aggregates had percentages of losses lower than Calcined Bauxite (CB).

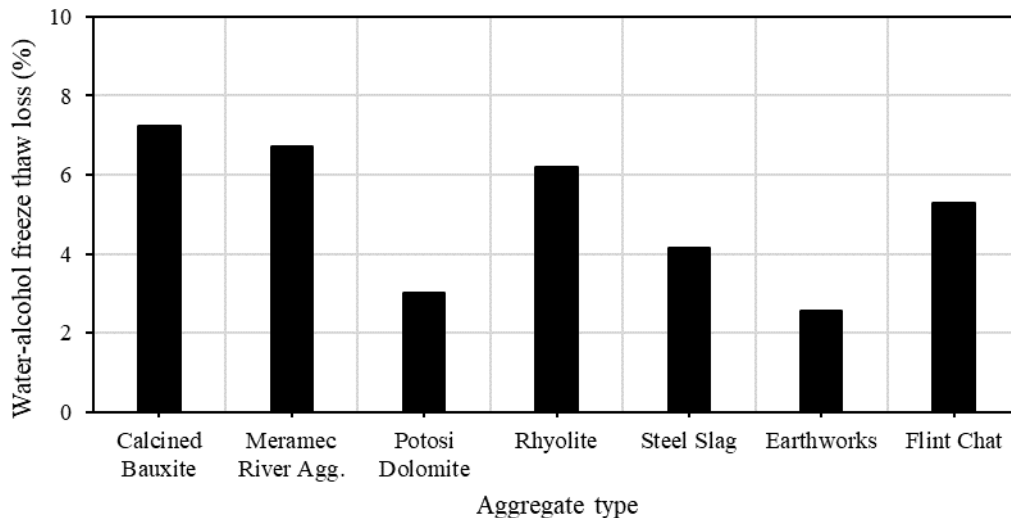


Figure 4-4 Water-alcohol freeze thaw test results.

4.2.2.4 Acid Insoluble Residue

Calcined Bauxite and alternative aggregates were tested for their acid-insoluble residues. The tests were run on the aggregates with (#6 - #8) size. The percentages of noncarbonate (insoluble) residue in carbonate aggregates were determined to identify the polishing susceptibility of the proposed aggregates using a hydrochloric acid solution to cause carbonates reactions. The percentages of insoluble residue are displayed in Figure 4-5. Potosi Dolomite had the lowest residue percentage, followed by Steel Slag. These percentages were under the acceptable level (80%). Quartzite had the highest residue percentage, followed by CB and then Rhyolite. The other aggregates were above the acceptable level but lower than Quartzite, CB, and Rhyolite.

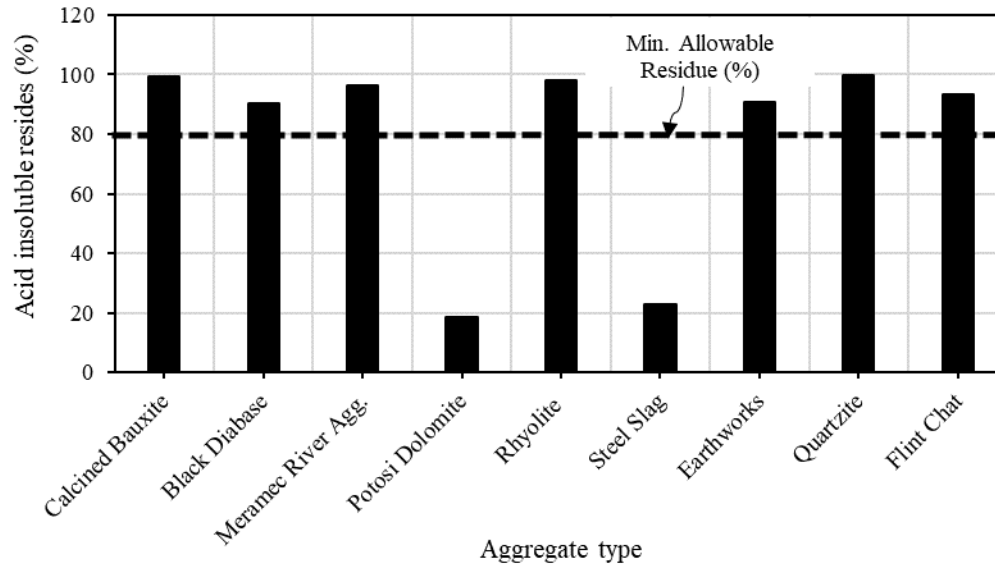


Figure 4-5 Acid insoluble residue percentages.

4.3 Part-II Testing

In this section, the results of the physical properties testing and durability testing [Los Angeles Abrasion (LAA)] conducted in Part-II testing were discussed. Different aggregates' sizes were used when compared to the aggregates' testing conducted in Part-I, note Table 3-3.

4.3.1 Aggregate Gradation

Table 4-3 summarizes the aggregate gradation for the received aggregates (as-delivered gradation). The aggregates where more than 50% of the materials retained on #4 are presented in bold font, while the aggregates where more than 50% of the materials passed #4 are indicated with an italic font.

4.3.2 Specific Gravity and Absorption

Table 4-3 summarizes the specific gravity and absorption results for the aggregates. Four aggregates were not tested as they did not have the proper gradations (i.e., fine aggregates). The results showed that three of Meramec River Aggregates had an absorption greater than 2% (5/16" crushed gravel of 3.0%, torpedo gravel of 2.8%, and C. gravel of 2.2%). One of the aggregates [3/8" × #3 Calcined Bauxite (CB)] had an absorption of 2.5% which is the highest in the group of CB aggregates. Additionally, the aggregates showed an absorption of 1.6% for Steel Slag, 1.4% for GRIP grain CB, 0.7% for #3 × 0 CB, 1.7% for #6 × #16 Rhyolite, and 1.9% for Earthworks. Aggregates in the Black Diabase group had the lowest absorption. Aggregate 1" Black Diabase had the lowest absorption of 0.4%, while 3/8" Black Diabase had 0.7% absorption, and 1/4" Black Diabase had 0.8% absorption. Quartzite had an absorption of 1.2%. Regarding the bulk specific gravity of the test aggregates, three aggregates had G_{sb} greater than 3.0 (GRIP grain CB had G_{sb} of 3.28, 3/8" × #3 CB had G_{sb} of 3.22, Steel Slag had G_{sb} of 3.17). By contrast, three of the aggregates showed a lower G_{sb} (#3 × 0 CB had G_{sb} of 2.74, #6 × #16 Rhyolite had G_{sb} of 2.52, and Earthworks had G_{sb} of 2.42). For Meramec River Aggregates, 5/16" crushed gravel had G_{sb} of 2.44 and 2.4 for torpedo gravel. For Black Diabase aggregates, two aggregates had the same G_{sb} of 2.9 (i.e., 1/4" and 3/8"), while the 1" Black Diabase had a G_{sb} of 2.96. Quartzite aggregate had G_{sb} of 2.60.

4.3.3 Uncompacted Void Content

Table 4-3 shows the Uncompacted Void Content (UVC) percentages of five aggregates. For more information about the aggregates' sizes used in this test, see Table 3-3. Steel Slag had the highest UVC

percentage (49%), followed by Rhyolite (47%), and Black Diabase (46%). Calcined Bauxite had the lowest UVC percentage of 35%. High Friction Surface Treatment (HFST) application using Steel Slag aggregates had higher Mean Texture Depth (MTD) (2.64 mm) when compared to HFST application with Calcined Bauxite (CB) aggregate that showed MTD of 2.19 mm, as discussed later in Chapter 5. These results demonstrated that higher UVC percentages resulted in higher MTD at the same aggregate gradation.

4.3.4 Los Angeles Abrasion

Table 4-3 presents the Los Angeles Abrasion (LAA) percentages for the aggregates. Thirteen aggregates were tested following grading D as presented in Table 3-3. Meanwhile and based on the aggregate gradations, two aggregates followed grading B, and one aggregate followed grading C (see Table 3-3). The results obtained for the aggregates followed grading D showed that two of the aggregates demonstrated higher abrasion resistance: GRIP grain CB had 13% LAA percentage, and #3 × 0 CB had 14% LAA percentage. By contrast, the other two aggregates of the same group had higher LAA (i.e., #6 × #16 Rhyolite had a LAA percentage of 22%, Earthworks had 20% LAA percentage, and Steel Slag aggregate had a LAA percentage of 17%). The Meramec River Aggregate group had similar results. The Meramec river coarse manufactured sand had a LAA percentage of 18%, and the 5/16" crushed gravel and torpedo gravel aggregates had LAA percentages of 17%. Furthermore, the Black Diabase group had the highest LAA. Aggregate 3/8" Black Diabase had a LAA percentage of 23%, and aggregate 1/4" Black Diabase had a LAA percentage of 20%. The 1/2" Rhyolite aggregate had a LAA percentage of 22%. Flint Chat had a LAA percentage of 25%. Quartzite aggregate had a LAA percentage of 29%, which was the lowest resistance to abrasion. The LAA results for grading B showed Meramec River Aggregate (C. gravel) had a LAA percentage of 21%, and the 1" Black Diabase had a LAA percentage of 20%. The results of grading C exhibited the lowest LAA percentage (i.e., 10%); however, gradings B and C did not conform with the required HFST gradation.

4.4 Summary

This chapter presented the aggregates' physical properties and durability testing results. The UVC test [conducted in Part-I testing (#6 - #8) and (#6 - #16)] for nine aggregates with two sizes [(#6 - #8) and (#6 - #16)] showed that Flint Chat had the highest UVC percentages followed by Black Diabase, Potosi Dolomite, Steel Slag, and CB. Meramec River Aggregate had the lowest UVC percentages. No observable difference was noted between the UVC percentages for the two sizes. However, the UVC test [implemented in Part-II testing (#8 - #100)] for five aggregates with (#8 - #100) gradation exhibited that Steel Slag had the highest UVC percentage followed by Rhyolite, Black Diabase, Meramec River Aggregate. The lowest UVC percentage was noted for CB. Note that Flint Chat, Quartzite, and Potosi Dolomite were not tested because they had the highest LAA percentages, and these percentages exceeded the maximum allowable limit (20%). No relationship was observed between the aggregates' sizes and the UVC percentages: it is rational that using smaller aggregates' sizes caused a reduction in the UVC percentages, which was observed for CB. However, Steel Slag and Rhyolite showed an increase in the UVC percentages with decreasing the aggregate's size. Moreover, Meramec River Aggregate revealed no difference. The specific gravity test—conducted in Part-I (#6 - #16) and Part-II testing (- #4)—deemed that CB had the highest specific gravity values followed by Steel Slag. However, Earthworks and Meramec River Aggregate had the lowest specific gravity values.

Based on Part-I (grading D) testing results for the LAA test, Meramec River Aggregate had the lowest LAA percentage followed by CB, Steel Slag, Rhyolite, and then Black Diabase. However, Potosi Dolomite had the highest LAA percentage. Based on the LAA results [Part-II testing (gradings B, C, or D were used)], CB had the lowest LAA percentage followed by Steel Slag, Meramec River Aggregate, Earthworks, Black Diabase, Rhyolite, and Flint Chat. Quartzite had the highest LAA percentage. Based on the LAA results—conducted in Part-I for grading D and Part-II testing for gradings B, C, or D—CB,

Steel Slag, and Meramec River Aggregate showed the lowest LAA percentages. Black Diabase and Rhyolite had the highest percentages.

Meramec River Aggregate had the best sodium sulfate soundness results (lowest mass losses) among the alternative aggregates followed by Rhyolite and then Steel Slag. The highest percentage lost was noted for Potosi Dolomite.

All alternative aggregates had lower percentages of water-alcohol freeze thaw mass losses when compared to Calcined Bauxite (CB); the lowest percentage of mass loss was recorded for Earthworks and then for Potosi Dolomite. However, CB had the highest water-alcohol freeze thaw mass losses followed by Meramec River Aggregate.

Based on the acid-insoluble residue results, Quartzite, Rhyolite, Meramec River Aggregate, and Flint Chat had comparable residues percentages with CB (the percentages were greater than 93%). However, Potosi Dolomite had the lowest residue percentage followed by Steel Slag (the percentages were less than 25%). It was concluded that Meramec River Aggregate was the most favorable alternative to CB followed by Rhyolite and then Steel Slag, based on the physical properties and durability testing results.

Table 4-3 Part-II physical properties and LAA results.

Aggregate Testing	Measured Parameters	Calcined Bauxite (CB) 3/8" x #3	CB #3 x 0	CB GRIP Grain	Earthworks #6 x #16	Meramec River Agg. (MRC) C Gravel	MRC 5/16" Crushed Gravel	MRC Torpedo Gravel	MRC Coarse Man. Sand	Steel Slag 1" x 0	Rhyolite (Rh) 1/2" x 0	Rh #6 x #16	Black Diabase (BD) 1"	BD 3/8"	BD 1/4"	BD Sand	Quartzite 1" x 0	Flint Chat (FC) #6 x #16	FC Larger Particle Size	
Aggregate Gradation	% Retained	1"				0							0				0		0	
		3/4"				26					0		12				1		1	
		1/2"				43				0	2		48	0			21		64	
		3/8"	0	0	0		22	0	0	0	57	15	0	26	5	0		14		12
		#4	100	4	0	0	8	11	76	0	30	36	1	14	76	5	0	20	0	10
		#8	0	18	51	38		36	24	23	8	20	55		18	34	1	11	53	6
		#16	0	23	48	60		25		34	2	11	39		0	25	17	6	46	3
		#30	0	16	2	2		14		22	1	6	3		0	10	27		1	
		#50	0	10	0	0		8		12	0	3	1		0	8	23		0	
		#100	0	8	0	0		4		6	0	2	0		0	7	16		0	
#200	0	6	0	0		1		2	1	2	0		0	5	10		0			
	Pan	0	14	0	0	0	0	0	0	1	2	0	0	0	5	7	27	0	4	
Specific Gravity & Absorption	G _{sb}	3.22	2.74	3.28	2.42	2.44	2.44	2.40	NA	3.17	2.57	2.52	2.96	2.90	2.90	NA	2.60	NA	NA	
	G _{sb SSD}	3.30	2.76	3.32	2.47	2.49	2.51	2.47		3.22	2.60	2.56	2.97	2.90	2.93		2.63			
	G _{sa}	3.50	2.79	3.43	2.54	2.58	2.63	2.57		3.34	2.64	2.63	2.99	3.00	2.98		2.68			
	% Absorption	2.5	0.7	1.4	1.9	2.2	3.0	2.8		1.6	1.0	1.7	0.4	0.7	0.8		1.2			
Uncompacted Void Content (UVC)	UVC Percentage (%)		35				43			49	47				46					
Los Angeles Abrasion (LAA)	LAA Percentage (%)	10	14	13	20	21	17	17	18	17	22	22	20	23	20		29	25		

CHAPTER 5: AGGREGATE PERFORMANCE TESTING

5.1 Introduction

This chapter discussed the aggregate performance testing results. The tests were conducted to compare the performance of Calcined Bauxite (CB) with alternative aggregates. The performance testing included Micro-Deval (MD), Aggregate Image Measurement System (AIMS), accelerated friction testing (sand patch test and dynamic friction test), British Pendulum (BP) test. Different aggregate sizes for each aggregate type were used in the MD, AIMS, and BP to explore the effect of the aggregate size on the aggregates' performance.

5.2 Micro-Deval Results

In this section, the MD results were discussed for coarse and fine aggregates. The MD results were indicators of the best alternative aggregates rather than CB by analyzing the mass losses after different polishing times. The polishing times were 105 and 180 minutes for the coarse aggregates. Contrarily, the polishing times for the fine aggregates were 5, 15, and 30 minutes. The following subsections explained the MD results.

5.2.1 Coarse Aggregate

The MD test was run for the coarse aggregates with (3/8" - #4) gradation (note Table 3-3). The samples were prepared according to the ASTM D6928 – 17 (Section 8.4). A total sample weight of 1500g was prepared by combining two portions. The first portion's weight was 750g that had (3/8" - 1/4") gradation. The second portion's weight was 750g that had (1/4" - #4) gradation. The percentages of masses lost After 105- and 180-minutes of Micro-Deval polishing times (AMD 105 and AMD 180) are presented in Figure 5-1. The highest percentages of mass loss were recorded for Potosi Dolomite. Black Diabase presented the highest percentages of mass loss after Potosi Dolomite. Contrarily, the lowest percentages of mass loss were noted for Meramec River Aggregate. Calcined Bauxite, Quartzite, and Steel Slag had approximately the same percentages of mass losses regarding AMD 105 and AMD 180. Rhyolite and Earthworks showed the same percentages of mass losses for AMD 105 and AMD 180, and they had lower percentages of mass losses than CB, Quartzite, and Steel Slag. Flint Chat aggregate showed a lower percentage of mass loss for AMD 105 than Earthworks, Rhyolite, and Steel Slag. However, for AMD 180, Flint Chat reflected a higher percentage of mass loss than Rhyolite and Earthworks.

According to the MD mass losses regarding 105 minutes, Meramec River Aggregate had the lowest mass loss's percentage followed by Flint Chat, Earthworks, Rhyolite, CB, Quartzite, Steel Slag, and Black Diabase. The highest percentage of mass loss was for Potosi Dolomite. Based on the MD mass losses after 180 minutes, Meramec River Aggregate had the lowest mass loss's percentage followed by Earthworks, Rhyolite, Flint Chat, CB, Quartzite, Steel Slag, and Black Diabase. The highest percentage of mass loss was for Potosi Dolomite.

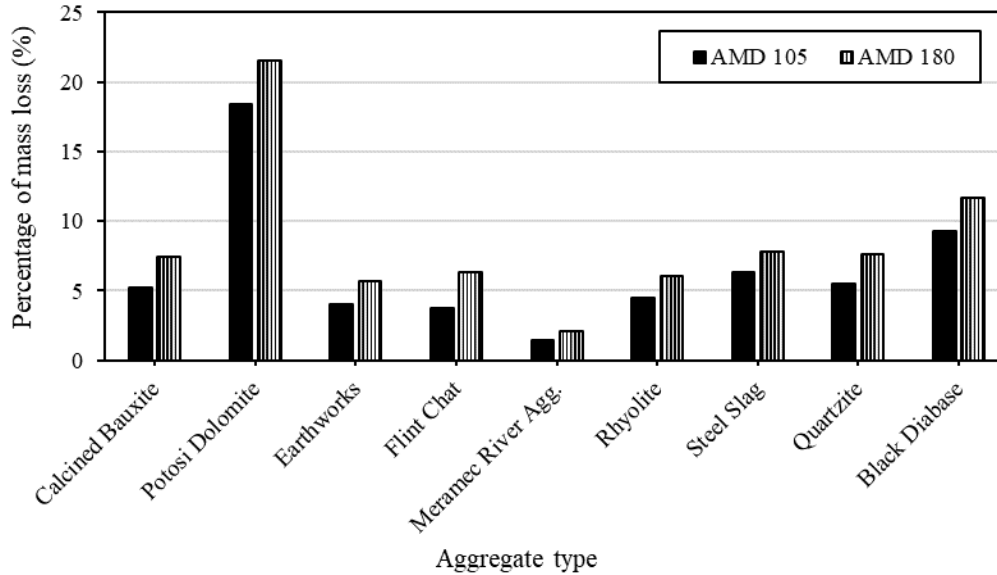


Figure 5-1 Micro-Deval mass losses' percentages with (3/8" - #4) gradation.

5.2.2 Fine Aggregate

The Micro-Deval (MD) test was run for the fine aggregates according to the ASTM D7428 – 15 with a sample weight of 500g. The test was implemented on the aggregates with (#6 - #16) gradation, as indicated in Table 3-3. Figure 5-2a shows the percentages of mass losses for aggregates with (#6 - #16) gradation; the mass losses were calculated for #6 - #16. The MD polishing times were 5, 15, and 30 minutes. Increasing the MD polishing time from 5 to 30 minutes increased the mass loss percentages, as indicated in Figure 5-2a. Calcined Bauxite had the lowest mass loss percentage for After 30-minutes of Micro-Deval polishing time (AMD 30) followed by Meramec River Aggregate, Earthworks, Rhyolite, Steel Slag, Flint Chat, Quartzite, and Black Diabase. However, Potosi Dolomite showed the highest mass loss percentage for AMD 30. Meramec River Aggregate had the same mass loss percentage as the Black Diabase and Quartzite for After 5-minutes of Micro-Deval polishing time (AMD 5); however, Meramec River Aggregate had less than the half the percentage of mass loss in reference to Quartzite and Black Diabase for AMD 30. Figure 5-2b depicts the percentages of mass losses for aggregates with (#6 - #16) gradation; the mass losses were estimated for #6 - #8. Increasing the MD polishing time from 5 to 30 minutes increased the mass loss percentages, as displayed in Figure 5-2b. The mass losses calculated for #6 - #8 were higher than the mass losses calculated for #6 - #16. This indicated that the larger aggregates' sizes had higher mass losses than the smaller aggregates' sizes. Meramec River Aggregate had the lowest mass loss percentage for AMD 30 followed by Calcined Bauxite (CB), Earthworks, Steel Slag, Black Diabase, Rhyolite, Flint Chat, and Quartzite. However, Potosi Dolomite showed the highest mass loss percentage for AMD 30. Meramec River Aggregate had the same mass loss percentage as the Black Diabase for AMD 5; however, Meramec River Aggregate had less than the half the percentage of mass loss in reference to Black Diabase for AMD 30.

Calcined Bauxite and three alternatives were run with the (#4 - #12) gradation (note Table 3-3 and Table 3-4) for After 15-minutes of Micro-Deval polishing time (AMD 15), and the CB was tested with another gradation (1/4" - #10). Table 5-1 shows the results of the percentage of mass loss. For (#4 - #12) gradation, the highest percentage of mass loss was noted for Potosi Dolomite followed by Steel Slag and then CB. The lowest percentage of mass loss was recorded for Meramec rive aggregate.

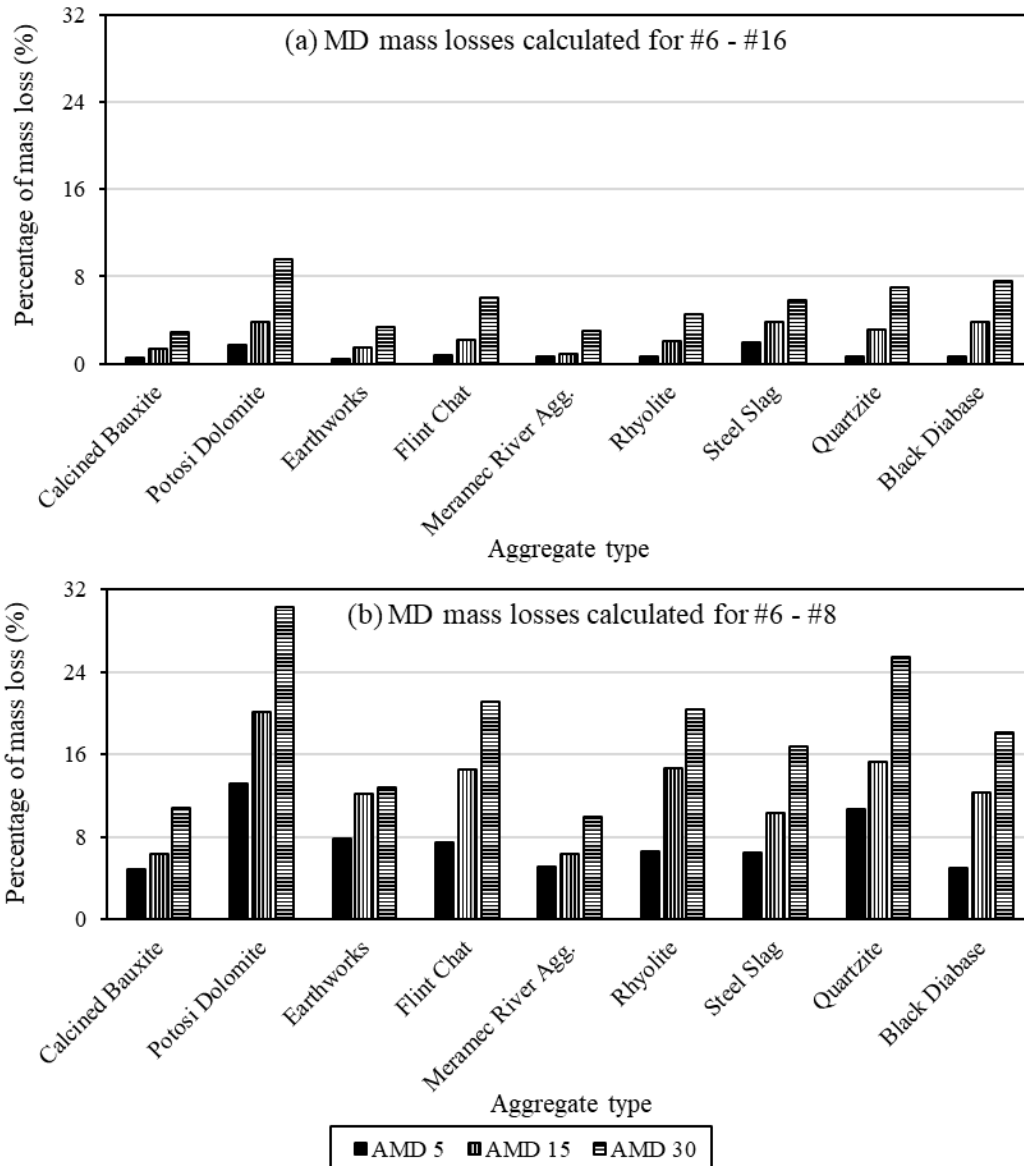


Figure 5-2 Micro-Deval mass losses' percentages with (#6 - #16) gradation.

Table 5-1 Micro-Deval mass losses' percentages with two gradations.

Aggregate Type	Percentage of Mass Loss AMD 15 for (#4 - #12) Gradation (%)	Percentage of Mass Loss AMD 15 for (1/4" - #10) Gradation (%)
Calcined Bauxite (CB)	1.80	1.32
Meramec River Agg.	0.74	
Steel Slag	2.26	
Potosi Dolomite	2.28	

5.3 Aggregate Image Measurement System

In this section, the Aggregate Image Measurement System (AIMS) Texture (TX) and Gradient Angularity (GA) indices—Before Micro-Deval polishing (BMD), After 105-minutes of Micro-Deval polishing time

(AMD 105), After 180-minutes of Micro-Deval polishing time (AMD 180)—were compared for aggregates. Two aggregate sizes were evaluated: (3/8" - 1/4") and (1/4" - #4) sizes (note Table 3-3).

5.3.1 Effect of Aggregate Size on Texture and Angularity Indices

Figure 5-3 shows the AIMS TX and GA indices for aggregates with two sizes (3/8" - 1/4" and 1/4" - #4) for BMD, AMD105, and AMD180. Decreasing the aggregates' sizes from (3/8" - 1/4") to (1/4" - #4) decreased the TX and GA indices for BMD, AMD 105, and AMD 180. However, Steel Slag yielded an increase in TX indices for BMD when the aggregate's size changed from (3/8" - 1/4") to (1/4" - #4). Moreover, Potosi Dolomite, Earthworks, and Flint Chat showed increases in GA indices regarding BMD with the decrease of the aggregates' sizes from (3/8" - 1/4") to (1/4" - #4). Calcined Bauxite had an increase in the GA indices for AMD 105 and AMD 180 when the aggregate's size was decreased.

Figure 5-4 demonstrates the percentages of increase or decrease in the AIMS TX and GA indices for aggregates regarding AMD 105 and AMD 180. Figure 5-4a displays that when using AMD, the TX indices decreased for 4 aggregate types. However, the TX indices increased using AMD 105 for Calcined Bauxite (CB), (1/4" - #4) size Flint Chat, and (1/4" - #4) size Steel Slag. Furthermore, the Meramec River Aggregate and (3/8" - 1/4") size Steel Slag TX indices increased for AMD 105 and AMD 180. Figure 5-4b shows that with AMD, the GA indices decreased for 4 types of aggregates. By contrast, the GA indices increased using AMD 105 for the (1/4" - #4) size Meramec River Aggregate and (3/8" - 1/4") size Steel Slag. Additionally, the GA indices increased regarding AMD 105 and AMD 180 for the (3/8" - 1/4") size Flint Chat. The aggregates' TX and GA indices increased after MD polishing time probably due to one of the reasons explained as follows (E. Mahmoud and Masad 2007; Masad et al. 2009; E. Mahmoud and Ortiz 2014):

- 1- Breaking of particles, instead of polishing, that exposed their internal surface TXs,
- 2- The aggregates had strong granular structures and were hard to polish,
- 3- Micro-Deval polishing exposed more textured surfaces that were previously covered by smoother surfaces,
- 4- Micro-Deval polishing did not have the expected effect on the aggregates with low TXs, and
- 5- Some aggregates (e.g., sandstone) had mineralogies that exposed new textured surfaces with Micro-Deval (MD) polishing.

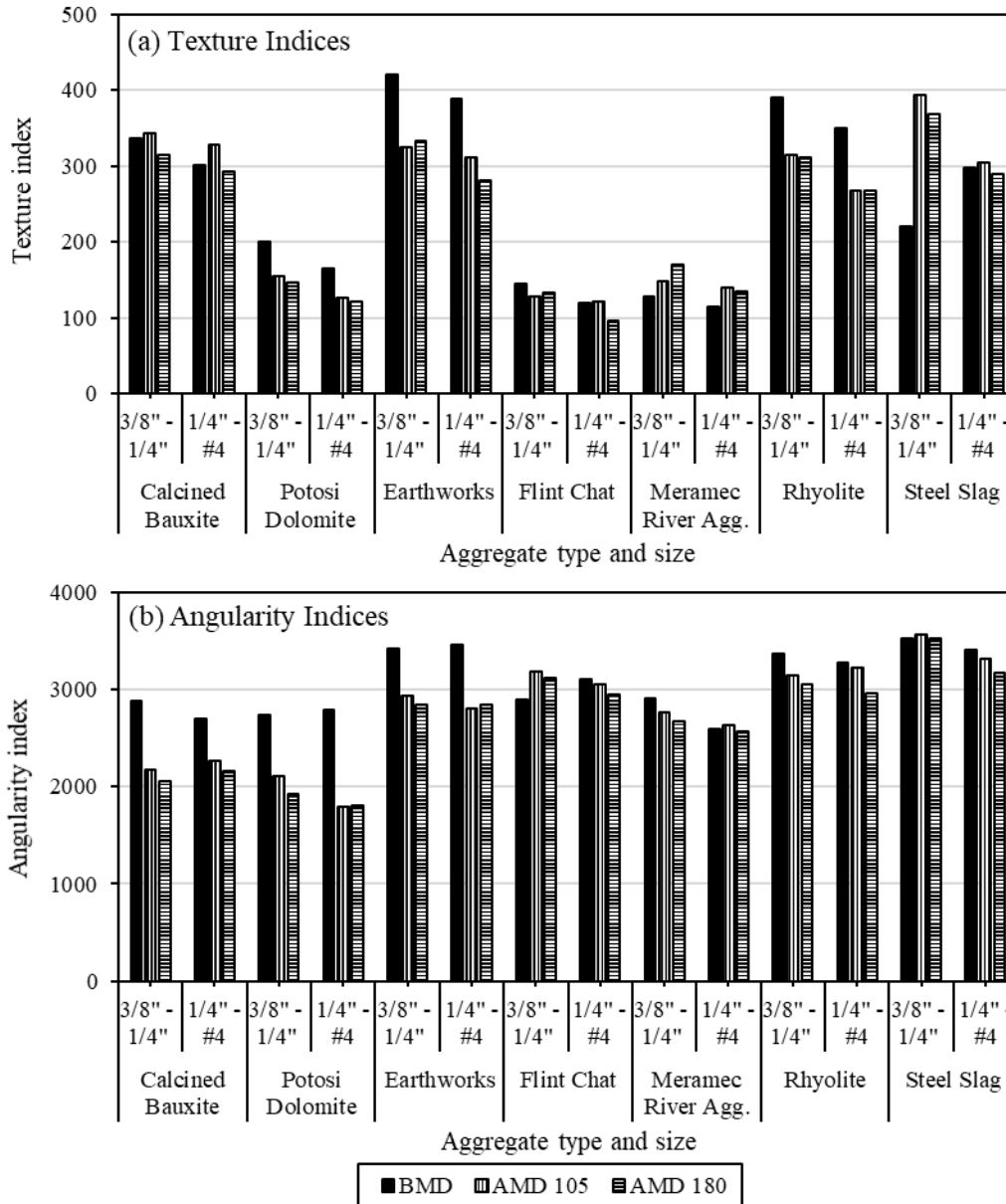


Figure 5-3 Texture and angularity indices.

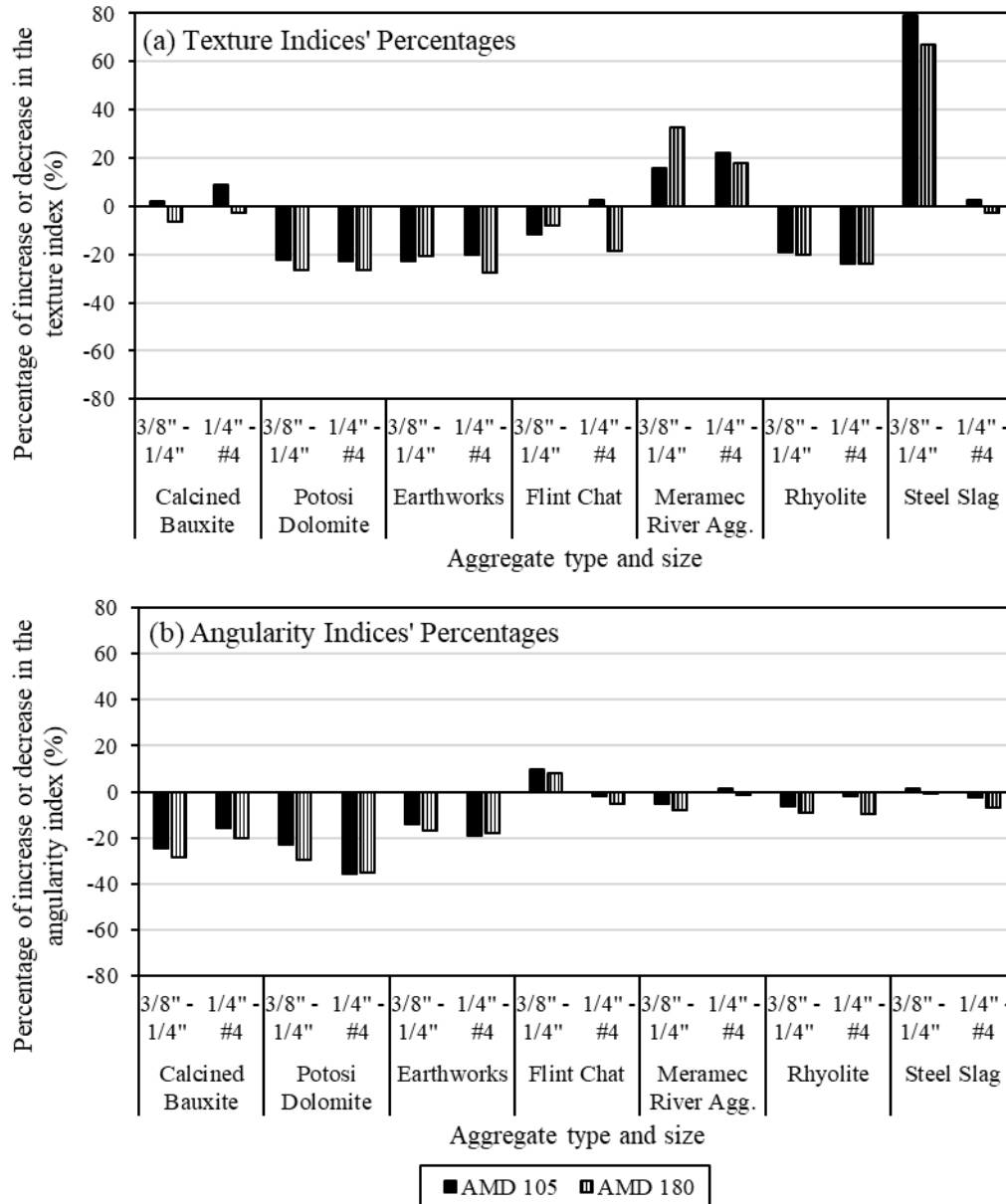


Figure 5-4 Percentages of increase or decrease in the texture and angularity indices.

5.3.2 Analysis of Average Texture and Angularity Indices

The Aggregate Image Measurement System (AIMS) indices were averaged for two aggregate sizes [(3/8" - 1/4") and (1/4" - #4)]. Average Texture (TX) and average Gradient Angularity (GA) indices for Before Micro-Deval polishing (BMD), After 105-minutes of Micro-Deval polishing time (AMD 105), and After 180-minutes of Micro-Deval polishing time (AMD 180) are illustrated in Figure 5-5. Earthworks had the highest average TX and average GA indices during BMD polishing, and Meramec River Aggregate presented the lowest average TX and average GA indices during BMD polishing. Steel Slag showed the highest average TX and average GA indices amid AMD 105 and AMD 180. Flint Chat had the lowest average TX indices for AMD 105 and AMD 180, and Potosi Dolomite showed the lowest average GA indices for AMD 105 and AMD 180. Average TX indices increased using AMD 105 for Meramec River Aggregate, and this increase continued when AMD 180 was used. This happened because the Micro-Deval (MD) polishing exposed a more textured surface that was previously covered by a smoother

surface, or the aggregates had mineralogies that exposed new textured surfaces with Micro-Deval (MD) polishing. For Calcined Bauxite (CB) and Steel Slag aggregates, average Texture (TX) indices increased with AMD 105 and decreased with AMD 180. This occurred due to the breaking of particles, instead of polishing, that exposed their internal surface TXs during AMD 105. However, for AMD 180, the polishing process took place on the old and the new exposed internal surface TXs. For Potosi Dolomite, Earthworks, Flint Chat, and Rhyolite, average TX indices decreased for AMD 105 and AMD 180 and reached the lowest values using AMD 180. Average GA indices decreased for all aggregates reaching the lowest value with AMD 180, except for Flint Chat aggregate that had steady values of average GA indices.

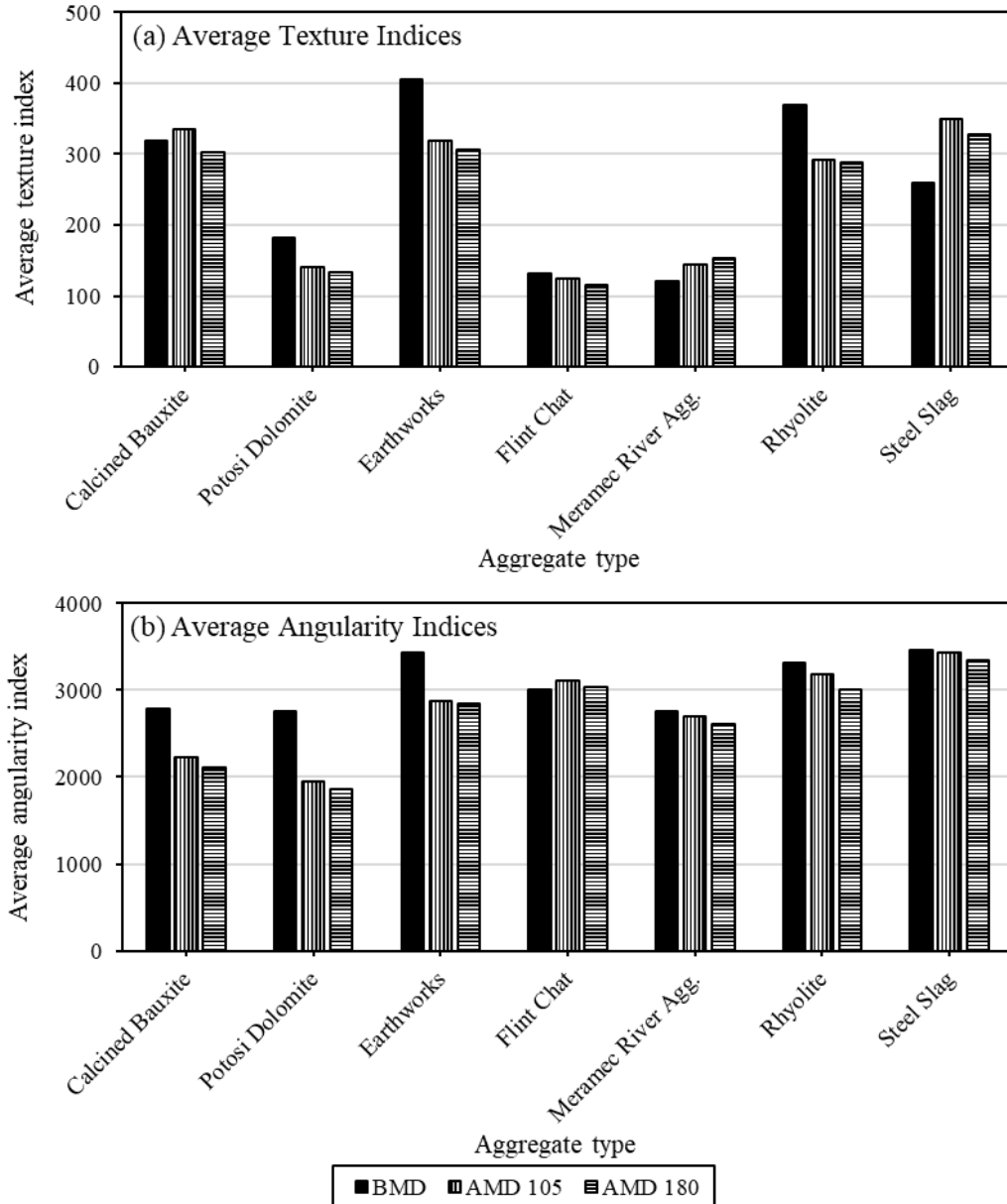


Figure 5-5 Average texture and average angularity indices.

The percentages of increase or decrease for average TX and average Gradient Angularity (GA) indices are presented in Figure 5-6. From Figure 5-6a, CB's average TX indices percentage for After 180-minutes

of Micro-Deval polishing time (AMD 180) decreased the least. Steel Slag showed the highest percentages of average Texture (TX) indices increases for After 105-minutes of Micro-Deval polishing time (AMD 105) and AMD 180. By contrast, Potosi Dolomite's average TX indices decreased the most for AMD 105 and AMD 180. All aggregates presented a decrease in average GA indices among AMD 105 and AMD 180, except for Flint Chat (Figure 5-5b and Figure 5-6b). From Figure 5-6b, the highest decrease percentages for average GA indices were noted for Potosi Dolomite. However, the lowest decrease in average GA indices was observed for Steel Slag.

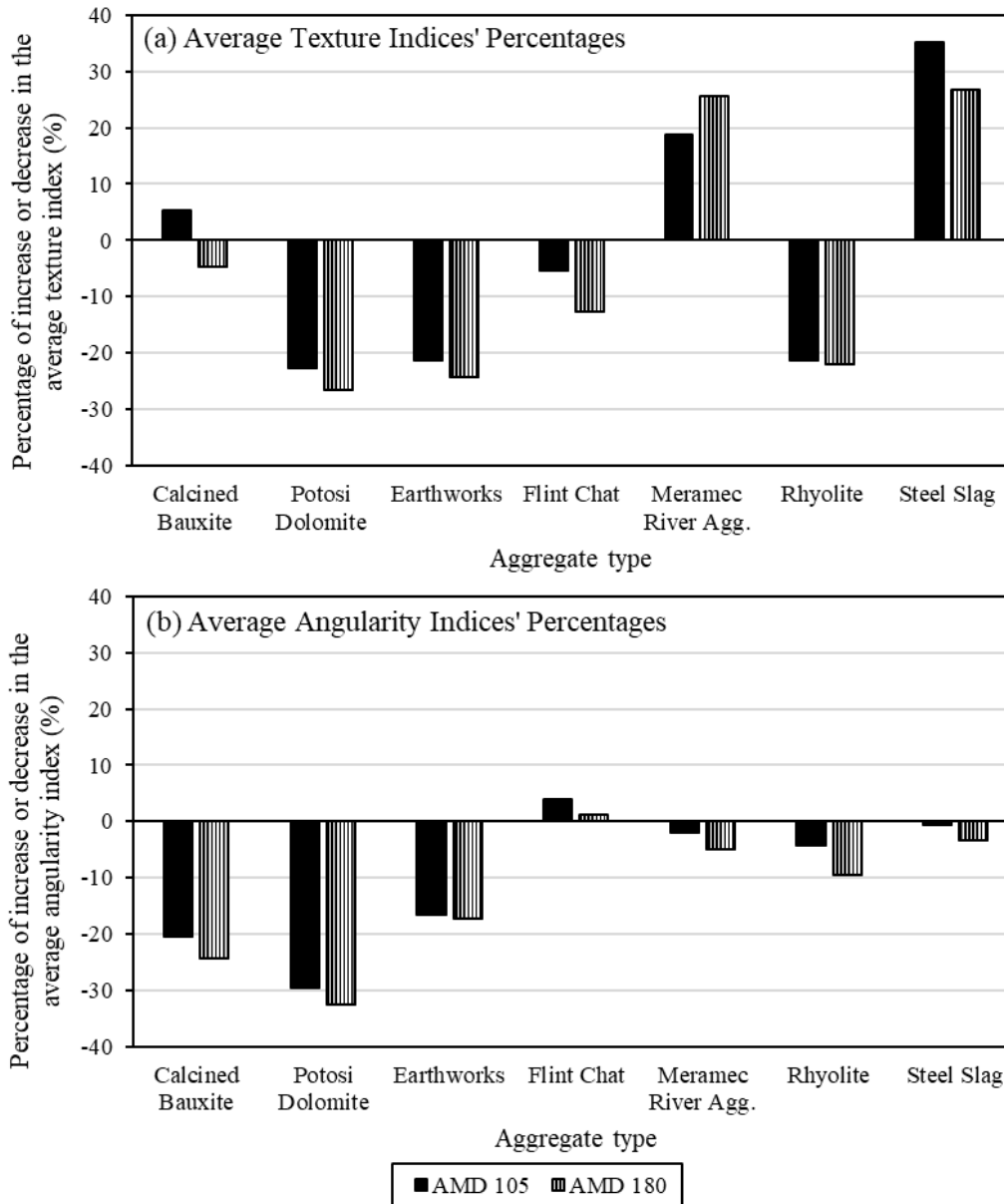


Figure 5-6 Percentages of increase or decrease in average texture and average angularity indices.

5.3.3 Relationship between Texture and Angularity Indices

In this section, the relationships between average TX and average Gradient Angularity (GA) indices for Before Micro-Deval polishing (BMD), After 105-minutes of Micro-Deval polishing time (AMD 105), and After 180-minutes of Micro-Deval polishing time (AMD 180) are shown in Figure 5-7. Aggregates

that had the highest average TX indices showed the highest average GA indices; however, no specific relationship is deduced from Figure 5-7. Earthworks showed the highest average Texture (TX) and average GA indices during BMD, and Steel Slag presented the highest average TX and average GA indices for AMD 105 and AMD 180. Meramec River Aggregate had the lowest average TX and average GA indices for BMD; Potosi Dolomite had the lowest average GA indices and the second-lowest average TX indices for AMD 105 and AMD 180.

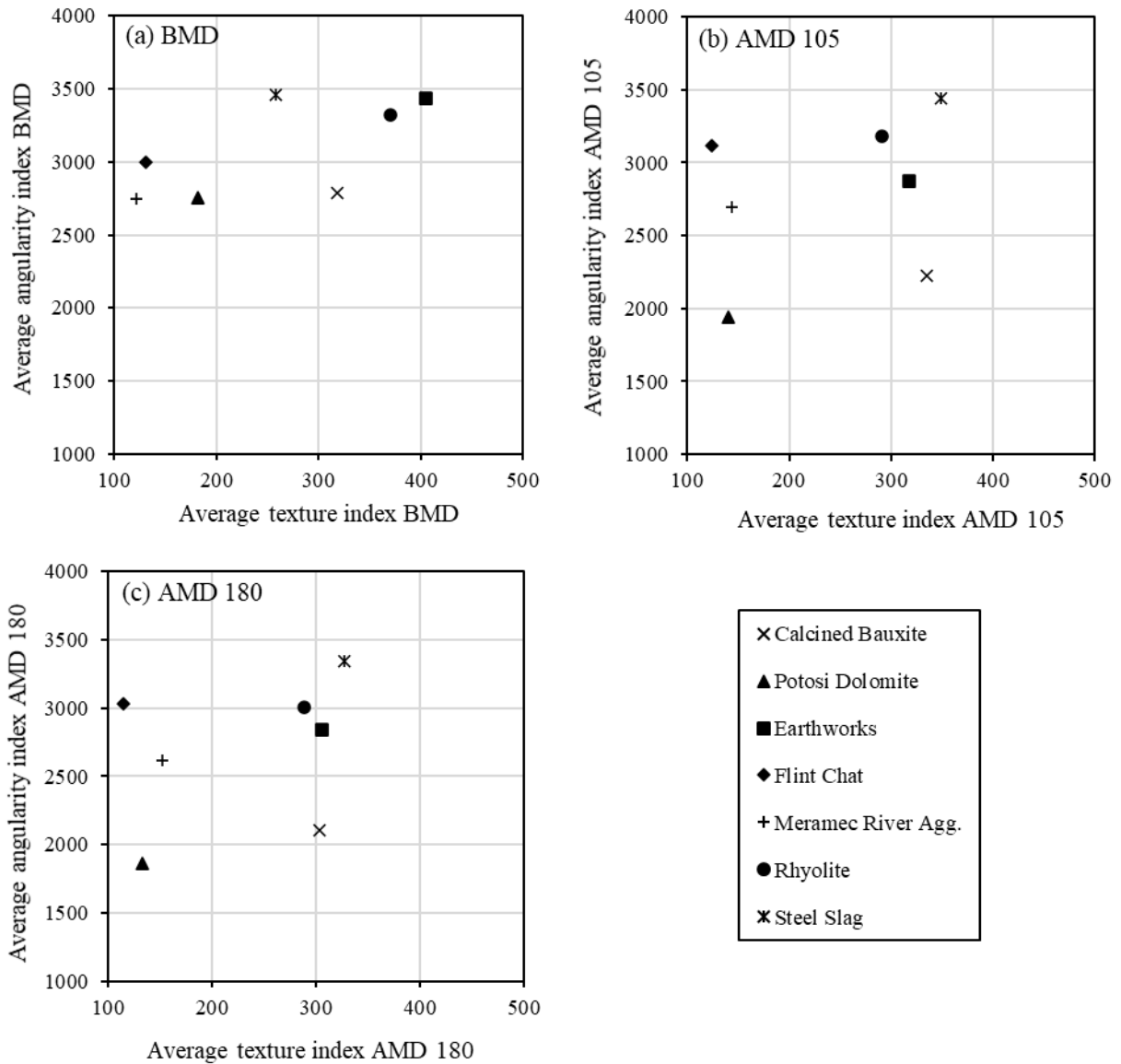


Figure 5-7 Relationships between average texture and average angularity indices.

Figure 5-8 shows the relationships between average TX and average Gradient Angularity (GA) indices considering Before Micro-Deval polishing (BMD), After 105-minutes of Micro-Deval polishing time (AMD 105), and After 180-minutes of Micro-Deval polishing time (AMD 180). No specific relationship is observed in Figure 5-8. After Micro-Deval (MD) polishing, the average TX and average GA indices decreased for four aggregates. Contrarily, Steel Slag, Calcined Bauxite (CB), and Meramec River Aggregate showed an increase in average TX indices for AMD 105. This TX index increase continued for AMD 180 with Meramec River Aggregate. This took place because one of the reasons explained in

Section 5.3.1. The average GA indices decreased for all aggregates with AMD 105 and AMD 180 except for Flint Chat that presented an increase in the average GA index using AMD 105. Steel Slag had the highest average GA indices BMD; however, it had lower average Texture (TX) indices than CB, Earthworks, and Rhyolite. Earthworks showed the highest average TX indices and the second-highest average GA indices during BMD. Meramec River Aggregate had the lowest average TX and average GA indices with BMD. Steel Slag had the highest average TX and average GA indices for AMD 105 and AMD 180. By contrast, Potosi Dolomite had the second-lowest average TX indices after Flint Chat, and it had the lowest average GA indices when AMD 105 and AMD 180 were applied.

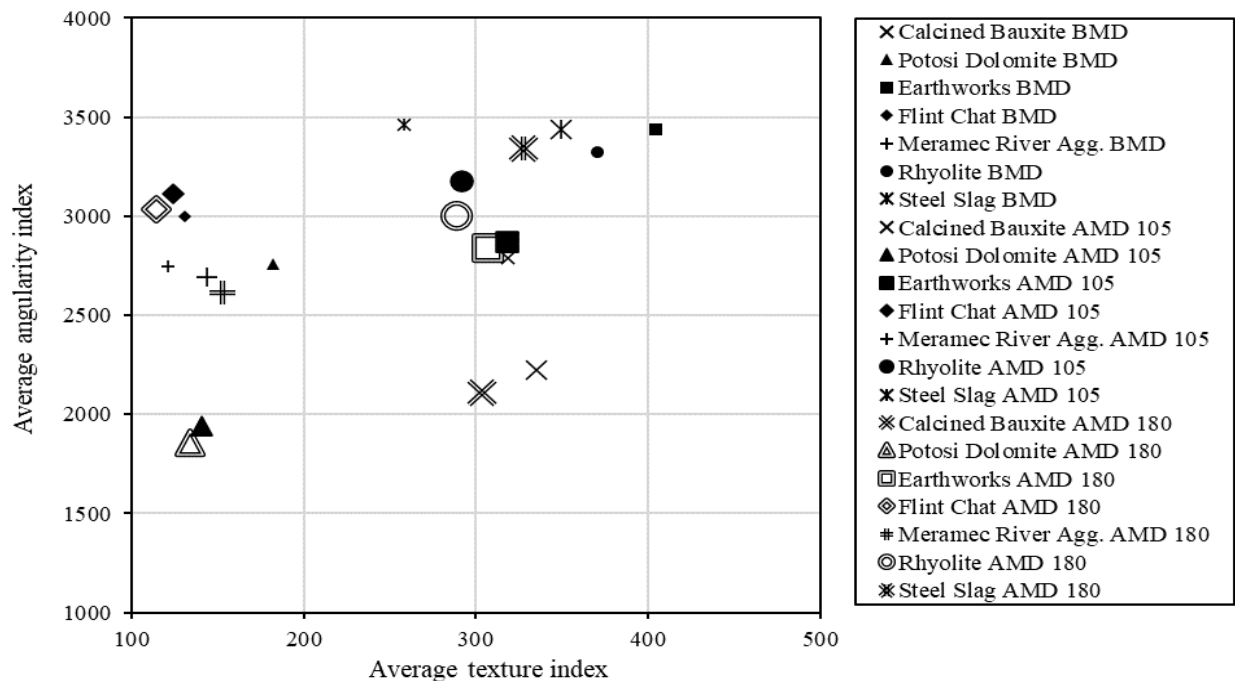


Figure 5-8 Relationship between average texture and average angularity indices.

5.4 Accelerated Friction Testing Results

Accelerated friction testing was conducted to evaluate the surface frictional characteristics of alternative aggregates compared to the control Calcined Bauxite (CB). The accelerated testing included measuring Mean Texture Depth (MTD) using the sand patch test and measuring the Coefficient of Friction (COF) using Dynamic Friction Tester (DFT). A Three-Wheel Polishing Device (TWPD) was used to polish the test surfaces to simulate the polishing of aggregates used in High Friction Surface Treatment (HFST) under traffic in the field. A DFT was used to measure the COF at different speeds (i.e., 20, 40, 60 km/hr) and different numbers of polishing cycles [i.e., 0 cycles (initial), 70k cycles, and 140k cycles (considered terminal)].

The researchers selected six aggregates, as presented in Table 3-3 for the accelerated friction testing. These aggregates included CB, Meramec River Aggregate, Flint Chat, Earthworks, Rhyolite, and Steel Slag. Three aggregates were excluded: Potosi Dolomite, Black Diabase, and Quartzite. Potosi Dolomite and Black Diabase had the highest MD mass losses. Additionally, Quartzite and Potosi Dolomite showed the highest LAA percentages. One size [i.e., (#6 - #8)] of the selected aggregates was considered. Two replicates (test slabs) were prepared and tested, and the results were based on the average of two replicates.

5.4.1 Sand Patch Test

Figure 5-9 displays MTD results for the HFST applications using aggregates before polishing. The MTD was the average of two replicates and four measurements were taken on each test surface. The measured MTD for all test surfaces ranged from 2.19 mm to 2.69 mm. The results showed that CB and Rhyolite surfaces had lower MTD measurements of 2.19 mm and 2.33 mm, respectively, compared to Steel Slag (2.64 mm) and Flint Chat (2.69 mm). The other surfaces (i.e., Meramec River Aggregate and Earthworks) had Mean Texture Depth (MTD) values greater than CB and Rhyolite. Flint Chat and Steel Slag had MTD values higher than Earthworks and Meramec River Aggregate. Different MTD values were observed due to aggregate surface properties [e.g., aggregate angularity and morphology].

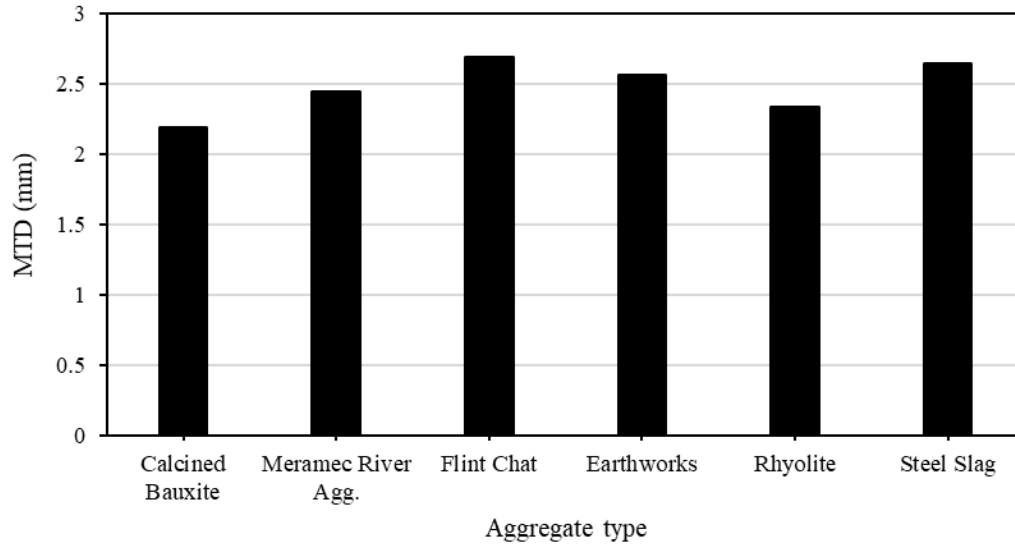


Figure 5-9 Mean texture depth values for the HFST applications.

5.4.2 Dynamic Friction Test

Coefficient of friction values were measured at different speeds (i.e., 20, 40, and 60 km/hr) and after different polishing cycles [i.e., 0 cycles (initial friction), 70k cycles, and 140k cycles (terminal friction)] for the six aggregates selected for accelerating friction testing. The Coefficient of Friction (COF) values were the average of two replicates. One friction measurement using Dynamic Friction Tester (DFT) was collected for each condition (polishing cycle and speed). Figure 5-10, Figure 5-11, and Figure 5-12 show the average COF values measured by the DFT for the two replicates at 20, 40, and 60 km/hr, respectively. The results showed that the COF decreased with polishing, as expected. Calcined Bauxite had higher initial and terminal COF values compared to the other alternative aggregates at the corresponding DFT speeds and polishing cycles. The Meramec River Aggregate had the lowest initial friction compared to all other aggregates, and it had comparable terminal friction to that of Earthworks.

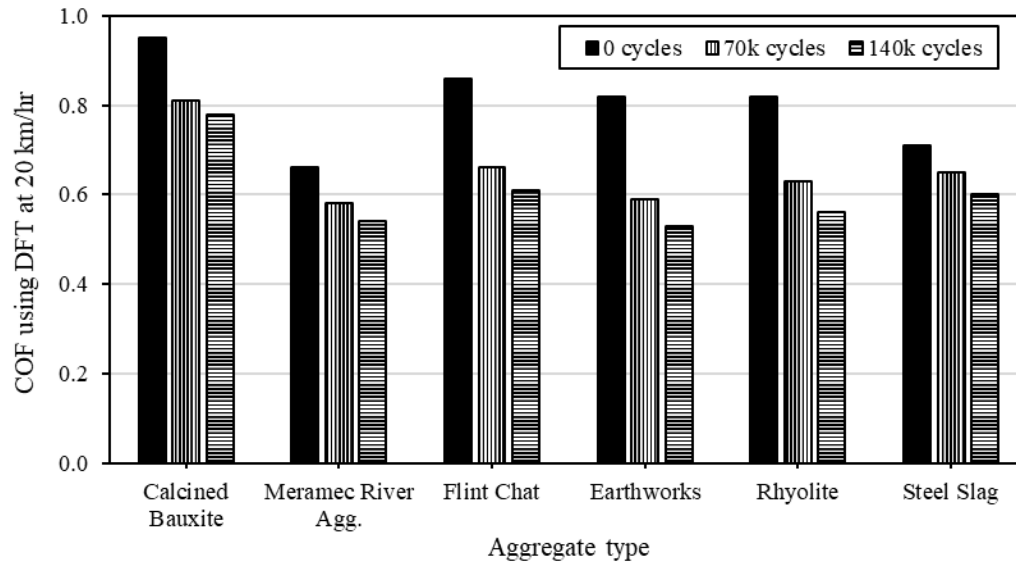


Figure 5-10 Coefficient of friction values using DFT at 20 km/hr.

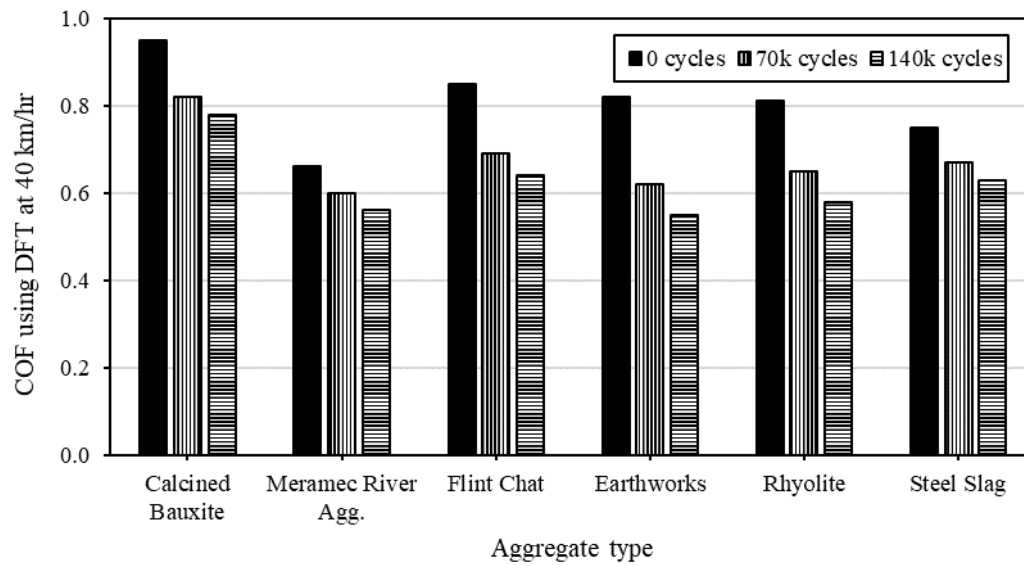


Figure 5-11 Coefficient of friction values using DFT at 40 km/hr.

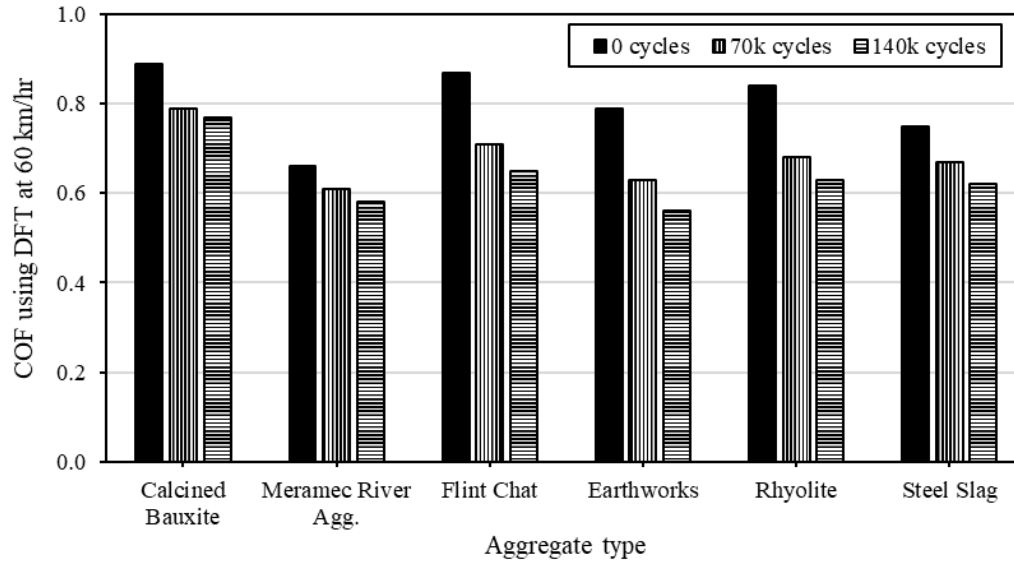


Figure 5-12 Coefficient of friction values using DFT at 60 km/hr.

The initial (0 cycles) and terminal (after 140k cycles of polishing) Coefficient of Friction (COF) values measured by Dynamic Friction Tester (DFT) at different speeds (20, 40, and 60 km/hr) for aggregates are displayed in Figure 5-13. Based on the terminal COF values, Flint Chat was considered the best choice after Calcined Bauxite (CB) and followed by Steel Slag and Rhyolite. The DFT speed had an inconsiderable impact on the initial COF values of Meramec River Aggregate. The COF values decreased for the CB (before and after polishing) and Earthworks (before polishing) with the increase in DFT speeds. However, the initial and terminal COF values increased with the increase in the DFT speed for the remaining alternative aggregates. The highest increase in COF values was noted for Rhyolite (after polishing): a 12.5% increase in the COF value by increasing the DFT speed from 20 to 60 km/hr.

Figure 5-14 shows the percentage of Coefficient of Friction (COF) value losses measured using Dynamic Friction Tester at 40 km/hr after 70k cycles and 140k cycles compared to the initial friction values (i.e., at 0 cycles). The results demonstrated that Meramec River Aggregate had the lowest COF loss percentage after 70k cycles and 140k cycles. This was because it had the lowest initial friction. Steel Slag and Calcined Bauxite (CB) had lower COF percentage losses after 140k cycles when compared to all other remaining aggregates. Earthworks had the highest COF loss percentage after 70k and 140k cycles.

5.4.3 Relationship between Dynamic Friction Test Results and Number of Polishing Cycles

There was a noticeable relationship between the COF values measured by DFT and the number of polishing cycles. Figure 5-15 displays the relationship between COF values measured by the Dynamic Friction Tester at 20 km/hr (DFT_{20}) and the number of polishing cycles (N). COF values exponentially decreased as the number of polishing cycles increased. Thus, an exponential regression was proposed for the prediction of DFT_{20} through the number of polishing cycles as shown in Equation 5.1. Fitting parameters values—for the (DFT_{20} - N) model—were estimated using Excel by reducing the sum of squared error (SSE), as summarized in Table 5-2. Figure 5-16 shows the measured DFT_{20} values and the predicted DFT_{20} values using the (DFT_{20} - N) model.

$$DFT_{20} = a + b \times e^{(-c \times N)} \quad \text{Equation 5.1}$$

where,

DFT_{20} is the Coefficient of Friction measured by the Dynamic Friction Tester at 20 km/hr, N is the number of polishing cycles, and $(a, b, \text{ and } c)$ are the fitting parameters.

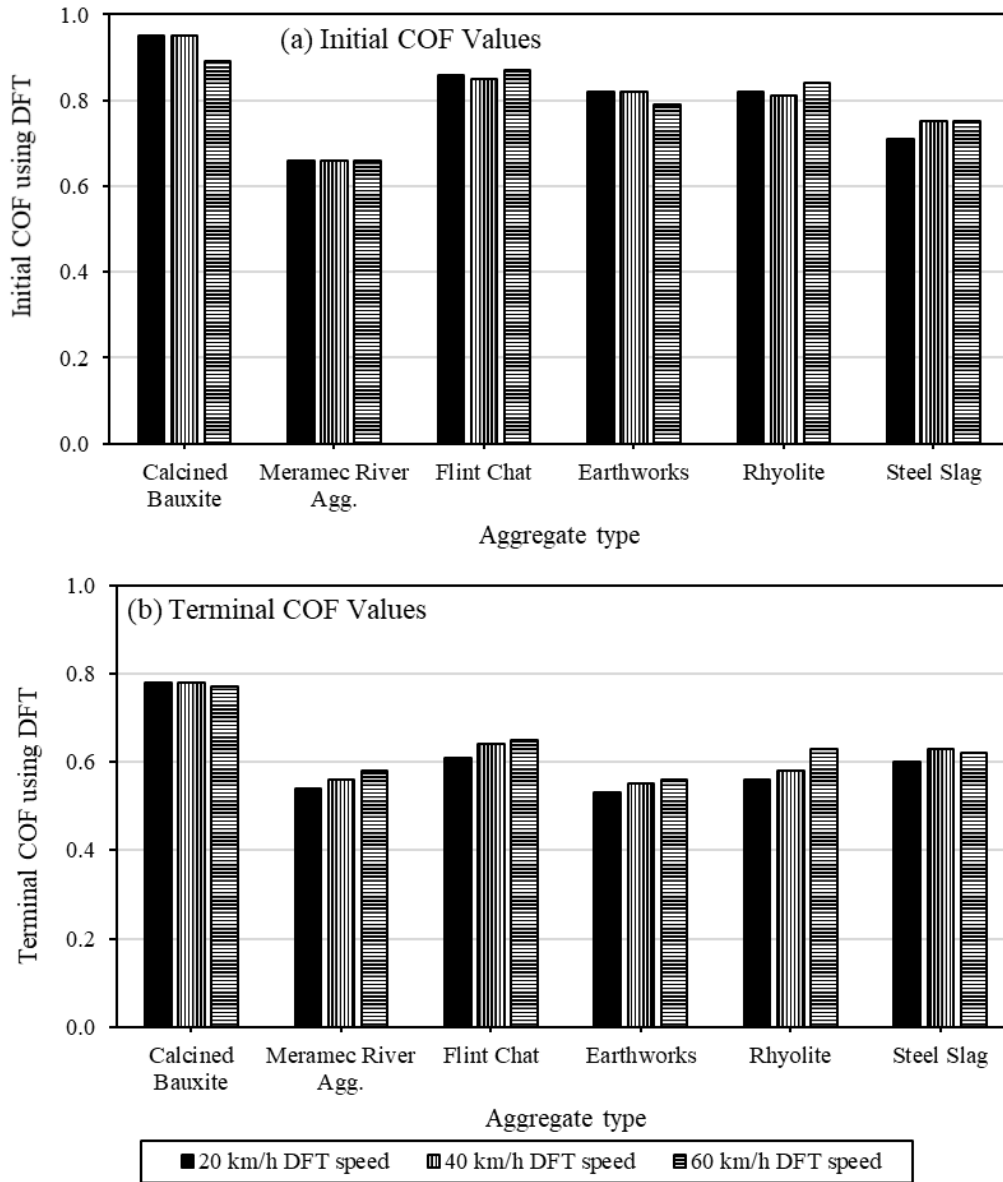


Figure 5-13 Initial and terminal COF values using DFT.

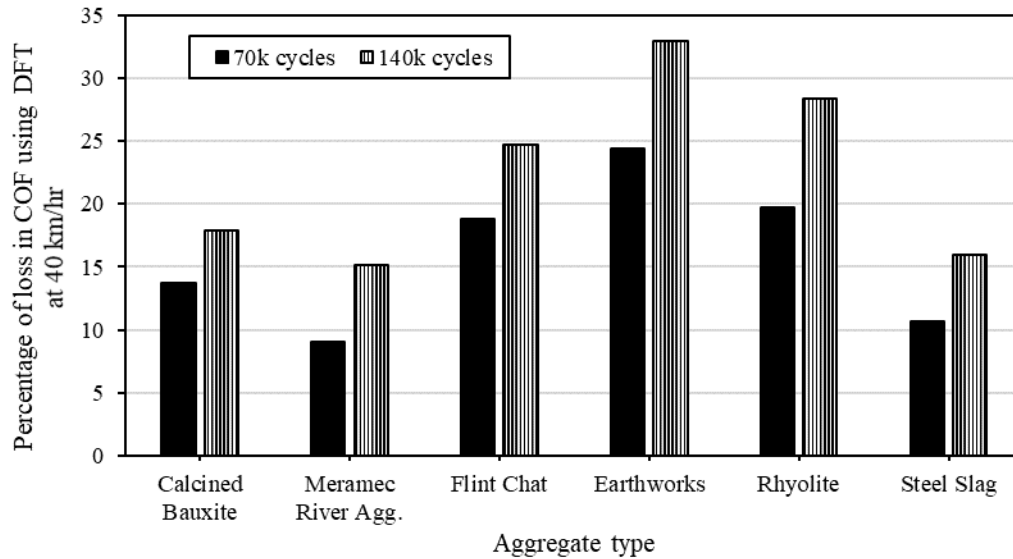


Figure 5-14 Percentages of losses in COF values after polishing.

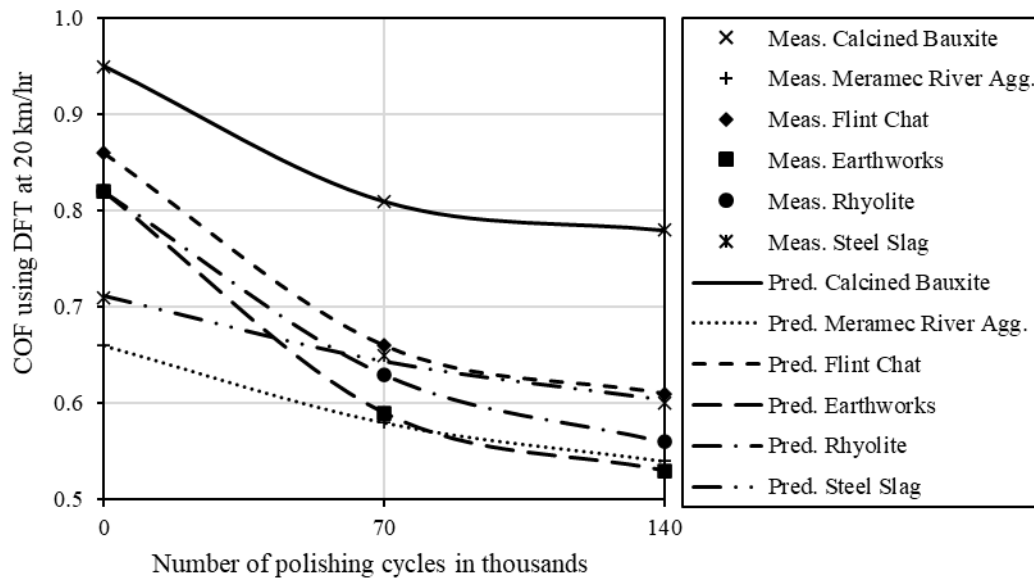


Figure 5-15 Relationship between COF values and the number of polishing cycles.

Table 5-2 Fitting parameters for (DFT_{20-N}) model.

Aggregate Type	<i>a</i>	<i>b</i>	<i>c</i>	<i>SSE</i>
Calcined Bauxite (CB)	0.7718	0.1782	0.022004	1.174E-11
Meramec River Agg.	0.50	0.1600	0.0099002	2.058E-11
Flint Chat	0.5933	0.2667	0.0198037	1.954E-12
Earthworks	0.5088	0.3112	0.0191958	1.493E-12
Rhyolite	0.5192	0.3008	0.0142638	9.063E-12
Steel Slag	0.5459	0.1663	0.0075436	5.512E-05

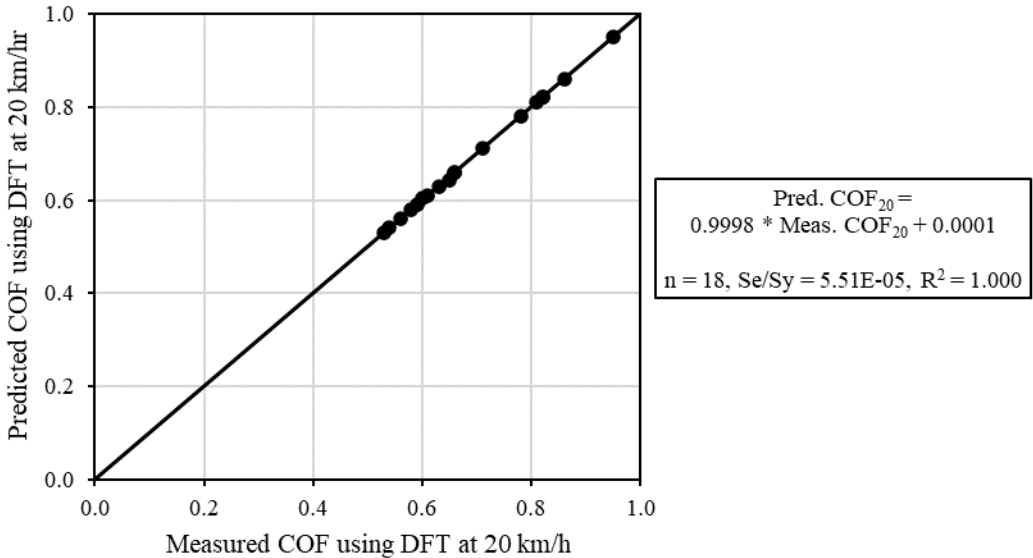


Figure 5-16 Measured versus predicted COF values.

5.4.4 Estimated Skid Number and International Friction Index

Figure 5-17 shows the estimated Skid Number measured at 40 mi/hr by a skid trailer with Ribbed tires (SN40R), using Equation B.36, for High Friction Surface Treatment (HFST) applications based on COF values measured by DFT at 40 km/hr (DFT₄₀). The initial estimated SN40R values were above 55 for all aggregates except for Meramec River Aggregate (i.e., 47). The results showed that Calcined Bauxite (CB) had the highest terminal estimated SN40R value of 58.1. Flint Chat and Steel Slag had relatively similar terminal estimated SN40R values of 45.2 and 44.2, respectively. Earthworks had the lowest terminal estimated SN40R value of 36.9, and it was followed by the Meramec River Aggregate with a value of 37.8.

The initial COF values measured by DFT at 20 km/hr (DFT₂₀) and Mean Texture Depth (MTD) measurements were used to calculate the initial International Friction Index (IFI) values as given in Equation B.1. The initial IFI values were then used to estimate the initial Skid Number measured at 50 mi/hr by a skid trailer with smooth tires [SN(50)] using a skid trailer with smooth tires (Equation B.10). However, these equations were calibrated with field measurements for Hot Mix Asphalt (HMA) surfaces, and no HFST surface treatments were included in this study (Masad, Rezaei, and Chowdhury 2011). Thus, the researchers used these formulas to estimate the initial IFI and initial SN(50) for the comparison purpose only, as these formulas are not calibrated for HFSTs.

The results of the estimated initial IFI (Figure 5-18) and the estimated initial SN(50) (Figure 5-19) further demonstrated that CB provided the highest IFI followed by Flint Chat, Earthworks, and Rhyolite. Note that the estimated initial Skid Number measured at 50 mi/hr by a skid trailer with smooth tires [SN(50)] values were relatively higher compared to Skid Number measured at 40 mi/hr by a skid trailer with Ribbed tires (SN40R), which was the opposite of expected. Therefore, these formulas should be calibrated with High Friction Surface Treatment (HFST) aggregates before being used to estimate SN(50).

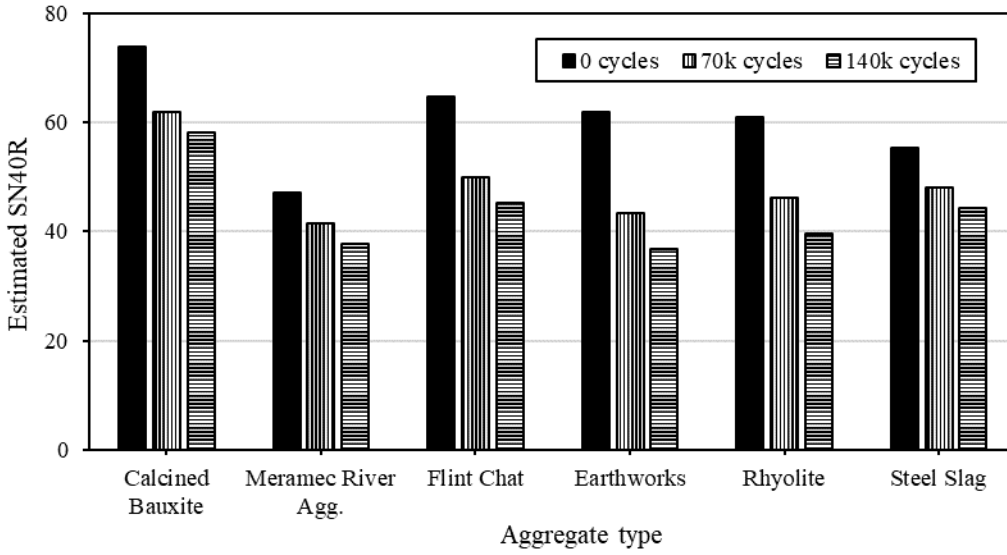


Figure 5-17 Estimated SN40R values for HFST applications.

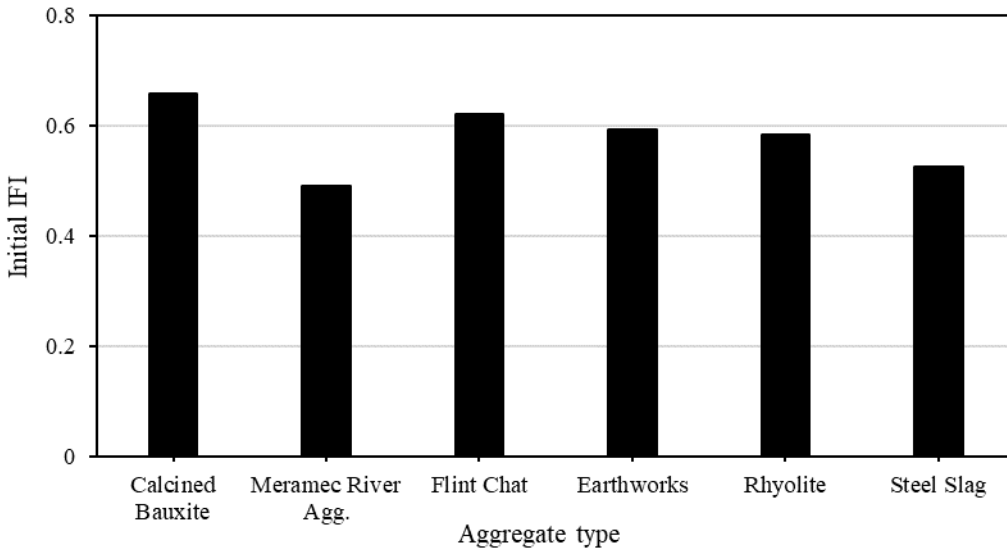


Figure 5-18 Estimated initial IFI values, based on DFT₂₀ and MTD measurements, for the HFST applications.

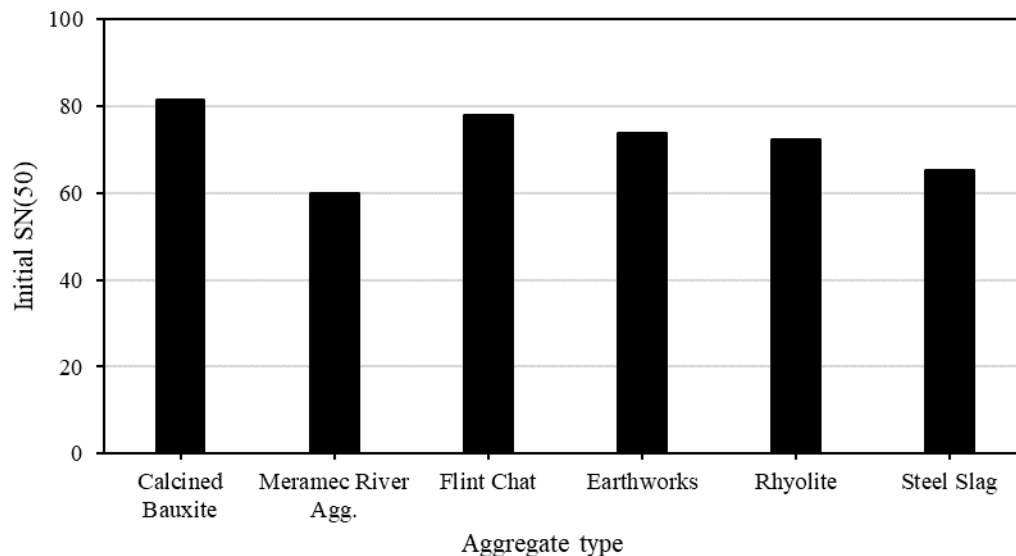


Figure 5-19 Estimated initial SN(50) values, based on DFT_{20} and MTD measurements, for the HFST applications.

5.5 British Pendulum Test Results

5.5.1 Effect of Aggregate Size on the British Pendulum Number Values

The British Pendulum Number (BPN) values measured before and after 10-hr polishing cycles in the British wheel are presented in Figure 5-20 for aggregates. Two aggregate sizes were used in the test. The first size was (#6 - #8), and the second size was (#4 - #6), note Table 3-3. For each aggregate size, two aggregate coupons were formed using two-components-epoxy binder and aggregate. Five BPN measurements were recorded before and after polishing for each aggregate coupon, and the average BPN was calculated. From Figure 5-20, before and after the polishing process, Potosi Dolomite showed the highest BPN values for both sizes [(#6 - #8) and (#4 - #6)]. However, Steel Slag presented the lowest pre-polish BPN values. Calcined Bauxite presented the second highest pre-polish and post-polish BPNs for the two aggregate sizes. Flint Chat, Earthworks, Rhyolite, and Meramec River Aggregate had comparable BPN values before the polishing process for the (#6 - #8) size. However, after polishing, the Meramec River Aggregate showed the highest BPN, and Rhyolite presented the lowest BPN. Before the polishing process, the aggregates' size (#4 - #6) showed higher BPN values than the aggregates' size (#6 - #8). This agreed with Aggregate Image Measurement System (AIMS) results: increasing the size of the aggregates from (1/4" - #4) to (3/8" - 1/4") caused an increase in the Texture (TX) and Gradient Angularity (GA) indices.

Figure 5-21 shows the percentages decrease or increase in the BPN values after the polishing process for aggregates with two sizes (#6 - #8) and (#4 - #6). The BPN values decreased after the polishing process for all aggregates except for Meramec River Aggregate (#6 - #8 size). This occurred because average TX indices for After 105-minutes of Micro-Deval polishing time (AMD 105) and After 180-minutes of Micro-Deval polishing time (AMD 180) showed an increase compared to the TX index for Before Micro-Deval polishing (BMD).

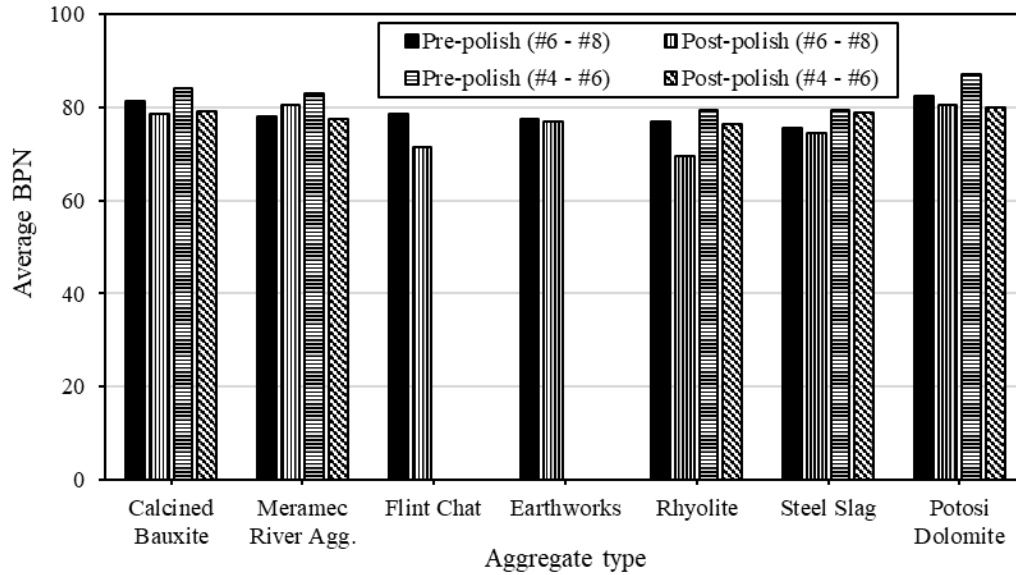


Figure 5-20 Average BPNs with two sizes.

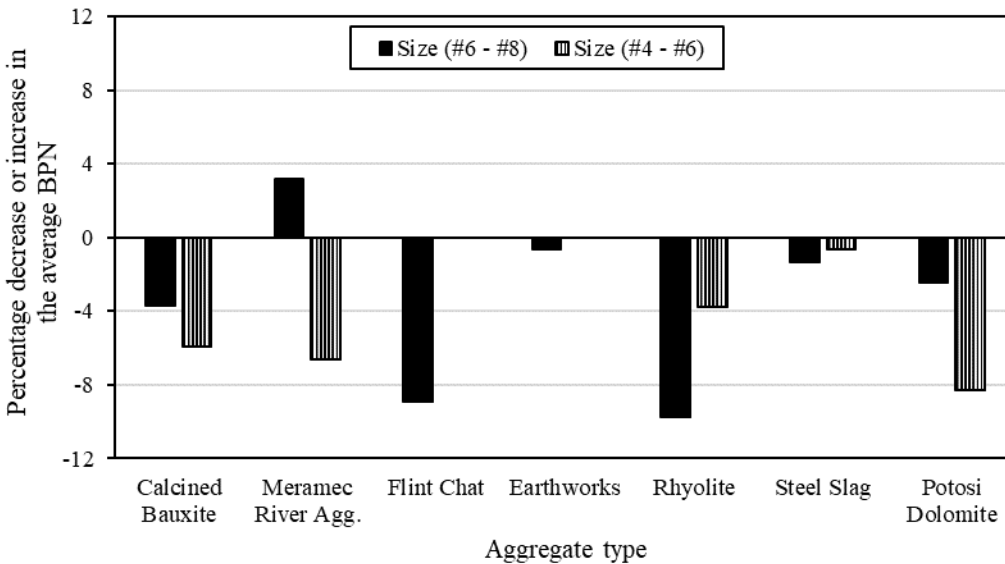


Figure 5-21 Percentages of decrease or increase in the average BPNs after the polishing process with two sizes.

5.5.2 Average British Pendulum Number Values

The average British Pendulum Number (BPN) values for aggregates' sizes (#6 - #8) and (#4 - #6) are exhibited in Figure 5-22. Potosi Dolomite had the highest average pre-polished BPN value followed by Calcined Bauxite (CB) and then Meramec River Aggregate. Potosi Dolomite showed the highest average post-polished BPN value followed by Meramec River Aggregate and then CB. The average BPN values before polishing were the same for Earthworks and Steel Slag (77.5). After polishing Earthworks had a higher BPN value than Steel Slag by 0.2. Rhyolite and Flint Chat had comparable average pre-polish BPN values; however, Flint Chat showed lower post-polish BPN values than Rhyolite.

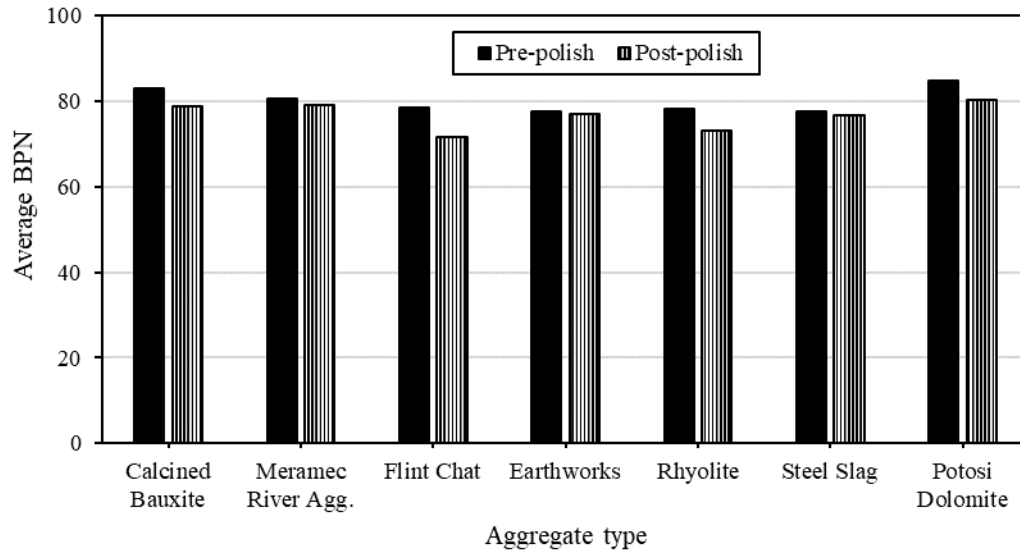


Figure 5-22 Average BPNs.

The decrease average British Pendulum Number (BPN) percentages for aggregates after polishing are displayed in Figure 5-23. Flint Chat percentages decreased the most in the average BPN (-8.9%), followed by Rhyolite (-6.7%), Potosi Dolomite (-5.4%), and then Calcined Bauxite (CB) (-4.8%). Earthworks, Steel Slag, and Meramec River Aggregate percentages decreased the least in the average BPN values (less than -2%).

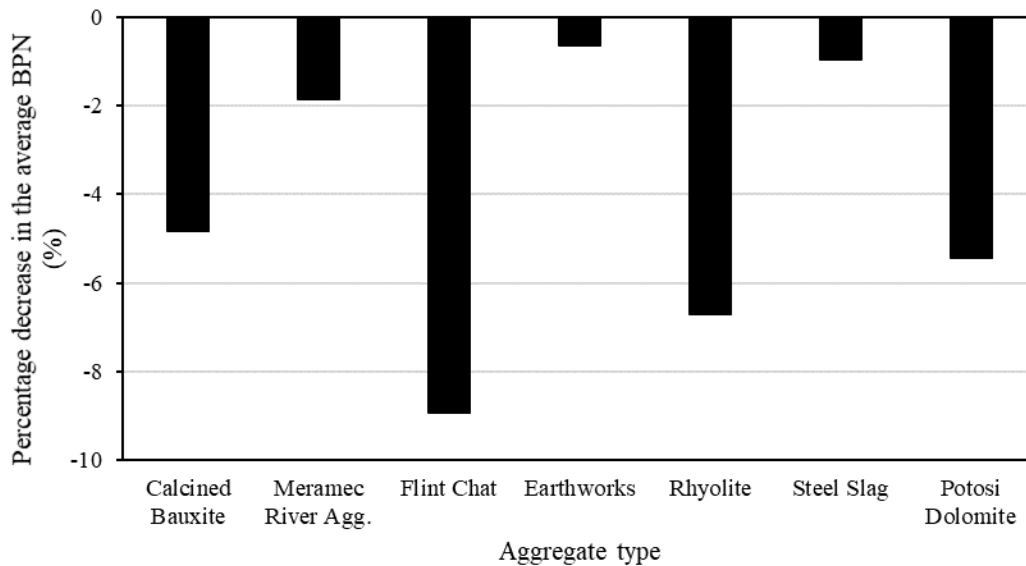


Figure 5-23 Percentages of decrease in the average BPNs after the polishing process.

5.6 Summary

This chapter discusses the performance testing results for aggregates through different testing. The Micro-Deval (MD) test was run on coarse (3/8" - #4) and fine (#6 - #16) aggregate gradations. The MD results after 180-minutes polishing time for the coarse gradation showed that Meramec River Aggregate had the lowest percentage of mass loss followed by Earthworks, Rhyolite, Flint Chat, Calcined Bauxite (CB), Quartzite, Steel Slag, and Black Diabase. The highest percentage of mass loss was recorded for Potosi

Dolomite. The MD results after 30-minutes polishing time for the fine gradation deemed that CB had the lowest percentage of mass loss, followed by Meramec River Aggregate, Earthworks, Rhyolite, Steel Slag, Flint Chat, Quartzite, and Black Diabase. The highest percentage of mass loss was for Potosi Dolomite. The MD results for aggregates with fine gradation showed that the mass losses calculated #6 - #8 were higher than the mass losses calculated for #6 - #16. This indicated that the larger aggregates' sizes had higher mass losses than the smaller aggregates' sizes.

The Aggregate Image Measurement System (AIMS) results deemed that the highest average Texture (TX) index based on After 180-minutes of Micro-Deval polishing time (AMD 180) was noted for Steel Slag followed by Earthworks, CB, Rhyolite, Meramec River Aggregate, and Potosi Dolomite. The lowest average TX index regarding AMD 180 was for Flint Chat. The highest average Gradient Angularity (GA) index AMD 180 was for Steel Slag, followed by Flint Chat, Rhyolite, Earthworks, Meramec River Aggregate, and CB. The lowest average GA index regarding AMD 180 was recorded for Potosi Dolomite. The Aggregate Image Measurement System (AIMS) results demonstrated that decreasing the aggregates' sizes from (3/8" - 1/4") to (1/4" - #4) showed mixed results. A decrease in the Texture (TX) and Gradient Angularity (GA) indices for before Micro-Deval (BMD), After 105-minutes of Micro-Deval polishing time (AMD 105), and After 180-minutes of Micro-Deval polishing time (AMD 180) was noted. However, there were exceptions for Steel Slag [TX (BMD)], Potosi Dolomite [GA (BMD)], Earthworks [GA (BMD)], Flint Chat [GA (BMD)], and CB [GA (AMD 105) and (AMD 180)]. No specific relationships were observed between average TX indices and average GA indices regarding BMD, AMD 105, and AMD 180.

The sand patch test results depicted that Flint Chat had the highest Mean Texture Depth (MTD) values followed by Steel Slag, Earthworks, Meramec River Aggregate, and Rhyolite. The lowest MTD value was for CB. The Dynamic Friction Tester (DFT) results showed that CB had the highest terminal Coefficient of Friction (COF) value followed by Flint Chat, Steel Slag, Rhyolite, and Meramec River Aggregate. The lowest terminal COF value was noted for Earthworks. The British Pendulum (BP) test results illustrated that Potosi Dolomite had the highest post-polish British Pendulum Number (BPN) value followed by Meramec River Aggregate, CB, Earthworks, Steel Slag, and Rhyolite. The lowest post-polish BPN value was recorded for Flint Chat. To compare the aggregates' physical properties, durability, and frictional performance, the researchers introduced Chapter 6 for this purpose.

CHAPTER 6: PHYSICAL PROPERTIES, DURABILITY, AND PERFORMANCE TESTING COMPARATIVE STUDIES

6.1 Introduction

The physical properties and durability testing were explained for the various aggregates and sizes in Chapter 4. Moreover, the aggregates' performance was presented in Chapter 5 through various testing. In this chapter, the physical properties, durability, and performance testing results of aggregates were compared. The physical properties testing involved specific gravity and Uncompacted Void Content (UVC). The durability testing contained Los Angeles Abrasion (LAA), sodium sulfate soundness, water-alcohol freeze thaw, and acid insoluble residue. The performance properties involved Micro-Deval (MD) mass losses and polishing times, Aggregate Image Measurement System (AIMS) Texture (TX) and Gradient Angularity (GA) indices, the Mean Texture Depth (MTD), British Pendulum Number (BPN) values, Coefficient of Friction (COF) values using Dynamic Friction Tester (DFT), and the predicted initial and terminal Skid Number (SN) values. The relationships between MD mass losses and AIMS TX or GA indices were explored, and the relationships between MD polishing times and AIMS TX or GA indices were confirmed. The percentages of mass losses through Los Angeles Abrasion (LAA) and MD testing were compared for the aggregates. The relationships between the UVC percentages for the aggregates and the MD polishing time, AIMS GA indices, or MTD values were investigated. The AIMS TX and GA indices were compared to the BPN values, and the AIMS TX or GA indices were compared to the COF values measured by the DFT. Additionally, the BPN values were compared to the COF values measured by the DFT.

6.2 Relationships between Micro-Deval and Aggregate Image Measurement System Results

6.2.1 Relationships between Micro-Deval Mass Losses and Texture or Angularity Indices

Mass losses, average AIMS TX indices, and average AIMS GA indices were assessed for After 105-minutes of Micro-Deval polishing time (AMD 105) and After 180-minutes of Micro-Deval polishing time (AMD 180); the relationships between mass losses and average AIMS TX indices or average AIMS GA indices are shown in Figure 6-1. The MD test was conducted on aggregates with (3/8" - #4) gradation, and the AIMS TX indices and AIMS GA indices were calculated based on the results of two sizes [(3/8" - 1/4") and (1/4" - #4)], note Table 3-3. No specific relationship is observed in Figure 6-1. Meramec River Aggregate had the lowest MD mass losses after 105- and 180-minutes polishing times; however, it had the third-lowest average TX and average GA indices regarding AMD 105 and AMD180. Potosi Dolomite had the highest MD mass losses, the lowest average GA indices, and the second-lowest average TX indices after 105- and 180-minutes polishing times. Steel Slag had the highest average TX and average GA indices; however, it had the second-highest MD mass loss after 105- and 180-minutes polishing times. Calcined Bauxite had comparable average TX indices with Steel Slag for AMD 105 and AMD 180. Nevertheless, Steel Slag had higher average GA indices than Calcined Bauxite (CB) for AMD 105 and AMD 180.

Figure 6-2 illustrates the relationships between the percentages of mass losses and the average TX indices (Figure 6-2a) or average GA indices (Figure 6-2b) for AMD (105- and 180-minutes polishing times). No specific relationships are noted in Figure 6-2a and Figure 6-2b. Aggregate with the highest mass loss for AMD—Potosi Dolomite—showed the lowest average GA indices. Steel Slag and CB had comparable MD mass losses and average TX indices after 105- and 180-minutes polishing times; however, Calcined Bauxite had lower average GA indices than Steel Slag. Rhyolite and Earthworks had comparable MD mass losses, average TX indices, and average GA indices after 105- and 180-minutes polishing times. Flint Chat had comparable MD mass losses and average GA indices with Earthworks and Rhyolite; however, Flint Chat had the lowest average TX indices considering 105- and 180-minutes polishing times.

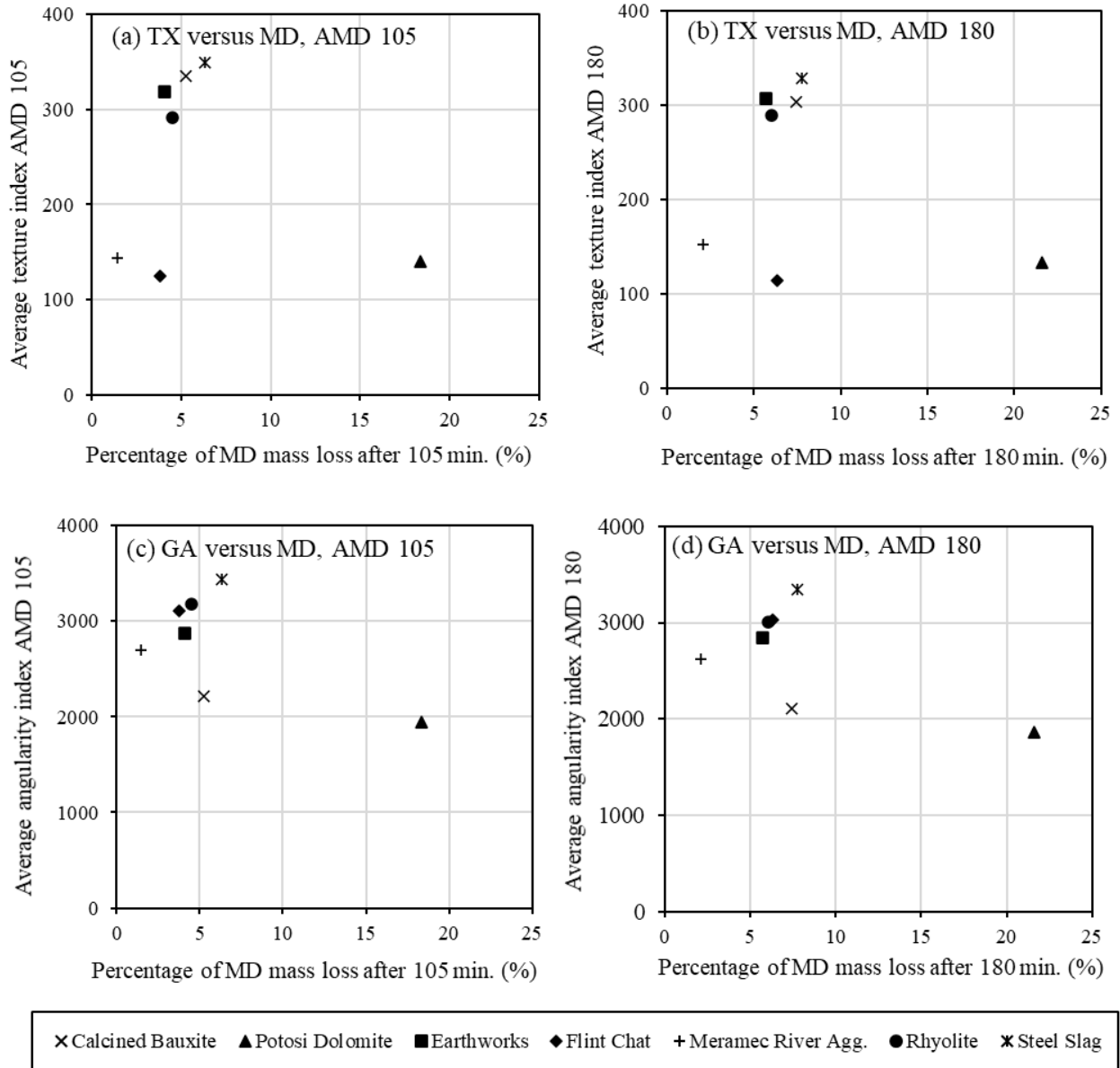


Figure 6-1 Relationships between MD percentages of mass losses and texture or angularity indices.

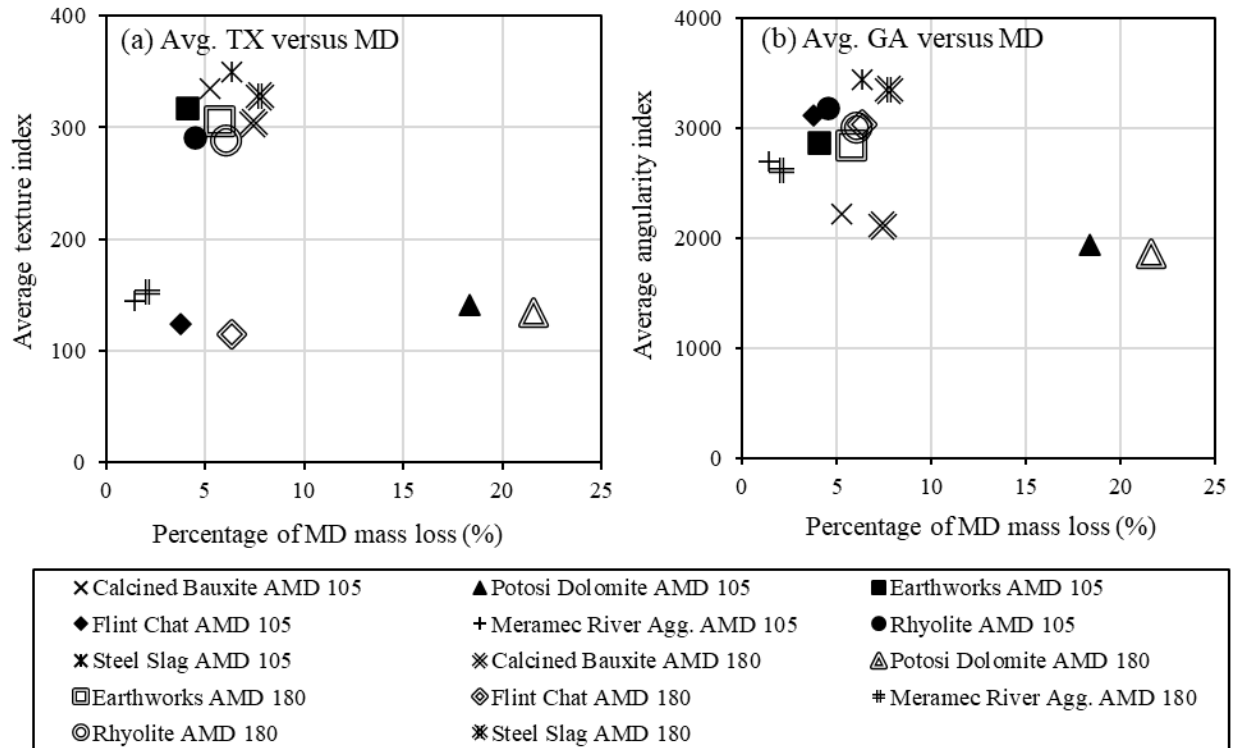


Figure 6-2 Relationships between MD percentages of mass losses and average TX indices or average GA indices.

Table 6-1 presents the rankings of the aggregates based on average Aggregate Image Measurement System (AIMS) Texture (TX) indices, average AIMS Gradient Angularity (GA) indices, and Micro-Deval (MD) mass losses results. The aggregates were ranked from 1 to 7 based on the average AIMS TX indices of After 180-minutes of Micro-Deval polishing time (AMD 180), average AIMS GA indices with AMD 180, and mass losses for AMD 180. Aggregates with the highest average TX indices for AMD 180, average GA indices for AMD 180, or lowest MD mass losses after 180-minutes were scored with 1. Except for Meramec River Aggregate and Steel Slag ranking, the rankings of the aggregates based on AIMS TX or GA indices in AMD 180 and mass losses for AMD 180 were similar.

Table 6-1 Ranking of aggregates based on AIMS and MD results.

Aggregate Type	Ranking		
	Based on Average AIMS TX Indices for AMD 180 [(3/8" - 1/4") and (1/4" - #4) Sizes]	Based on Average AIMS GA Indices for AMD 180 [(3/8" - 1/4") and (1/4" - #4) Sizes]	Based on Micro-Deval (MD) Mass Losses for AMD 180 [(3/8" - #4) Gradation]
Calcined Bauxite (CB)	3	6	5
Earthworks	2	4	2
Flint Chat	7	2	4
Meramec River Agg.	5	5	1
Rhyolite	4	3	3
Steel Slag	1	1	6
Potosi Dolomite	6	7	7

6.2.2 Relationships between Micro-Deval Polishing Times and Texture or Angularity Indices

The relationships between the Texture (TX) indices and Micro-Deval (MD) polishing times for aggregates are illustrated in Equation 6.1. The fitting parameters and the estimated SSE for the (TX-MD t) model are presented in Table 6-2.

$$TX = a_{TX} + b_{TX} \times e^{(-c_{TX} \times t)} \quad \text{Equation 6.1}$$

where,

TX is the texture index,

t is the MD polishing time,

a_{TX} is the terminal texture index. It should be greater than or equal to zero,

$(a_{TX} + b_{TX})$ is the initial texture index, and

c_{TX} is the rate of texture change.

The relationships between the Gradient Angularity (GA) indices and MD polishing times for aggregates are illustrated in Equation 6.2. The fitting parameters and the estimated SSE for the (GA-MD t) model using are presented in Table 6-3.

$$GA = a_{GA} + b_{GA} \times e^{(-c_{GA} \times t)} \quad \text{Equation 6.2}$$

where,

GA is the gradient angularity index,

t is the Micro-Deval polishing time,

a_{GA} is the terminal angularity index. It should be greater than or equal to zero,

$(a_{GA} + b_{GA})$ is the initial angularity index, and

c_{GA} is the rate of angularity change.

Table 6-2 Fitting parameters for (TX-MD t) model.

Aggregate Type	a_{TX}	b_{TX}	c_{TX}	SSE
Calcined Bauxite (CB)	0.0	325.136	2.03E-04	432.445
Meramec River Agg.	164.461	-43.112	7.12E-03	8.5465E-06
Flint Chat	0.0	132.009	7.25E-04	5.907
Earthworks	302.444	102.156	1.79E-02	1.6614E-07
Rhyolite	288.424	81.726	3.27E-02	6.5805E-07
Steel Slag	338.650	-80.100	1.89E-01	231.125

Table 6-3 Fitting parameters for (GA-MD t) model.

Aggregate Type	a_{GA}	b_{GA}	c_{GA}	SSE
Calcined Bauxite (CB)	2048.457	740.946	1.39E-02	2.573E-05
Meramec River Agg.	0.0	2755.595	2.71E-04	332.778
Flint Chat	683.521	2365.629	0.0	7050.485
Earthworks	2840.29	597.013	2.84E-02	5.0E-05
Rhyolite	0.0	3333.264	5.39E-04	1527.033
Steel Slag	0.0	3476.260	1.85E-04	1421.615

6.3 Relationships between Micro-Deval and Los Angeles Mass Losses

6.3.1 Micro-Deval Mass Losses for Coarse Gradation Versus Los Angeles Abrasion for Grading D

The relationships between the Los Angeles Abrasion (LAA) for Part-I testing (grading D) and Micro-Deval (MD) mass losses for (3/8" - #4) size are illustrated in Figure 6-3a and Figure 6-3b. Two MD polishing times were used for the coarse gradation [105 minutes (Figure 6-3a) and 180 minutes (Figure 6-3b)]. According to the maximum allowable LAA percentage (NJSP-15-13B requirements), Potosi Dolomite and Black Diabase were out of the requirements. The MD mass losses increased with increasing the polishing time from 105 to 180 minute. There were direct linear relationships between the LAA and MD test results. Aggregates with the highest LAA percentage had the highest MD mass loss (e.g., Potosi Dolomite). Meramec River Aggregate had the lowest LAA percentage and MD mass loss. The MD mass losses percentages were observed to be much lower than the LAA percentages. The MD mass losses were more sensitive than the LAA percentages. For instance, Steel Slag and Meramec River Aggregate had similar LAA percentage (14.06% for Meramec River Aggregate and 15.53% for Steel Slag). However, the MD mass losses for the two aggregates were completely different. The MD mass losses for Meramec River Aggregate and Steel Slag after 105 minutes of polishing were 1.4% and 6.3%, respectively. Furthermore, the MD mass losses for Meramec River Aggregate and Steel Slag after 180 minutes of polishing were 2.1% and 7.8%, respectively.

6.3.2 Micro-Deval Mass Losses for Fine Gradation Versus Los Angeles Abrasion for Grading D

The relationships between the LAA for Part-II testing (grading D) and MD mass losses for (#6 - #16) gradation are shown in Figure 6-3c and Figure 6-3d. The MD mass losses for one polishing time (30 minutes) was discussed. The MD mass losses were calculated for the (#6 - #8) size and for the total gradation (#6 - #16), as presented in Figure 6-3c and Figure 6-3d, respectively. Based on the maximum allowable LAA percentage (NJSP-15-13B requirements), Rhyolite, Flint Chat, and Quartzite were out of the requirements. The mass losses calculated for (#6 - #8) were higher than the mass losses calculated for (#6 - #16). This reflected that the larger aggregates' sizes had higher mass losses than the smaller aggregates' sizes. There were linear direct relationships between the LAA and MD test results. Aggregates with the highest LAA percentage had the highest MD mass loss. Meramec River Aggregate and CB had lower LAA percentages and MD mass losses when compared to the remaining aggregates. The MD mass losses percentages were noted to be much lower than the LAA percentages. The MD mass losses were more sensitive than the LAA percentages. For example, Earthworks and Black Diabase had the same LAA percentage (20%). Nevertheless, the MD mass losses for the two aggregates were completely different. The MD mass losses for Earthworks and Black Diabase after 30 minutes of polishing for (#6 - #8) size were 12.7% and 18.1%, respectively. Moreover, the MD mass losses for Earthworks and Black Diabase after 30 minutes of polishing for (#6 - #16) size were 3.4% and 7.5%, respectively. The same findings were noted for Meramec River Aggregate and Steel Slag. Both aggregates showed similar LAA percentages; however, they had different MD mass losses. Both Flint Chat and Quartzite had LAA percentages higher than Black Diabase; however, the two aggregates had lower MD mass losses than Black Diabase (see Figure 6-3d). Based on these findings, the MD was found to be more sensitive for aggregate screening than LA.

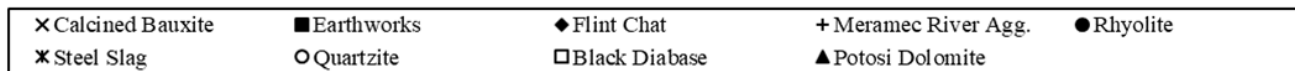
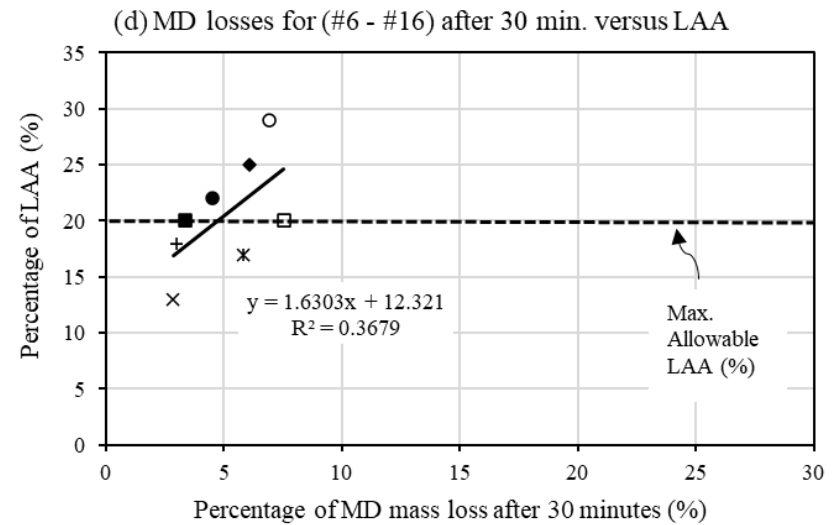
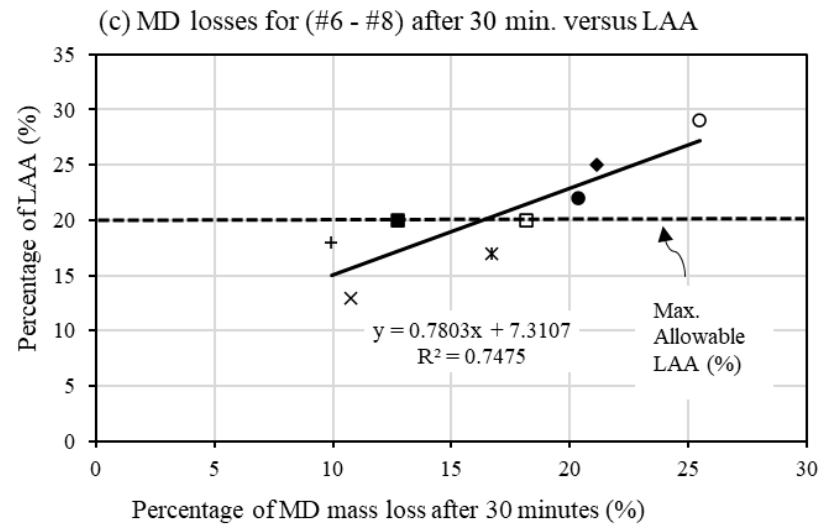
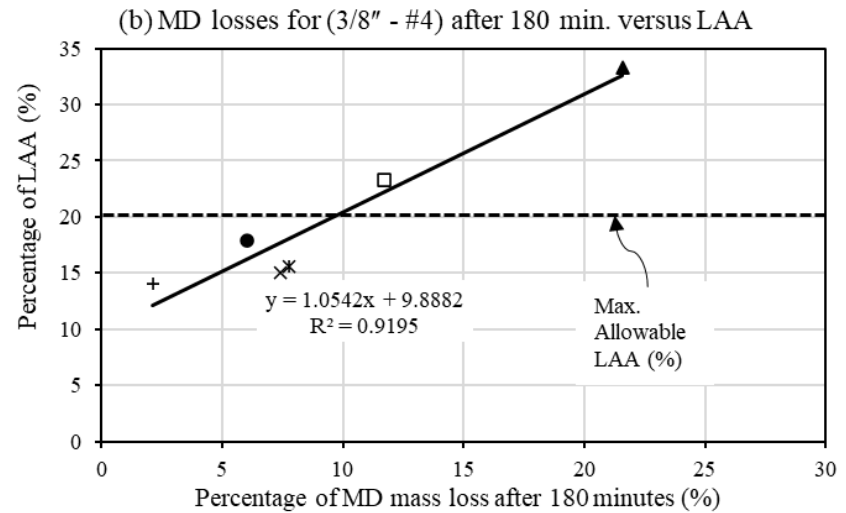
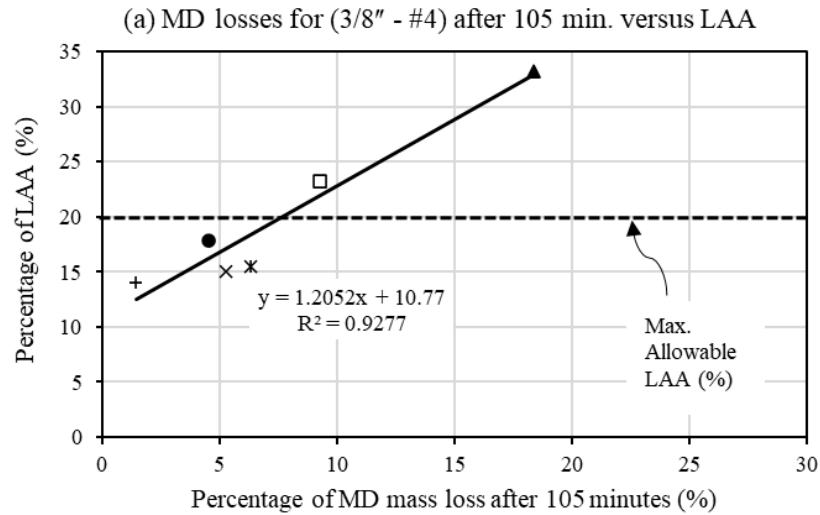


Figure 6-3 Relationships between the MD mass losses and LAA.

6.4 Relationship between Uncompacted Void Content, Micro-Deval, Sand Patch, and Aggregate Image Measurement System Results

6.4.1 Effect of Micro-Deval Polishing Time on the Uncompacted Void Content Percentages

Figure 6-4 shows the percentages of Uncompacted Void Content (UVC) for aggregates using (#6 - #16) gradation and (#6 - #8) size (see Table 3-3). The percentages were calculated for the aggregates using Before Micro-Deval polishing (BMD), After 5-minutes of Micro-Deval polishing time (AMD 5), After 15-minutes of Micro-Deval polishing time (AMD 15), and After 30-minutes of Micro-Deval polishing time (AMD 30). The percentages of UVC decreased and reached the lowest values after 30-minutes MD polishing time. Flint Chat had the highest percentages of UVC before and after polishing. Meramec River Aggregate showed the lowest percentages of UVC, and after polishing, it showed steady low percentages of UVC. The relationship between the times of MD polishing and percentages of UVC was explored based on the results discussed in Figure 6-4. The relationship between UVC percentages and MD polishing times is presented in Equation 6.3 [(UVC-MD t) model]. Figure 6-5 displays the relationship between the MD polishing times and the percentages of the UVC for Rhyolite using Equation 6.3. The goodness-of-fit for Rhyolite is shown in Figure 6-6. The fitting parameters and the goodness-of-fit using the remaining aggregates are presented in Table 6-4. Fitting parameter values were evaluated using Excel by minimizing the SSE.

$$UVC = a + b \times e^{(-c \times t)} \quad \text{Equation 6.3}$$

where,

UVC is the uncompacted void content percentage,
(a , b , and c) are the fitting parameters, and
 t is the Micro-Deval (MD) polishing time in minutes.

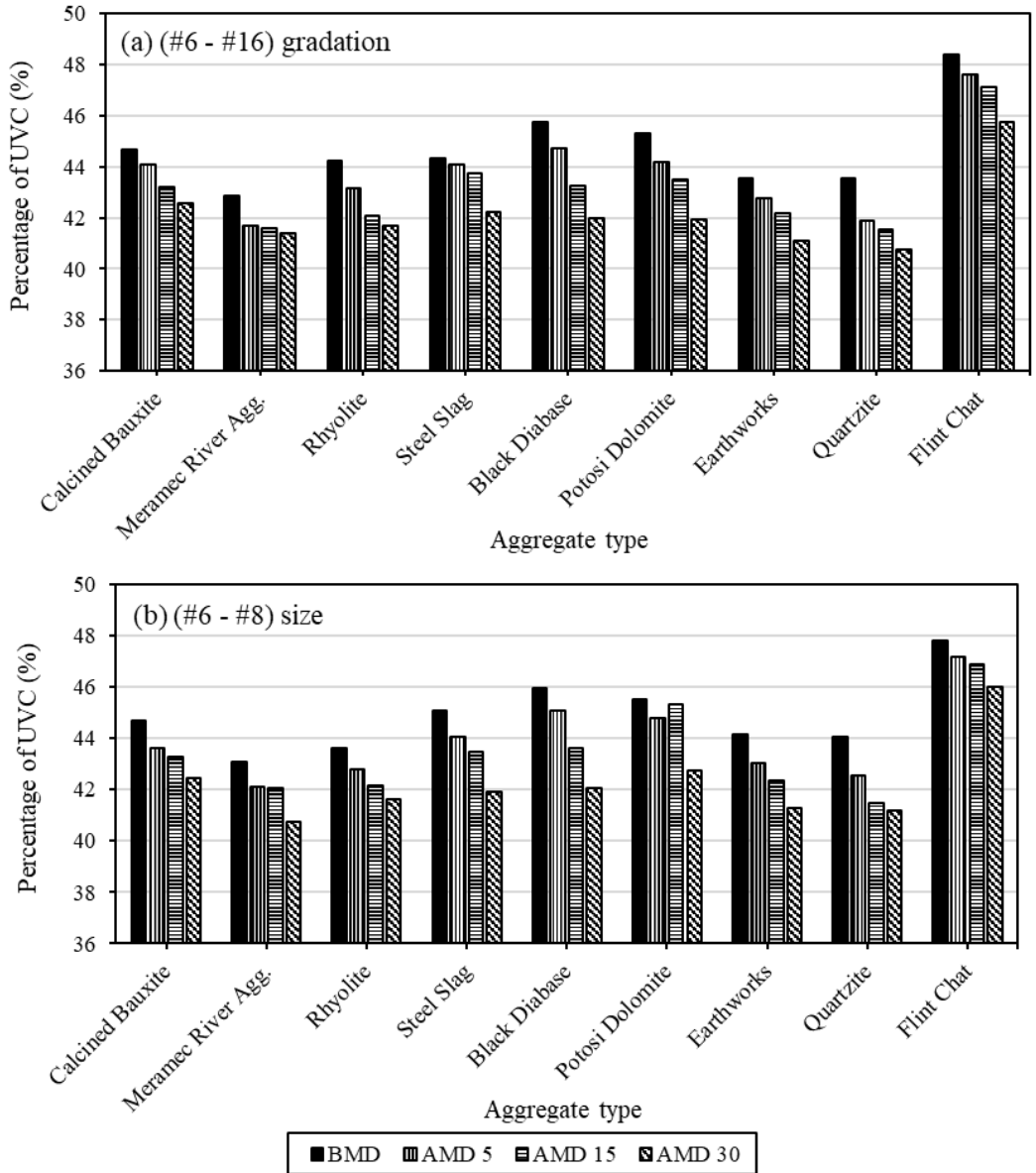


Figure 6-4 Effect of MD polishing times on the UVC percentages with two sizes.

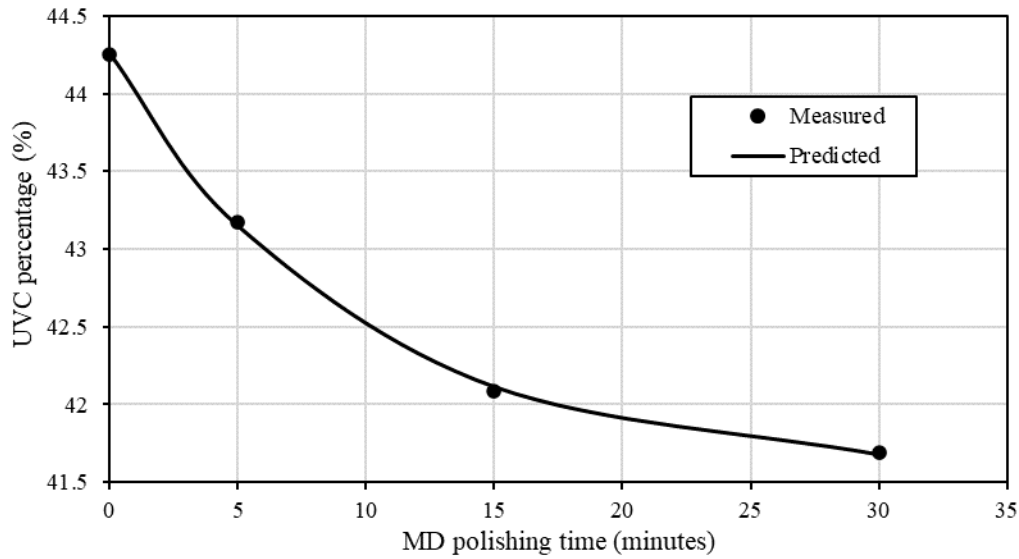


Figure 6-5 Relationship between the MD polishing times and the UVC percentages for Rhyolite.

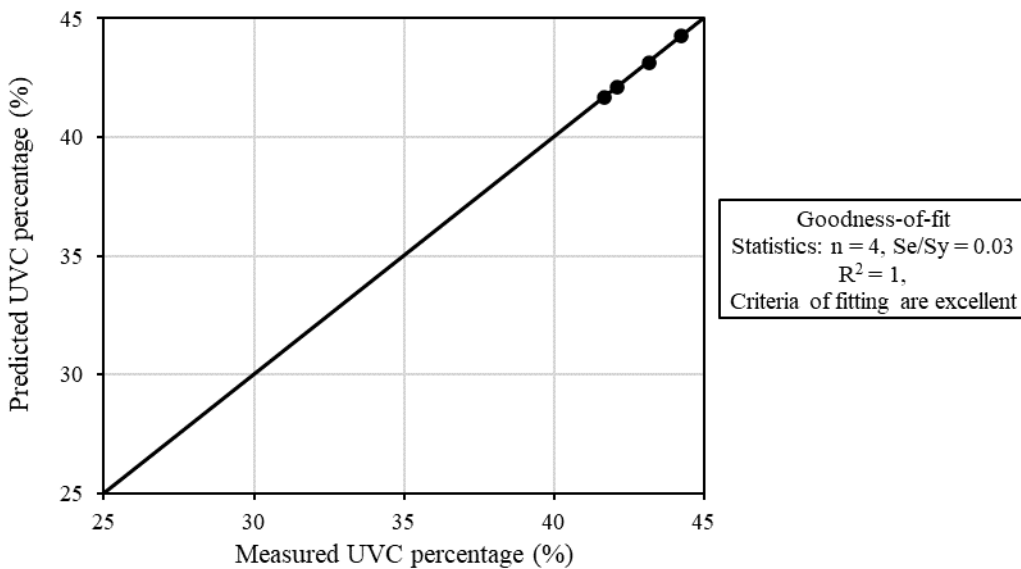


Figure 6-6 Predicted versus measured UVC percentages for Rhyolite.

Table 6-4 Fitting parameters for (UVC-MD t) model.

Aggregate Type	<i>a</i>	<i>b</i>	<i>c</i>	<i>SSE</i>	<i>S_e/S_y</i>	<i>R</i> ²
Calcined Bauxite (CB)	41.971	2.732	0.052	1.207E-03	0.037	1.000
Meramec River Agg.	41.466	1.380	0.347	1.963E-02	0.211	0.985
Rhyolite	41.565	2.692	0.106	1.211E-03	0.030	1.000
Steel Slag	10.000	34.453	0.002	1.635E-01	0.432	0.938
Black Diabase	40.551	5.214	0.044	3.213E-05	0.003	1.000
Potosi Dolomite	38.496	6.668	0.022	1.272E-01	0.251	0.979
Earthworks	39.334	4.141	0.028	4.340E-02	0.200	0.987
Quartzite	40.943	2.569	0.162	2.248E-01	0.398	0.947
Flint Chat	40.150	8.167	0.012	8.589E-02	0.261	0.977

Figure 6-7 presents the effect of the aggregate size [(#6 - #8) size and (#6 - #16) gradation] on the Uncompacted Void Content (UVC) percentages regarding Before Micro-Deval polishing (BMD), After 5-minutes of Micro-Deval polishing time (AMD 5), After 15-minutes of Micro-Deval polishing time (AMD15), and After 30-minutes of Micro-Deval polishing time (AMD 30). There was an inconsiderable change in the percentage of UVC with changing the size of the aggregates.

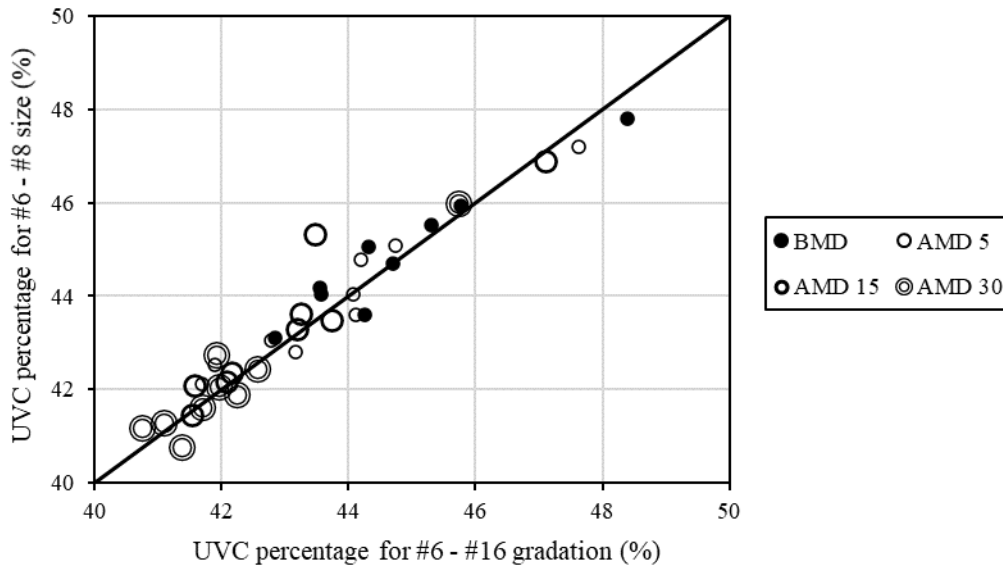


Figure 6-7 Relationship between UVC percentages for two sizes.

6.4.2 Relationship between Percentages of Uncompacted Void Content and Angularity Indices

The percentages of the UVC were used as indirect measures of the fine aggregate angularity. Thus, the relationship between Aggregate Image Measurement System (AIMS) Gradient Angularity (GA) indices BMD polishing for (1/4" - #4) size and the percentages of the UVC of standard graded [(#8 - #100) gradation, see Table 3-3] aggregates are illustrated in Figure 6-8. No specific relationship is noted in Figure 6-8. The highest GA index and percentage of UVC were recorded for Steel Slag. Nevertheless, Calcined Bauxite (CB) provided the lowest percentage of UVC and the second-lowest GA index after Meramec River Aggregate.

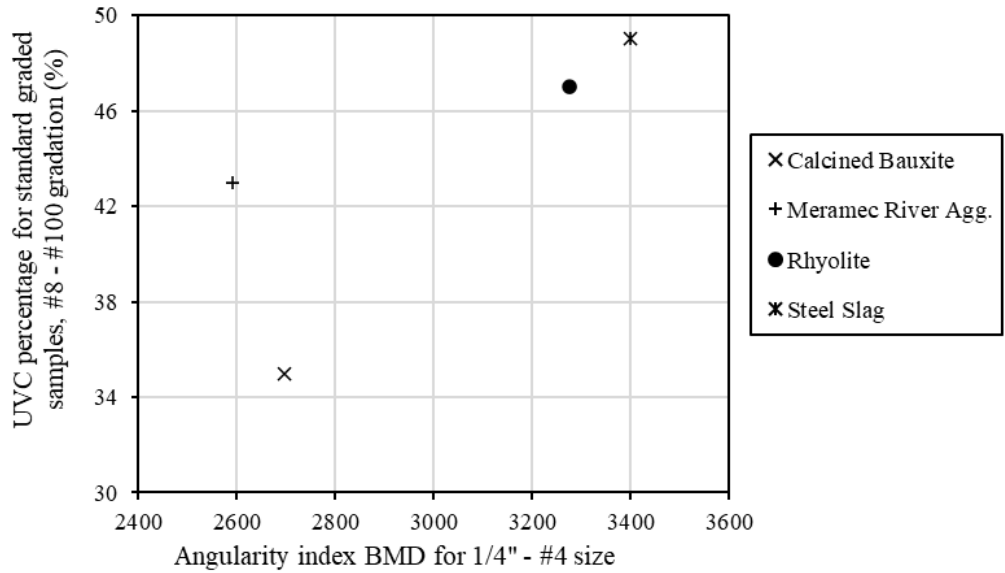


Figure 6-8 Relationship between UVC percentages with (#8 - #100) gradation and the GA indices.

Figure 6-9 shows the relationship between Aggregate Image Measurement System (AIMS) Gradient Angularity (GA) indices Before Micro-Deval polishing (BMD) for (1/4" - #4) size and the percentages of the Uncompacted Void Content (UVC) of (#6 - #8) size; see Table 3-3 for more details. No specific relationship is observed in Figure 6-9. Meramec River Aggregate had the lowest UVC percentage and the lowest GA index. The highest GA index was for Earthworks, and the highest percentage of the UVC was recorded for Flint Chat.

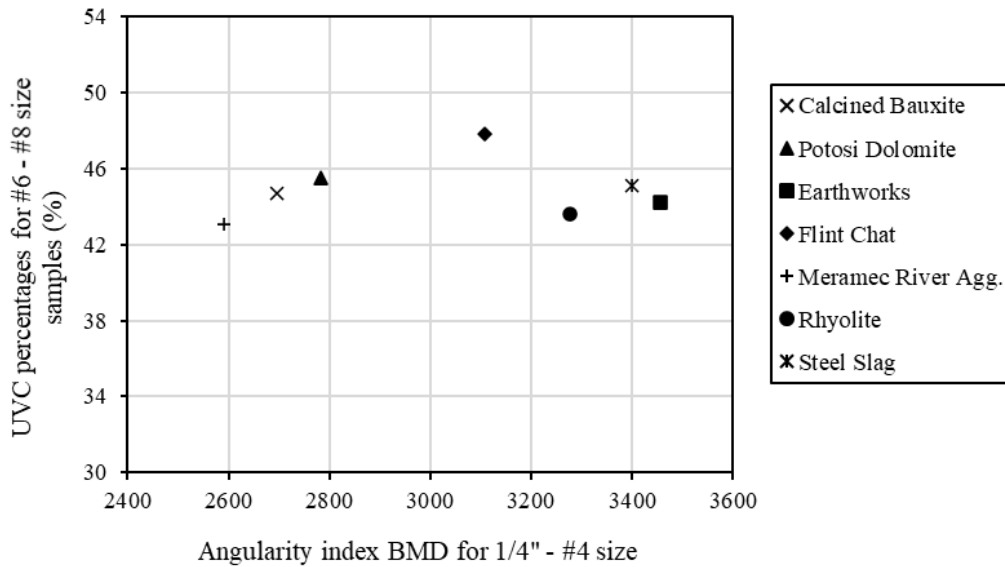


Figure 6-9 Relationship between UVC percentages with (#6 - #8) size and the GA indices.

Figure 6-10 displays the relationship between AIMS Gradient Angularity (GA) indices BMD for (1/4" - #4) size and the percentages of the UVC of Calcined Bauxite (CB), along with six alternatives using CB gradation [(#6 - #16), see Table 3-3]. No specific relationship is noted in Figure 6-10. Meramec River Aggregate had the lowest Uncompacted Void Content (UVC) percentage and the lowest GA index. Note

that the highest GA index was for Earthworks, and the highest percentage of the UVC was recorded for Flint Chat.

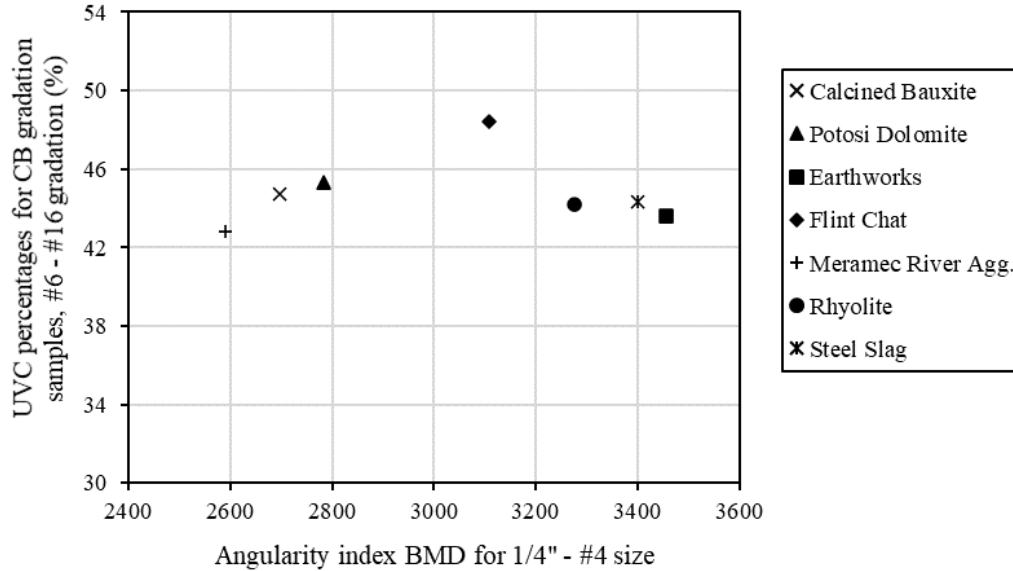


Figure 6-10 Relationship between UVC percentages with (#6 - #16) gradation and the GA indices.

6.4.3 Relationship between Percentages of Uncompacted Void Content and Mean Texture Depth Values

Figure 6-11 displays the relationship between the percentages of the UVC for standard graded [(#8 - #100) gradation, note Table 3-3] aggregates and the Mean Texture Depth (MTD) for (#6 - #8) size aggregates before polishing. No specific relationship is observed in Figure 6-11. Steel Slag had the highest MTD and percentage of UVC, and Calcined Bauxite (CB) showed the lowest MTD and percentage of UVC.

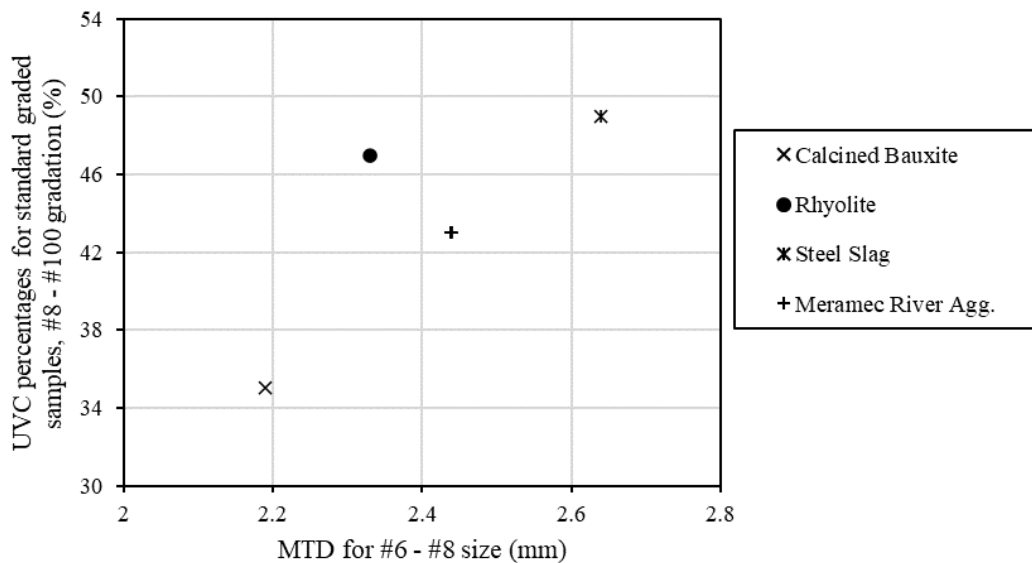


Figure 6-11 Relationship between UVC percentages with (#8 - #100) gradation and the MTD values.

Figure 6-12 exhibits the relationship between Uncompacted Void Content (UVC) percentages and MTD values for aggregates with (#6 - #8) size before polishing, note Table 3-3. Figure 6-13 displays the

relationships between UVC percentages for aggregates with CB gradation [(#6 - #16), Table 3-3] and MTD data for (#6 - #8) size aggregates before polishing. No specific relationships are noted between the UVC percentages and Mean Texture Depth (MTD) values. In both figures, Flint Chat had the highest MTD values and UVC percentages. The lowest UVC percentages were for Meramec River Aggregate, and the lowest MTD values were for Calcined Bauxite (CB).

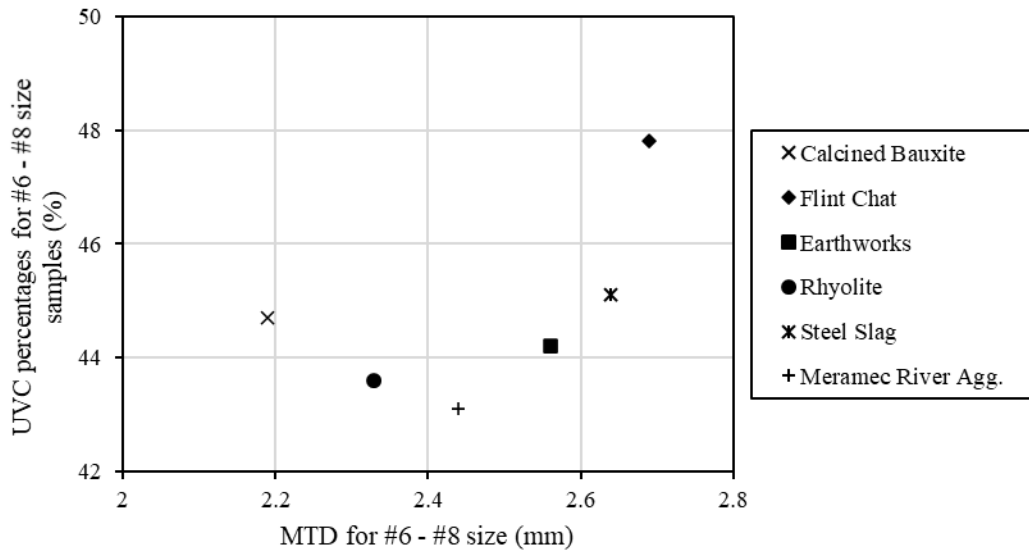


Figure 6-12 Relationship between UVC percentages with (#6 - #8) size and the MTD values.

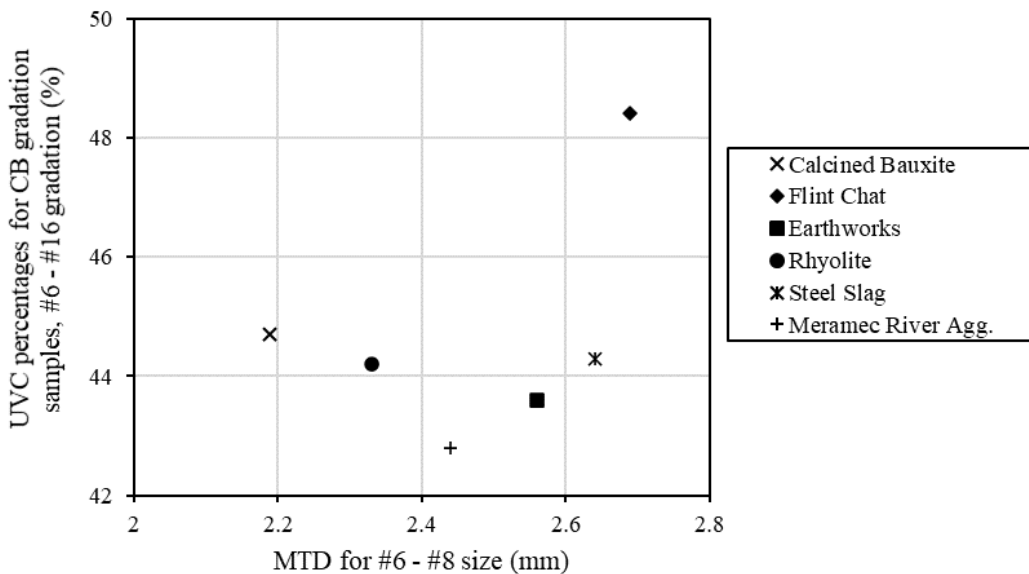


Figure 6-13 Relationship between UVC percentages with (#6 - #16) gradation and the MTD values.

6.4.4 Relationship between Mean Texture Depth Values and Angularity Indices

Figure 6-14 depicts the relationship between Aggregate Image Measurement System (AIMS) Gradient Angularity (GA) indices for (1/4" - #4) size and (#6 - #8) size MTD values for aggregates before polishing. No specific relationship is observed between the MTD values and GA indices. Calcined Bauxite showed the lowest MTD value, and Flint Chat exhibited the highest MTD value. Flint Chat had the highest Uncompacted Void Content (UVC) percentages in Figure 6-12 and Figure 6-13. Meramec River

Aggregate had the lowest GA index, and Earthworks had the highest GA index. Meramec river aggregates had the lowest UVC percentages in Figure 6-12 and Figure 6-13.

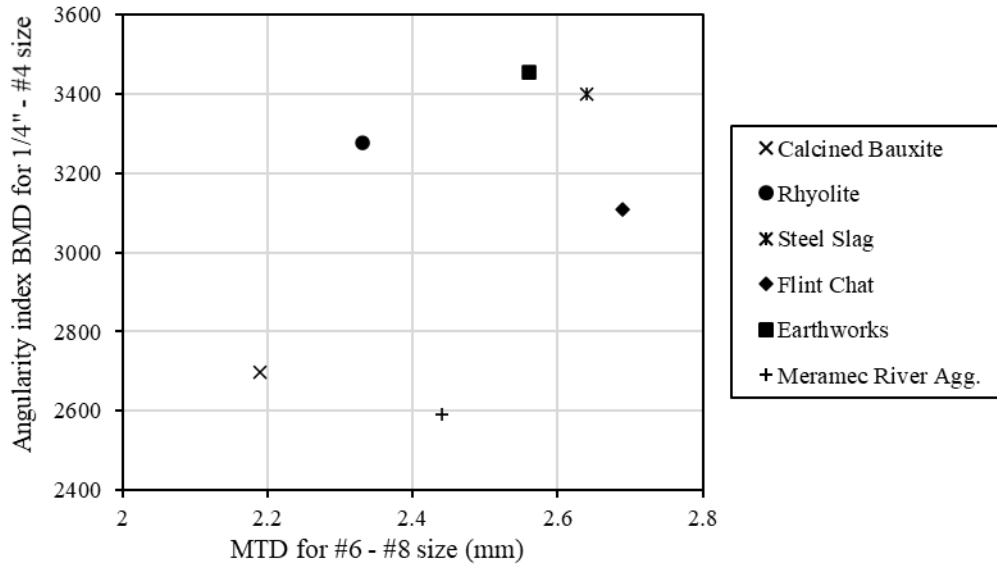


Figure 6-14 Relationship between GA indices and the MTD values.

6.5 Comparing Aggregate Image Measurement System and British Pendulum Test Results

In this section, average Aggregate Image Measurement System (AIMS) Texture (TX) and Gradient Angularity (GA) indices for (3/8" - 1/4") and (1/4" - #4) aggregate sizes were compared with average British Pendulum Number (BPN) values for (#4 - #6) and (#6 - #8) aggregate sizes. Figure 6-15 shows average BPN and AIMS results for aggregates. Average pre-polish BPN values were compared with average AIMS TX and GA indices Before Micro-Deval polishing (BMD) (Figure 6-15a and Figure 6-15b). Furthermore, average post-polish BPN values were compared with average AIMS TX and GA indices for After 180-minutes of Micro-Deval polishing time (AMD 180) (Figure 6-15c and Figure 6-15d). No specific trend was noted between AIMS and BPN results. Potosi Dolomite presented the highest BPN values before and after polishing; however, it showed the lowest GA indices for BMD and AMD 180, the second-lowest TX index for AMD 180, and the third-lowest TX index for BMD. Furthermore, Potosi Dolomite depicted the highest mass loss percentages for After 105-minutes of Micro-Deval polishing time (AMD 105) and AMD 180.

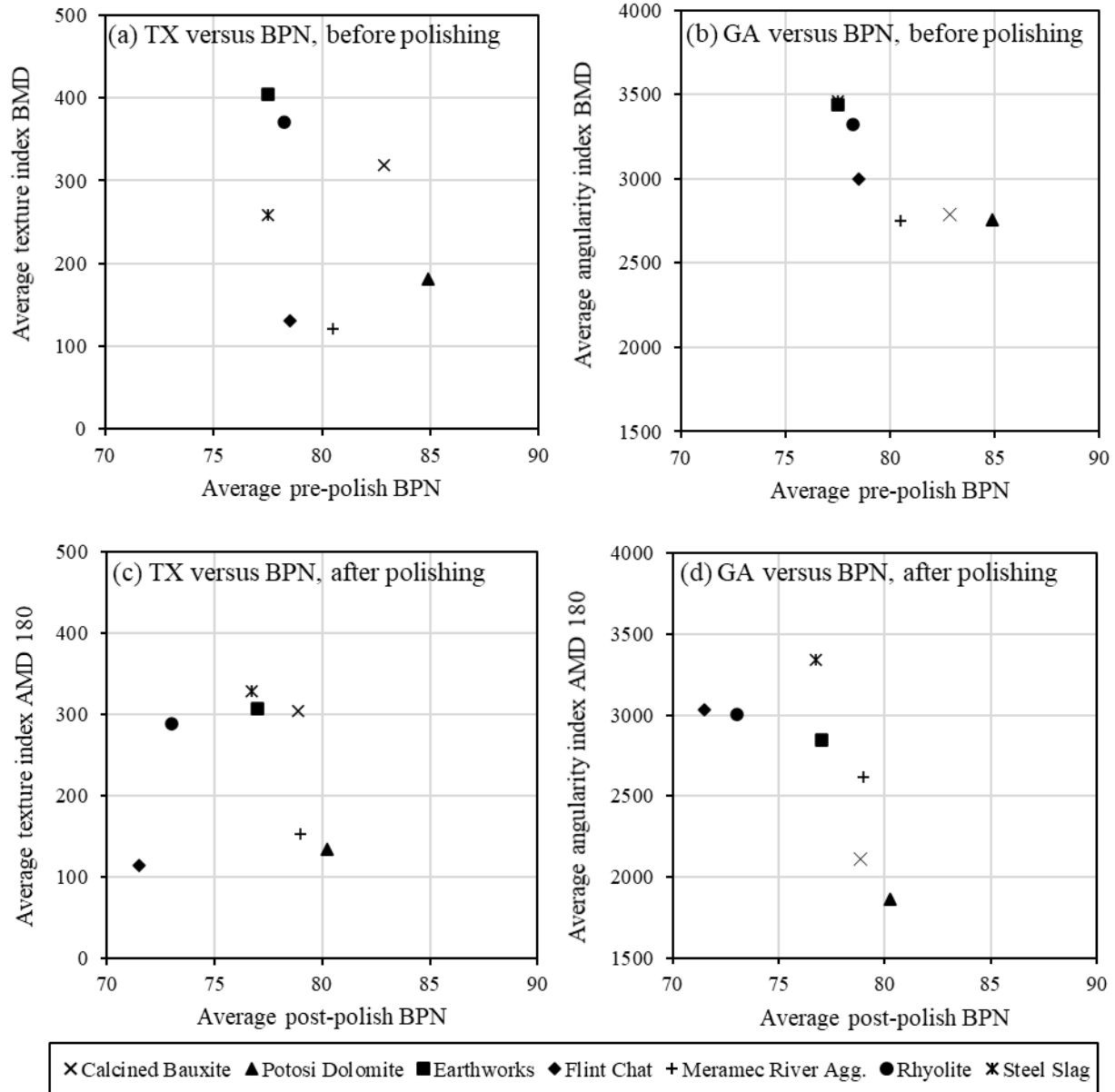


Figure 6-15 Relationships between AIMS and BP results.

6.6 Comparing Aggregate Image Measurement System and Dynamic Friction Test Results

Average Aggregate Image Measurement System (AIMS) Texture (TX) and Gradient Angularity (GA) indices for (3/8" - 1/4") and (1/4" - #4) aggregate sizes were compared with the average Coefficient of Friction (COF) values measured by DFT at 40 km/hr (DFT₄₀) for (#6 - #8) aggregate size. Figure 6-16 exhibits average DFT₄₀ and AIMS results for aggregates. Average initial DFT₄₀ were compared with average AIMS TX and GA indices Before Micro-Deval polishing (BMD) (Figure 6-16a and Figure 6-16b). Average terminal DFT₄₀ were compared with average AIMS TX and GA indices for After 180-minutes of Micro-Deval polishing time (AMD 180) (Figure 6-16c and Figure 6-16d). There were no significant relationships between AIMS and Dynamic Friction Tester (DFT) results. Calcined Bauxite had the highest initial and terminal DFT₄₀; however, it yielded the lowest GA indices for BMD and AMD 180. Steel Slag resulted in the lowest initial DFT₄₀ after Meramec River Aggregate; however, it had the

highest AIMS GA indices for BMD and AMD 180. Earthworks had the lowest terminal DFT₄₀; however, it had the second-highest AIMS TX index for AMD 180.

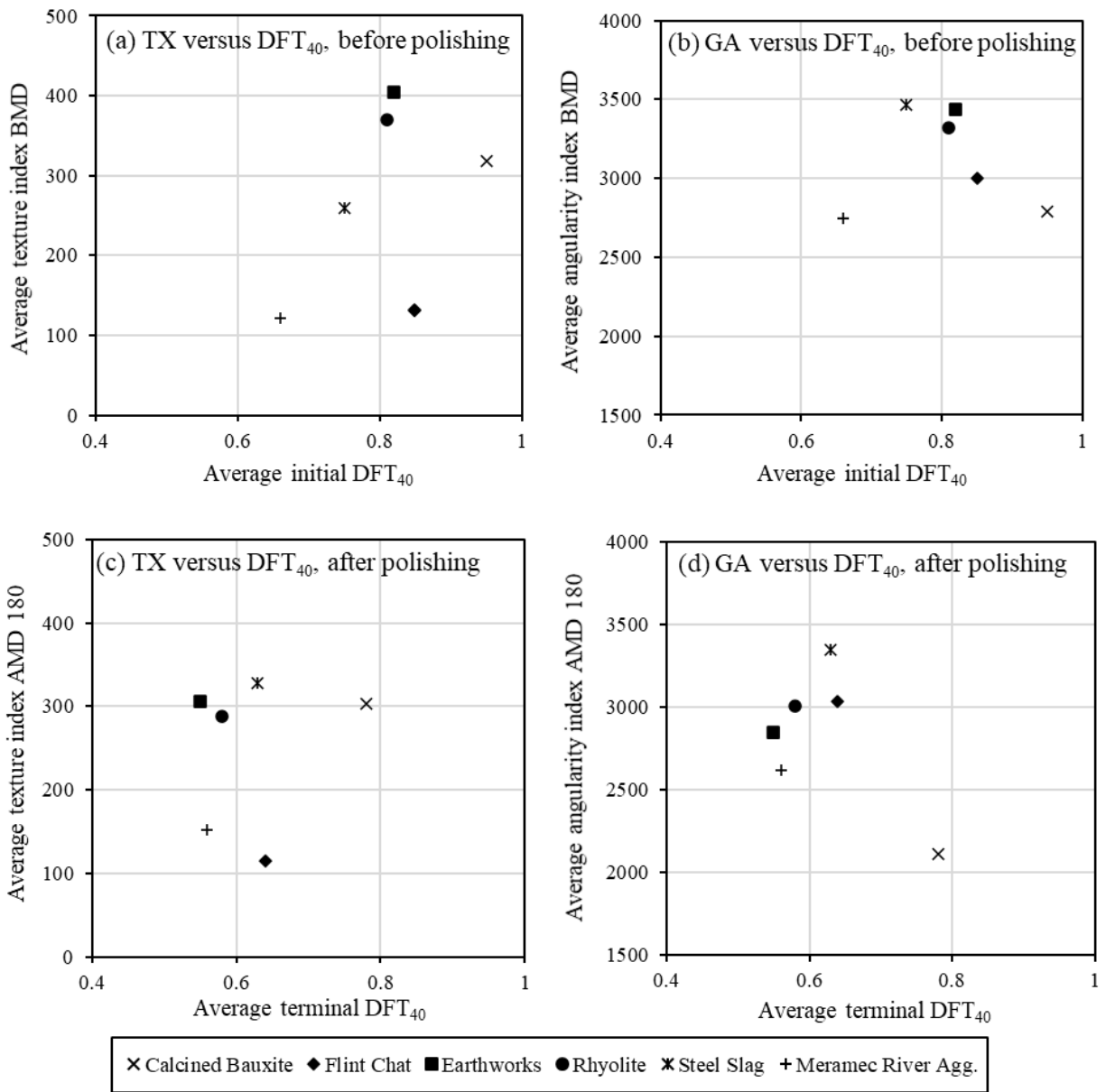


Figure 6-16 Relationships between AIMS and DFT results.

6.7 Comparing British Pendulum Test and Dynamic Friction Test Results

Relationships between Coefficient of Friction (COF) values measured by DFT at 40 km/hr (DFT₄₀) and British Pendulum Number (BPN) values are shown in Figure 6-17; they include aggregates with (#6 - #8) size before and after polishing. The relationships between average initial DFT₄₀ and averaged pre-polish BPN are presented in Figure 6-17a. Calcined Bauxite had the highest average initial DFT₄₀ and the highest average pre-polish BPN values. Steel Slag had the lowest average pre-polish BPN value, and Meramec River Aggregate had the lowest average initial DFT₄₀. Figure 6-17b exhibits the relationship between average terminal DFT₄₀ and average post-polish BPN results. No specific relationship is noted

from this figure. Calcined Bauxite showed the highest average terminal DFT₄₀, and Meramec River Aggregate had the highest average post-polish BPN values. However, Rhyolite had the lowest values.

Figure 6-17c presents the relationship between average DFT₄₀ and average British Pendulum Number (BPN) values. No specific relationship is noted from the figure. Before the polishing process, by the Three-Wheel Polishing Device (TWPD) or the British wheel, aggregates presented the highest COF using Dynamic Friction Tester (DFT) and the BPN results. By contrast, after polishing, the DFT₄₀ and the BPN values decreased. Calcined Bauxite had the highest DFT₄₀ and the highest BPN values before and after polishing. Before polishing, Steel Slag had the lowest average pre-polish BPN value, and Meramec River Aggregate had the lowest average initial DFT₄₀. After polishing, Rhyolite had the lowest values.

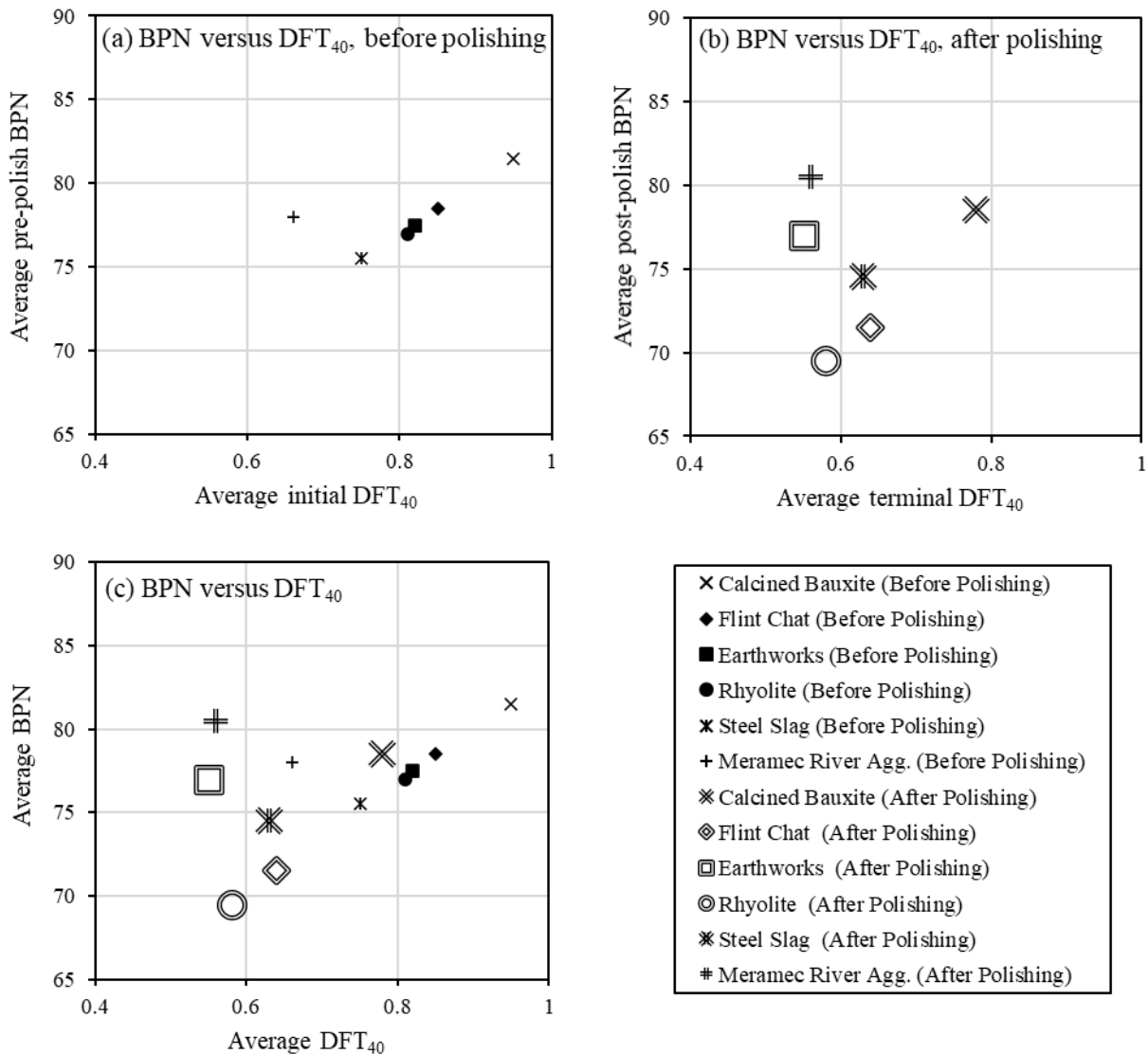


Figure 6-17 Relationships between BP and DFT results.

Table 6-5 presents the rankings of aggregates based on British Pendulum Number (BPN) and Coefficient of Friction (COF) values measured by DFT at 40 km/hr (DFT₄₀). The aggregates were ranked from 1 to 6 based on the average BPN values and average DFT₄₀. Aggregates with the highest average BPN values or average DFT₄₀ were scored with 1. The aggregate rankings based on initial DFT₄₀ showed that Calcined

Bauxite (CB) was the best followed by Flint Chat, and Meramec River Aggregate was the worst. The aggregate rankings based on the pre-polish BPN values illustrated that CB was the best followed by Flint Chat and then Meramec River Aggregate. However, Steel Slag was the worst. The aggregate rankings based on terminal DFT₄₀ showed that Calcined Bauxite (CB) was the best followed by Flint Chat. However, Meramec River Aggregate had the best ranking followed by CB based on the post-polish BPN values. The aggregate ranking for the terminal DFT₄₀ exhibited that Earthworks aggregate was the worst. However, Rhyolite had the worst ranking based on the post-polish BPN values.

Table 6-5 Ranking of aggregates based on DFT and BP results.

Aggregate Type	Ranking			
	Based on Average Initial DFT ₄₀ for (#6 - #8) Size	Based on Average Terminal DFT ₄₀ for (#6 - #8) Size	Based on Average Pre-Polish BPN for (#6 - #8) Size	Based on Average Post-Polish BPN for (#6 - #8) Size
Calcined Bauxite (CB)	1	1	1	2
Earthworks	3	6	4	3
Flint Chat	2	2	2	5
Rhyolite	4	4	5	6
Steel Slag	5	3	6	4
Meramec River Agg.	6	5	3	1

6.8 Comparing the Predicted Initial and Terminal Skid Number Values for Alternatives

In this section, the predicted initial and terminal Skid Number (SN) values were calculated from Skid Number measured at 50 mi/hr by a skid trailer with smooth tires [SN(50)] or Skid Number measured at 40 mi/hr by a skid trailer with Ribbed tires (SN40R) prediction models (Equation B.23, Equation B.36, and Equation B.37). The Aggregate Image Measurement System (AIMS), British Pendulum (BP), and Coefficient of Friction (COF) values measured by DFT at 40 km/hr (DFT₄₀) results were used to obtain the SN values from the prediction models. AIMS results were used to predict the SN(50) (Equation B.23); however, the British Pendulum Number (BPN) or Coefficient of Friction (COF) using DFT₄₀ results were utilized to calculate the SN40R (Equation B.36 and Equation B.37). Figure 6-18 illustrates the predicted initial SN values for High Friction Surface Treatment (HFST) applications. Based on the predicted initial SN values, CB had the highest values followed by Meramec River Aggregate, Potosi Dolomite, and Flint Chat aggregates. Furthermore, Potosi Dolomite showed the highest predicted initial SN40R based on BP results. Steel Slag presented the lowest predicted initial SN values. No differences were observed between the predicted initial SN values for Rhyolite and Earthworks.

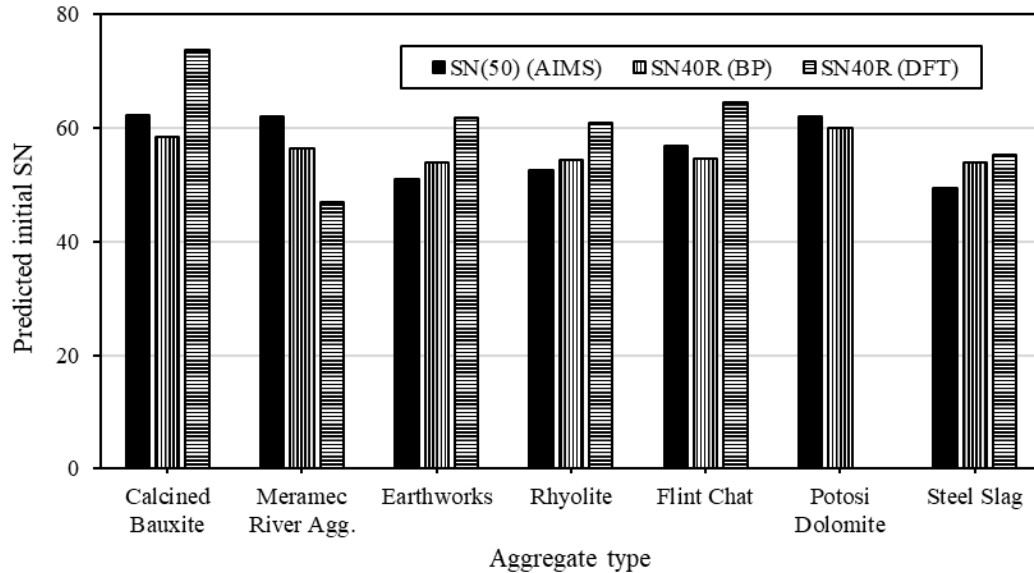


Figure 6-18 Predicted initial SN values for HFST applications.

Figure 6-19 exhibits the predicted terminal Skid Number (SN) values for High Friction Surface Treatment (HFST) applications. The predicted terminal SN values—indicated in Figure 6-19—decreased compared to the initial SN values (presented in Figure 6-18). The highest SN values were recorded for the Skid Number measured at 40 mi/hr by a skid trailer with Ribbed tires (SN40R), as predicted. Nevertheless, the lowest SN values were observed for the Skid Number measured at 50 mi/hr by a skid trailer with smooth tires [SN(50)], as predicted. It was rational for SN(50) values to be the lowest of SN values because the SN(50) values were predicted at 50 mi/hr by a skid trailer with smooth tires. Note that the SN40R values were predicted at 40 mi/hr by a skid trailer with ribbed tires. The SN values for the Flint Chat had an opposite trend: the SN(50) value was greater than the SN40R value. This happened because Flint Chat was the only aggregate that had an increase in the Aggregate Image Measurement System (AIMS) Gradient Angularity (GA) indices after Micro-Deval (MD) polishing. Based on the predicted terminal SN values, Calcined Bauxite (CB), Meramec River Aggregate, and Flint Chat aggregates had high SN values. Steel Slag had the lowest terminal SN(50) value; however, it had comparable SN40R values to Flint Chat, Rhyolite, and Earthworks. Potosi Dolomite showed the highest terminal SN40R based on British Pendulum (BP) results; however, it presented the third-lowest terminal SN(50) value based on AIMS results.

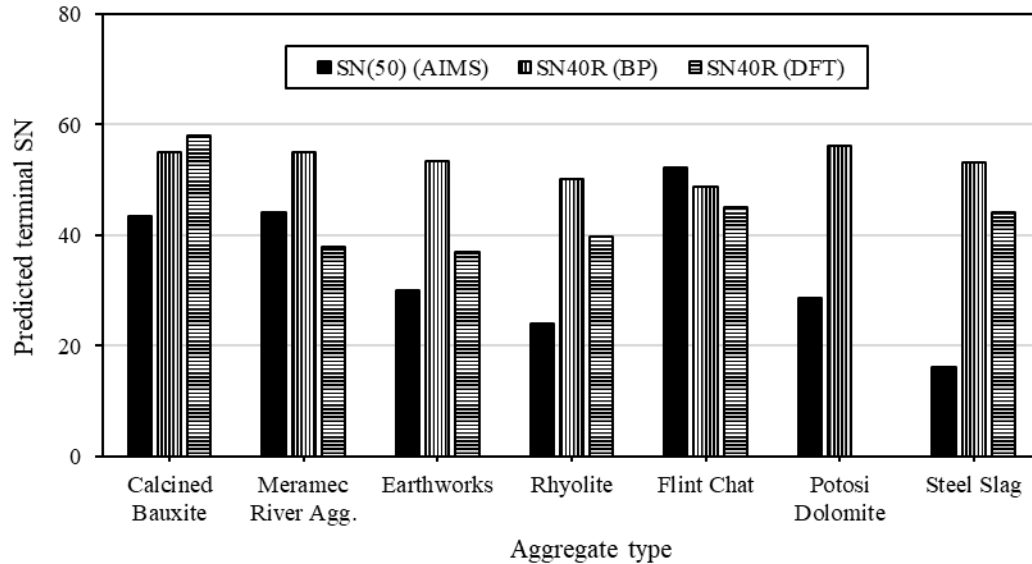


Figure 6-19 Predicted terminal SN values for HFST applications.

Table 6-6 presents ranking comparisons of High Friction Surface Treatment (HFST) aggregates based on Skid Number (SN) values for aggregates. Potosi Dolomite was excluded from this comparison because the dynamic friction test was not implemented for this aggregate. HFST aggregates were ranked from 1 to 6 based on the SN values: 1 indicated the aggregates with the highest SN values, and 6 indicated the aggregates with the lowest SN value. According to the rankings based on the initial SN values, Calcined Bauxite (CB) was the best followed by Flint Chat and Meramec River Aggregate. Steel Slag had the worst aggregate ranking. Based on the terminal SN values, CB was the best followed by Meramec River Aggregate and Flint Chat. Rhyolite was the worst aggregate.

Table 6-6 Ranking of aggregates based on predicted SN values.

Aggregate Type	Ranking					
	Predicted Initial SN(50) Based on AIMS	Predicted Initial SN40R Based on BP	Predicted Initial SN40R Based on DFT ₄₀	Predicted Terminal SN(50) Based on AIMS	Predicted Terminal SN40R Based on BP	Predicted Terminal SN40R Based on DFT ₄₀
Calcined Bauxite (CB)	1	1	1	3	2	1
Earthworks	5	5	3	4	3	6
Rhyolite	4	4	4	5	5	4
Flint Chat	3	3	2	1	6	2
Steel Slag	6	5	5	6	4	3
Meramec River Agg.	2	2	6	2	1	5

6.9 Relating Physical Properties and Durability Testing to Performance Testing

6.9.1 Relating Uncompacted Void Content Percentages to Angularity Indices and Mean Texture Depth

By analyzing Uncompacted Void Content (UVC) results [(#6 - #8) and (#6 - #16) sizes], Meramec River Aggregate had the lowest UVC percentage, and Steel Slag had higher UVC percentage than CB. The UVC results [(#8 - #100) gradation] showed that Meramec River Aggregate had the second lowest UVC percentage after CB, and Steel Slag had the highest UVC percentage. No specific relationships were observed between the Gradient Angularity (GA) indices and the UVC percentages, and no specific relationships were noted between the Mean Texture Depth (MTD) and the UVC percentages.

6.9.2 Relating Durability Testing to Performance Testing

Earthworks and Meramec River Aggregate had the lowest specific gravity, and Steel Slag had the highest specific gravity after CB. The Los Angeles Abrasion (LAA) Part-I test (grading D) results demonstrated that Meramec River Aggregate had the lowest LAA percentage. Steel Slag had the third lowest LAA percentage after Meramec River Aggregate and CB. For Part-II testing (gradings B, C, or D), CB had the lowest percentage of LAA, followed by Steel Slag, Meramec River Aggregate, and Earthworks. According to the HFST requirements for LAA (NJSP-15-13B), Part-I testing (grading D), Black Diabase (1/4") and Potosi Dolomite (9/16" Clean) exceeded the maximum LAA limit (20%). For part-II testing (gradings B, C, or D), Rhyolite, Black Diabase (3/8"), Meramec River Aggregate (C. gravel), Quartzite, and Flint Chat (#6 × #16) exceeded the LAA maximum limit. Meramec River Aggregate had the best sodium sulfate soundness results (lowest mass losses) among the alternative aggregates followed by Rhyolite and then Steel Slag. The highest percentage lost was noted for Potosi Dolomite. Meramec River aggregate, Earthworks, and Steel Slag had lower percentages of water-alcohol freeze thaw mass losses when compared to CB. The acid-insoluble residue results showed that Meramec River Aggregate and Earthworks had comparable residues percentages with CB; however, Steel Slag had percentage lower than the minimum allowable limit.

For the performance testing, for the coarse gradation (3/8" - #4), Meramec River Aggregate had the lowest Micro-Deval (MD) mass loss percentage after 180-minutes polishing time followed by Earthworks. Steel Slag had lower mass losses percentages than Black Diabase and Potosi Dolomite (the worst aggregate). For the fine gradation (#6 - #16), CB had the lowest MD mass loss followed by Meramec River Aggregate, and then Earthworks. Steel Slag had lower MD mass losses than Flint Chat, Quartzite, Black Diabase, and Potosi Dolomite. The Dynamic Friction Tester (DFT) results for (#6 - #8) size showed that CB had the highest terminal Coefficient of Friction (COF) value followed by Flint Chat, Steel Slag, Rhyolite, and Meramec River Aggregate. The lowest terminal COF value for (#6 - #8) size was noted for Earthworks. The initial COF values showed that CB had the highest value followed by Flint Chat, Earthworks, Rhyolite, and then Steel Slag. Meramec River Aggregate had the lowest value. The average pre-polish British Pendulum Number (BPN) values for (#6 - #8) and (#4 - #6) sizes deemed that Potosi Dolomite had the highest value followed by CB, Meramec River Aggregate, Flint Chat, Rhyolite, Earthworks. However, Steel Slag had the lowest value. Based on the average post-polish BPN values for (#6 - #8) and (#4 - #6) sizes, Potosi Dolomite had the highest value followed by Meramec River Aggregate, CB, Earthworks, Steel Slag, Rhyolite. By contrast, Flint Chat aggregate had the lowest value.

6.9.3 Relating Micro-Deval Mass Losses and Los Angeles Abrasion to the British Pendulum Number

The Micro-Deval (MD) mass losses and Los Angeles abrasion (LAA) percentages were related to the British Pendulum Number (BPN) values for the aggregates used in each testing. The MD test was conducted for aggregates with (#6 - #16) gradation and calculated for (#6 - #8) after 30 minutes polishing time. The post-polish BPN values for the same aggregates with (#6 - #8) size, and the LAA percentages were conducted based on Part-I testing (grading D). An inverse relationship was observed between the MD mass losses and BPN values (see Figure 6-20a), and between the LAA percentages and BPN values (note Figure 6-20b). The relationship between the MD mass losses and BPN values was stronger than the relationship between the LAA percentages and BPN values. This occurred because the MD test could reflect the aggregates' performance more than the LAA test.

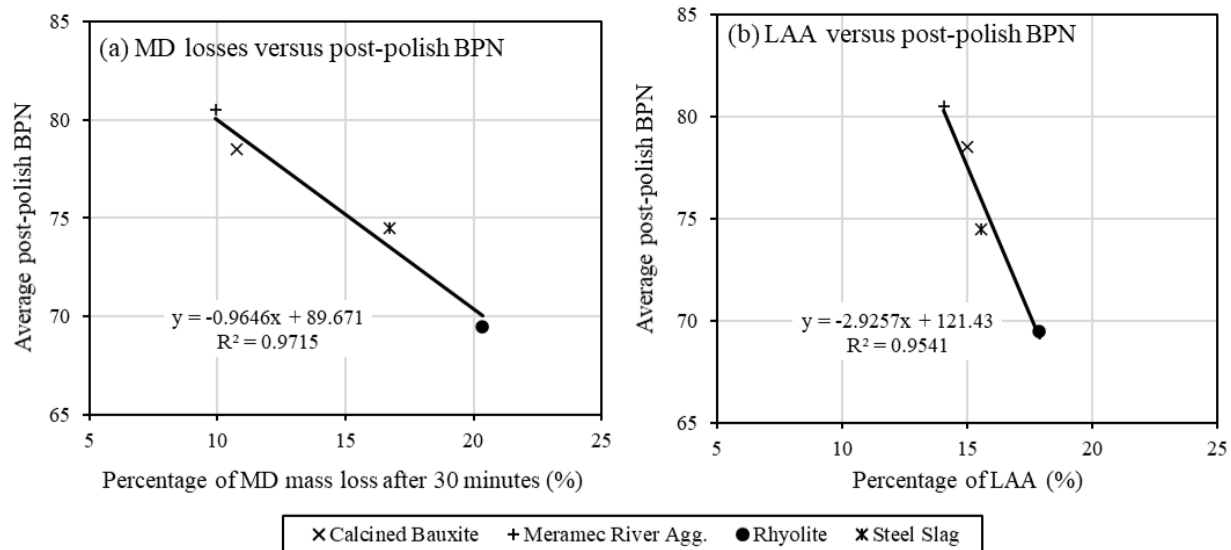


Figure 6-20 Relationships between MD mass losses' percentages or LAA percentages and BPN values.

6.10 Summary

The relationships between Micro-Deval (MD) mass losses and Aggregate Image Measurement System (AIMS) Texture (TX) indices or AIMS Gradient Angularity (GA) indices explored that no specific relationships were found. There was a direct linear relationship between the Los Angeles Abrasion (LAA) and MD mass losses. The MD was found to be more sensitive for aggregate screening than LA. The relationship between the Uncompacted Void Content (UVC) percentages and MD polishing times depicted that increasing the MD polishing times decreased the UVC percentages. This happened due to the change in the GA indices with polishing. However, no specific relationship was observed between the Mean Texture Depth (MTD) values and GA indices. Moreover, no specific relationships were observed between the GA indices and the Uncompacted Void Content (UVC) percentages. No significant relationships were found between British Pendulum (BP) and AIMS results, and between AIMS and Dynamic Friction Tester (DFT) results. This reflected that AIMS could not reflect the friction performance of aggregates; however, it was considered a good tool to explore the changes that occurred in the TX and GA indices. The relationship between the BP and DFT results before the British wheel and Three-Wheel Polishing Device (TWPD) polishing processes illustrated that aggregates with the highest Coefficient of Friction (COF) value had the highest British Pendulum Number (BPN) value [e.g., Calcined Bauxite (CB)]. After the polishing processes, no specific relationship was reflected from the relationship between the BP and DFT results. The Skid Number measured at 50 mi/hr by a skid trailer with smooth tires [SN(50)] values were predicted based on the AIMS TX and GA indices; however, the predicted Skid Number measured at 40 mi/hr by a skid trailer with Ribbed tires (SN40R) values were estimated based on the COF values measured by DFT at 40 km/hr (DFT₄₀) and BPN values. The aggregates were ranked based on the predicted initial and terminal Skid Number (SN) values [SN(50) and SN40R]. According to the rankings based on the initial SN values, CB was the best followed by Flint Chat and Meramec River Aggregate. Steel Slag had the worst aggregate ranking. Based on the terminal SN values, CB was the best followed by Meramec River Aggregate and Flint Chat. Rhyolite was the worst aggregate.

CHAPTER 7: ECONOMIC STUDY

7.1 Introduction

The purpose of using Life Cycle Cost Analysis (LCCA) was to evaluate the short- and long-term economic efficiencies between competing alternatives [i.e., High Friction Surface Treatment (HFST) applications using Calcined Bauxite (CB) and alternative aggregates]. The LCCA incorporates initial and discounted future costs incurred by the agency, user, and other stakeholders over the lifetime of the proposed alternatives. The initial cost includes—but is not limited to—mobilization, labor, epoxy-binder, correct gradation effort costs, and of the aggregate itself.

The LCCA approach estimated the service life of HFST and/or alternative aggregates to provide accurate analyses. Skid analysis of asphalt pavement software was developed mainly for Hot Mix Asphalt (HMA) and seal coat surfaces and will be adopted in this research (Chowdhury et al. 2016). The estimated service life, of HFST and alternative aggregates, needs to be compared to those in MoDOT records to ensure accuracy and consistency. The estimated Skid Number (SN) depends on aggregate Texture (TX) and Gradient Angularity (GA) before and after the Micro-Deval (MD) polishing, aggregate gradation, and traffic level. Furthermore, other prediction models were used to correlate the SN with the Dynamic Friction Tester (DFT) or British Pendulum (BP) results. The research team developed simple procedures through an Excel application based on the developed performance modeling of HFST to be used by MoDOT for evaluating alternative aggregates. The NPVs were estimated for the HFST applications. Based on the Net Present Values (NPVs), the best HFST application was selected. The major purpose of this LCC program was to present a rational method for converting different input data (material and project specifics) into comparable output data (NPV) that facilitated comparison between different alternatives.

7.2 Calculation Process of LCCA

The researchers developed a simple LCC program using Excel to conduct LCCA for the HFST application based on Aggregate Image Measurement System (AIMS), DFT, or BP results. The LCC program interfaces based on AIMS input data are presented in Appendix D; the material specifics are illustrated in Figure D-1, the project specifics input data are shown in Figure D-2, and the output data are deemed in Figure D-3. The LCC program was used to predict the NPVs for HFST applications. Figure 7-1 shows the calculation process of LCCA. The major input data were categorized into material and project specifics. The performance prediction models were used to convert the input data into SN values. The predicted terminal SN was compared with the recommended (or adopted) terminal SN based on the rehabilitation matrix as shown in Table 7-1. This matrix was proposed based on the predicted and recommended terminal SN values. The recommended terminal SN controlled by the program user. The recommended terminal Skid Number measured at 50 mi/hr by a skid trailer with smooth tires [SN(50)] was selected to be 21 [based on Table B-1 (Chowdhury et al. 2016)], and the recommended terminal Skid Number measured at 40 mi/hr by a skid trailer with Ribbed tires (SN40R) was 40 [based on Table B-5 (John J. Henry 2000)]. If the predicted terminal SN value was greater than or equal to the recommended terminal SN value, then nothing should be done. If the predicted terminal SN value was less than the recommended terminal SN value, then it was recommended to remove the old HFST application and add a new one. Finally, the output data were calculated; these data presented the NPVs for the HFST applications. Based on the lowest NPV, the best HFST application was selected. For more details about the input and output data, see Appendix D.

7.3 Performance Prediction

The performance prediction models used in the LCC program were selected, as discussed in Appendix B. The first model (Equation B.23) was used to predict the Skid Number measured at 50 mi/hr by a skid

trailer with smooth tires [SN(50)] from AIMS TX and GA indices for Before Micro-Deval polishing (BMD), After 105-minutes of Micro-Deval polishing time (AMD 105), and After 180-minutes of Micro-Deval polishing time (AMD 180) (Chowdhury et al. 2016; Aldagari et al. 2020). This model was calibrated based on the surface treatments (seal coats) results; however, it was used to compare the performance of the HFST applications. The second model (Equation B.36) aimed to predict the Skid Number measured at 40 mi/hr by a skid trailer with Ribbed tires (SN40R) from the COF values measured by DFT at 40 km/hr (DFT₄₀) before and after polishing. The prediction model presented in Equation B.36 was developed by Heitzman et al. (Heitzman, Turner, and Greer 2015). The third model (Equation B.37) correlated the British Pendulum (BP) results and SN40R (John Jewett Henry and Wambold 1992).

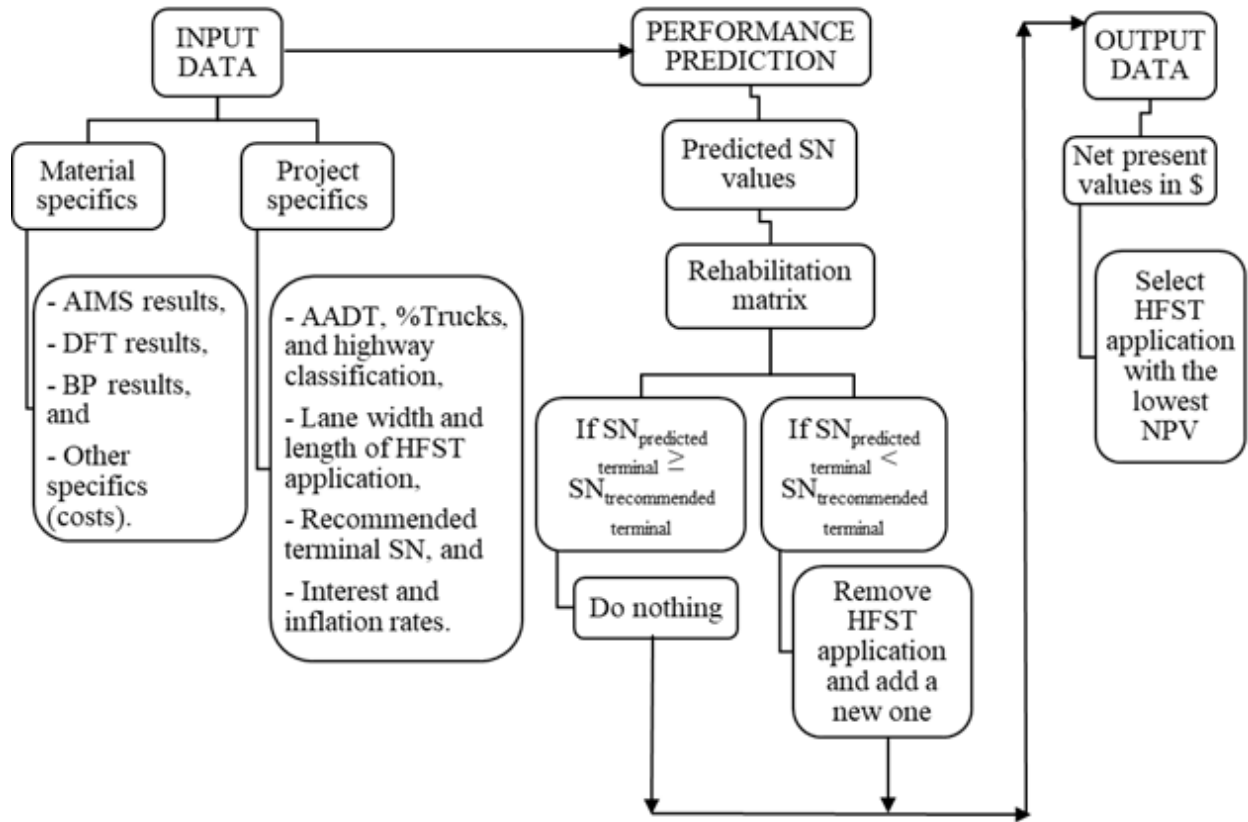


Figure 7-1 LCCA calculation process.

Table 7-1 Rehabilitation matrix for HFST applications.

What if?	Action
Predicted terminal Skid Number (SN) \geq recommended terminal SN	Do nothing
Predicted terminal SN < recommended terminal SN	Remove the old HFST application & add a new one

7.4 LCCA Results

The following subsections discussed the economic analysis results—obtained from the LCC program—based on the Aggregate Image Measurement System (AIMS), Dynamic Friction Tester (DFT), and BP input data. Then, a comparative economic study was conducted to select the appropriate High Friction Surface Treatment (HFST) application based on the Net Present Value (NPV) obtained from Life Cycle Cost Analysis (LCCA) studies.

7.4.1 Skid Number

Figure 7-2a displays the predicted initial Skid Number measured at 50 mi/hr by a skid trailer with smooth tires [SN(50)] values and SN(50) values after 5 years of service—considered as terminal—based on AIMS input data for HFST applications. The Skid Number measured at 50 mi/hr by a skid trailer with smooth tires [SN(50)] values decreased most after 5 years. Calcined Bauxite had the highest initial SN(50), and Steel Slag had the lowest value. Flint Chat presented the highest terminal SN(50) value, and Steel Slag yielded the lowest value. Potosi Dolomite had the third-highest initial SN(50) value; Calcined Bauxite (CB) and Meramec River Aggregate ranked above it. Potosi Dolomite showed the third-lowest terminal SN(50) value after Steel Slag and Rhyolite. Based on the initial and terminal SN(50) values, Potosi Dolomite had the lowest polishing process resistance. By contrast, Flint Chat presented the highest resistance to the polishing process.

Figure 7-2b illustrates the predicted Skid Number measured at 40 mi/hr by a skid trailer with Ribbed tires (SN40R) based on Dynamic Friction Tester (DFT) input data initially (0 polishing cycles) and terminally (after 140k polishing cycles) for High Friction Surface Treatment (HFST) applications. Calcined Bauxite displayed the highest initial and terminal SN40R values followed by Flint Chat. Meramec River Aggregate had the lowest initial and terminal SN40R values. Earthworks had a higher initial SN40R value than Meramec River Aggregate; however, the SN40R values were comparable after polishing. Earthworks and Rhyolite presented higher initial SN40R values than Steel Slag yielded. Nevertheless, Steel Slag had higher SN40R values than Earthworks and Rhyolite after polishing.

Figure 7-2c depicts the predicted SN40R based on the British Pendulum (BP) input data for the initial (pre-polish) and terminal (post-polish) stages of HFST applications. The polishing process decreased the SN40R values. Potosi Dolomite had the highest initial and terminal SN40R values. The second highest SN40R was recorded for Calcined Bauxite (CB) followed by Meramec River Aggregate. Flint Chat had the lowest terminal SN40R followed by Rhyolite.

7.4.2 Net Present Value

The Net Present Values (NPVs) for the HFST applications based on Aggregate Image Measurement System (AIMS) input data is shown in Figure 7-3a. The best choice was the HFST application using Meramec River Aggregate because it had the lowest NPV (\$93,380). The second-best choice was Potosi Dolomite with a NPV of \$100,304, and it was followed by Flint Chat with a NPV of \$104,764. Earthworks and Rhyolite had comparable NPVs. Calcined Bauxite had the second highest NPV after Steel Slag. The worst choice was the HFST application using Steel Slag; it had a NPV of \$259,296. The high NPV for CB occurred because of its high cost: it showed the highest cost when compared to the alternative aggregates' costs. However, Steel Slag showed the highest NPV because of it had the lowest terminal SN(50); the HFST application using Steel Slag was the only application that required replacement after 5 years of service.

The NPVs for the HFST applications based on DFT input data is shown in Figure 7-3b. The best choice was the HFST application using Steel Slag because it had the lowest NPV (\$97,633). This occurred because Steel Slag had the lowest cost, and no HFST replacement was required when it reached the terminal SN40R value. The second-best choice was Flint Chat with a NPV of \$104,764. Flint Chat had the third-lowest cost after Steel Slag and Meramec River Aggregate. When the aggregates reached their terminal SN40R values, no replacement took place for the HFST application using Flint Chat, and replacement happened for HFST application using Meramec River Aggregate. Thus, HFST application using Flint Chat had a lower NPV than the HFST application using Meramec River Aggregate. Calcined Bauxite was the third choice with a NPV of \$126,725. Calcined Bauxite had the highest cost between the aggregates; however, no HFST application replacement was needed when it reached the terminal SN40R value. Furthermore, Calcined Bauxite had the highest terminal SN40R value (see Figure 7-2b).

Earthworks and Rhyolite were the worst choices because they showed the highest NPV (more than \$302,000) followed by Meramec River Aggregate with a NPV of \$267,159. Earthworks and Rhyolite had the costs lower than CB and higher than the remaining aggregates. Moreover, HFST applications using Earthworks or Rhyolite required replacement when the aggregates reached the terminal values.

Figure 7-3c exhibits the Net Present Values (NPVs) for the HFST applications based on the BP input data. Figure 7-3c deemed the lowest NPVs when compared to Figure 7-3a and Figure 7-3b. This took place because no HFST applications' replacement happened when the aggregates reached the terminal Skid Number measured at 40 mi/hr by a skid trailer with Ribbed tires (SN40R) values. The best choice was the High Friction Surface Treatment (HFST) application using Steel Slag because it had the lowest NPV valued at \$97,633. Steel Slag had the lowest aggregate's cost, and no HFST applications' replacement happened when the aggregates reached the terminal SN40R values. The second-best choice was Meramec River Aggregate with a NPV of \$98,380 followed by Potosi Dolomite with a NPV of \$100,304. Calcined Bauxite was the worst choice because it presented the highest NPV (\$126,725) followed by Rhyolite with a NPV of \$116,223.

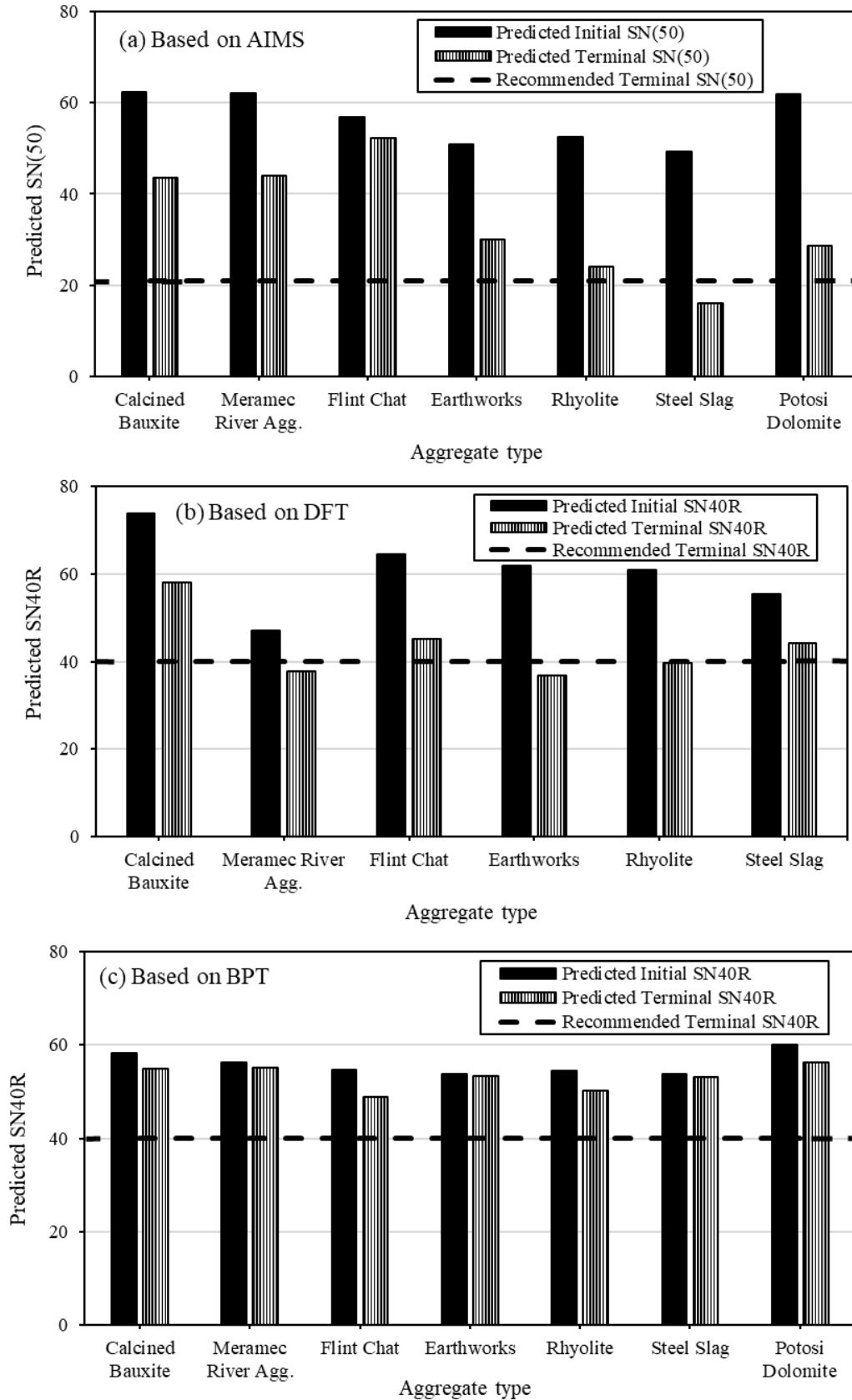


Figure 7-2 Predicted initial and terminal SN values for HFST applications.

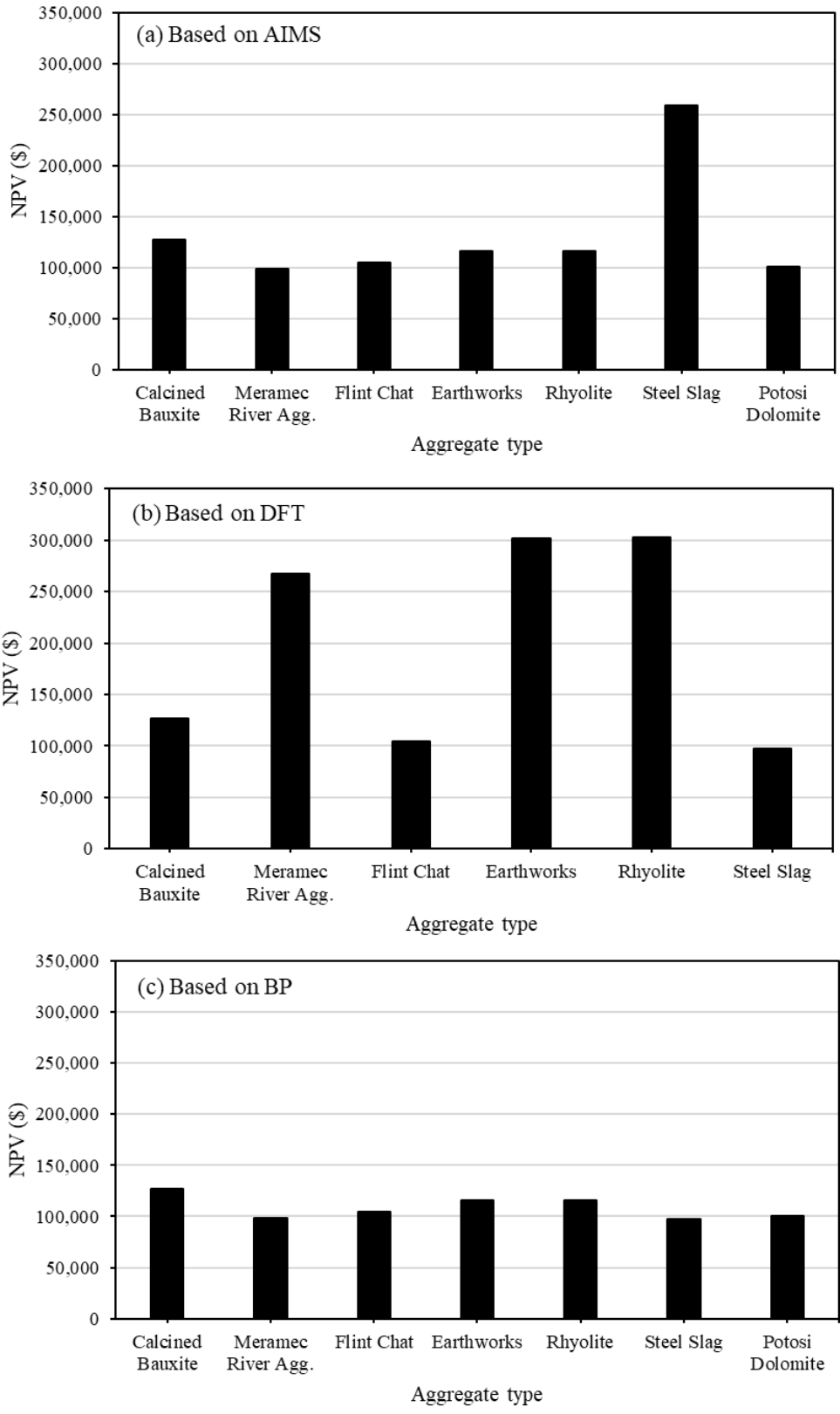


Figure 7-3 Net present values for HFST applications.

7.5 A Comparative Economic Study

In this section, the Net Present Value (NPV) data obtained from the LCC program were compared for the High Friction Surface Treatment (HFST) applications. The HFST application using Potosi Dolomite was excluded from the comparison because it was not tested using the Dynamic Friction Tester (DFT). The NPV ranked 1 to 6. The HFST application with the lowest NPV ranked 1, and the HFST application with the highest NPV ranked 6. Table 7-2 presents the HFST applications' rankings based on NPV.

Aggregates' rankings were considered high for 1 or 2, moderate for 3 or 4, and low for 5 or 6. Calcined Bauxite, Earthworks, and Rhyolite NPV rankings were between moderate to low. Steel Slag NPV rankings were between high (based on DFT or BP) and low [based on Aggregate Image Measurement System (AIMS)]. Flint Chat and Meramec River Aggregate NPV rankings were considered between high and moderate.

Table 7-2 Ranking of HFST applications based on the NPV.

Aggregate Type	Ranking		
	Based on AIMS	Based on DFT	Based on BP
Calcined Bauxite (CB)	5	3	6
Earthworks	3	5	4
Rhyolite	4	6	5
Flint Chat	2	2	3
Steel Slag	6	1	1
Meramec River Agg.	1	4	2

7.6 Summary

In this chapter, the economic analysis of HFST applications was discussed. The researchers developed a LCC simple program using Excel to predict the NPV for the HFST applications. The predicted terminal Skid Number (SN) values for the HFST applications were compared with the recommended terminal SN values, and the decision for maintenance of the HFST was taken. Based on economic analysis, Flint Chat and Meramec River Aggregate had the lowest NPVs followed by Steel Slag and then Earthworks. By contrast, Rhyolite showed the highest NPVs followed by Calcined Bauxite.

SUMMARY, CONCLUSIONS, AND RECOMMENDATIONS

8.1 Summary

The High Friction Surface Treatment (HFST) application is used to reduce roadway crashes on risky locations and horizontal curves, and to compensate for the deficiencies of geometric designs. Currently, Calcined Bauxite (CB) is the primary aggregate used for HFST in Missouri. Calcined Bauxite has very limited sources, which makes it more expensive than locally available aggregates. This research evaluated CB's feasible alternative aggregates through a comprehensive experimental program for use in HFST applications. The alternative aggregates were Earthworks, Meramec River, Steel Slag, Rhyolite, Black Diabase, Quartzite, Flint Chat, and Potosi Dolomite aggregate sources.

Three categories of testing were followed in the experimental program: the first category was for the physical properties testing, the second category was for durability testing, and the third category was for performance testing. Physical testing included aggregate gradation, specific gravity & absorption, and Uncompacted Void Content (UVC) of fine aggregates. Durability testing included Los Angeles Abrasion (LAA), Micro-Deval (MD) polishing; discussed under performance testing, sodium sulfate soundness, water-alcohol freeze thaw, and acid-insoluble residue. Physical properties and durability tests were run to classify the aggregates and identify the routine tests that investigate the performance of the proposed aggregates as HFST materials. Performance testing included Micro-Deval (MD) polishing, Aggregate Image Measurement System (AIMS), dynamic friction testing, and British Pendulum (BP) testing. The MD results reflected the aggregates' resistances to polishing and abrasion. The AIMS explored the changes that occurred to the Texture (TX) and Gradient Angularity (GA) indices for the coarse aggregates before, after 105-, and after 180-minutes polishing times in MD. The Dynamic Friction Tester (DFT) examined the Coefficient of Friction (COF) values before and after polishing cycles at different speeds. The polishing process was conducted using the Three-Wheel Polishing Device (TWPD). Finally, the BP evaluated the aggregates' surface frictional properties before and after 10-hr polishing time using the British Wheel.

The researchers developed a LCC simple process using Excel to calculate the Net Present Value (NPV) for HFST applications based on AIMS, DFT, or BP results. The major input data for the LCC program were categorized into material and project specifics. Performance prediction models were used to convert the input data into Skid Number (SN) values. The predicted terminal SN was compared with the recommended terminal SN using rehabilitation matrix. This matrix was proposed based on the predicted and recommended terminal SN values. Finally, the output data was calculated; this data presented the NPVs for the HFST applications. Based on the lowest NPV, the best HFST application was selected.

8.2 Conclusions

Two main categories of conclusions related to aggregate sources in HFST applications were noted: the alternative aggregate sources to Calcine Bauxite and the use of performance testing to evaluate aggregate sources.

8.2.1 Alternative Aggregate Sources to Calcined Bauxite in HFST.

The results of this study indicated that quality aggregate sources compare to calcined bauxite following the MoDOT HFST aggregate criteria. The following statements justify this conclusion.

1. Meramec River Aggregate, Earthworks, and Steel Slag were the most favorable alternative to Calcined Bauxite (CB). Flint Chat had favorable testing scores as CB alternative except its Los Angles Abrasion (LAA) percentage exceeded the HFST limits (NJSP-15-13B); its Micro-Deval scores were average among other alternatives.

2. The Uncompacted Void Content (UVC) results for (#6 - #8) size and (#6 - #16) gradation showed that Flint Chat had the highest UVC percentages followed by Black Diabase, Potosi Dolomite, Steel Slag, and CB. For #8 - #100 gradation, Steel Slag had the highest UVC percentage followed by Rhyolite, Black Diabase, Meramec River Aggregate. The specific gravity test—conducted on (- #4) size and (#6 - #16) gradation—deemed that CB had the highest specific gravity values followed by Steel Slag. However, Earthworks and Meramec River Aggregate had the lowest specific gravity values.
3. Calcined Bauxite, Steel Slag, and Meramec River Aggregate showed the lowest LAA percentages. Meramec River Aggregate had the best sodium sulfate soundness results (lowest mass losses) among the alternative aggregates followed by Rhyolite and then Steel Slag. The highest percentage lost was noted for Potosi Dolomite. All alternative aggregates had lower percentages of water-alcohol freeze thaw mass losses when compared to CB; the lowest percentage of mass loss was recorded for Earthworks and then for Potosi Dolomite. Based on the acid-insoluble residue results, Quartzite, Rhyolite, Meramec River Aggregate, and Flint Chat had comparable residues percentages with CB.
4. Meramec River Aggregate, Calcined Bauxite, and Earthworks had the best Micro-Deval (MD) mass losses' percentages after 180-minutes polishing time for the coarse gradation (3/8" - #4) or 30-minutes polishing time for the fine gradation (#6 - #16).
5. The relationship between the UVC percentages and MD polishing times depicted that increasing the MD polishing times decreased the UVC percentages. No specific relationship was observed between the Mean Texture Depth (MTD) values and GA indices, and no specific relationships were observed between the GA indices and the UVC percentages.

8.2.2 The Use of Performance Testing to Evaluate Aggregate Sources for HFST Applications

The conducted performance systems including Micro-Deval (MD) and Aggregate Image Measurement System (AIMS), dynamic friction testing, and British Pendulum (BP) testing, and the Dynamic Friction Testing (DFT) seem applicable to HFST aggregates. There are no strong correlations between the three systems; mainly because they are based on different mechanisms of measuring the aggregate friction properties. The following conclusions were noted:

6. Calcined Bauxite had the highest terminal Coefficient of Friction (COF) value in the Dynamic Friction Tester (DFT) results followed by Flint Chat, Steel Slag, Rhyolite, and Meramec River Aggregate. The lowest terminal COF value was noted for Earthworks. The initial COF values showed that CB had the highest value followed by Flint Chat, Earthworks, Rhyolite, and then Steel Slag. Meramec River Aggregate had the lowest value.
7. Potosi Dolomite had the highest average pre-polish British Pendulum Number (BPN) values followed by Calcined Bauxite, Meramec River Aggregate, Flint Chat, Rhyolite, Earthworks. Steel Slag had the lowest value. Potosi Dolomite had the highest average post-polish BPN values followed by Meramec River Aggregate, Calcine Bauxite, Earthworks, Steel Slag, Rhyolite. By contrast, Flint Chat aggregate had the lowest value.
8. There was a direct linear relationship between the LAA and MD mass losses. The MD was found to be more sensitive for aggregate screening than LA. Relationships were observed between the Micro-Deval or Los Angeles mass losses' percentages and BPN values.

9. No specific relationships were observed between average Aggregate Image Measurement System (AIMS) Texture (TX) and Gradient Angularity (GA) indices regarding (3/8" - #4) size. No relationships were detected between MD mass losses and AIMS TX or GA indices.
10. No specific relationships were found between British Pendulum (BP) and AIMS results, and no significant relationships were found between AIMS and DFT results. The relationship between the BP and DFT results before the polishing processes illustrated that aggregate source with the highest COF value had the highest BPN value (e.g., CB). After the polishing processes, no specific relationship was detected between the BP and DFT results.
11. Based on cost analysis, Flint Chat and Meramec River Aggregate had the lowest Net Present Values (NPVs) followed by Steel Slag and then Earthworks. Contrarily, Rhyolite showed the highest NPVs followed by CB. The high initial cost of CB affected its NPV Compared to other aggregate sources.

8.3 Recommendations

1. It is recommended to construct High Friction Surface Treatment (HFST) field sections using the selected alternative aggregates. This will evaluate the field performance of the selected aggregates. The DFT and BP results in the field could be compared to the results conducted in the lab.
2. It is recommended to update current MoDOT specifications on aggregate requirements for HFST following the findings of this research. Micro-Deval testing can be used for preliminary screening of HFST aggregate selection.
3. It is recommended to extend the use of high friction aggregate sources, with larger sizes, in HMA applications particularly in mixes with high recycled aggregate contents, for example, mixes with high RAP contents. RAP materials have been subjected to weathering and traffic for years resulting in potentially degraded skid resistance properties.
4. It is recommended to adopt the developed LCCA program as a rational tool to compare the aggregate source alternatives for HFST applications.
5. Due to the limited scope of this study, strong relations between the aggregate tested properties and the performance characteristics could not be developed. It is recommended to increase the scale of the presented research in future research to include more aggregates with various sizes. This will help the researchers to confirm the obtained results on a large scale.

REFERENCES

- Alabama DOT. 2014. "Section 431 High Friction Surface Treatments for Asphalt Pavements." Alabama Standard Specifications.
- Alaska DOT. 2004. "Section 405 High Friction Surface Treatment." Special Provision.
- Aldagari, S., M. Al-Assi, E. Kassem, A. Chowdhury, and E. Masad. 2020. "Development of Predictive Models for Skid Resistance of Asphalt Pavements and Seal Coat." *International Journal of Pavement Engineering*, May, 1–13. <https://doi.org/10.1080/10298436.2020.1766685>.
- Bloem, D.L. 1971. *Skid Resistance: The Role of Aggregates and Other Factors*. National Sand and Gravel Association.
- California DOT. n.d. "10-1.32 High Friction Surface Treatment." Contract No. 11-403704.
- Chowdhury, A., E. Kassem, S. Aldagari, and E. Masad. 2016. "Validation of Asphalt Mixture Pavement Skid Prediction Model and Development of Skid Prediction Model for Surface Treatments." Technical Report 0-6746-01-1, Texas A&M Transportation Institute, College Station, TX, U.S.A.
- Crouch, L.K., J.D. Gothard, G. Head, and W.A. Goodwin. 1995. "Evaluation of Textural Retention of Pavement Surface Aggregates." *Transportation Research Record*, no. 1486: 124–129.
- Cuelho, E., R. Mokwa, K. Obert, and A. Miller. 2007. "Comparative Analysis of Coarse Surfacing Aggregate Using Micro-Deval, L.A. Abrasion and Sodium Sulfate Soundness Tests." Final Project Report, FHWA/MT-06-016/8117-27, Western Transportation Institute, Montana State University, Bozeman, MT, U.S.A.
- FHWA. 2019. "High Friction Surface Treatments (HFST)." Accessed March 15, 2021. https://safety.fhwa.dot.gov/roadway_dept/pavement_friction/high_friction/.
- FHWA. 2020. "High Friction Surface Treatment (HFST) Quick Reference." DTFH61-13-D-00001, Task B9. Accessed March 4, 2021. <https://www.fhwa.dot.gov/publications/research/safety/highfriction/High-Friction-Surface-Treatment-final.pdf>.
- FHWA-CAI-14-019. n.d. "Frequently Asked Questions about High Friction Surface Treatments (HFST)." FHWA. Accessed March 9, 2021. https://www.fhwa.dot.gov/innovation/everydaycounts/edc-2/pdfs/fhwa-cai-14-019_faqs_hfst_mar2014_508.pdf.
- Florida DOT. 2014. "Section 333 High Friction Surface Treatment."
- Georgia DOT. 2017. "High Friction Surface Treatment - Section 419."
- Greer, M. 2015. "Evaluation of the AIMS-II and Micro-Deval for Friction Characteristics of Aggregates." M.Sc. Thesis, Auburn University, Auburn, Alabama, U.S.A.
- Harkey, D.L., R. Srinivasan, J. Baek, F.M. Council, K. Eccles, N. Lefler, B. Persaud, et al. 2008. "Accident Modification Factors for Traffic Engineering and ITS Improvements." (NCHRP) Report 617, Washington, D.C., U.S.A.: Transportation Research Board. <https://doi.org/10.17226/13899>.
- Heitzman, M., and J. Moore. 2017. "Evaluation of Laboratory Friction Performance of Aggregates for High Friction Surface Treatments." NCAT Report 17-01, National Center for Asphalt Technology at Auburn University, Auburn, AL, U.S.A.
- Heitzman, M., P. Turner, and M. Greer. 2015. "High Friction Surface Treatment Alternative Aggregates Study." NCAT Report 15-04, National Center for Asphalt Technology at Auburn University, Auburn, AL, U.S.A.
- Henry, J.J. 2000. "Evaluation of Pavement Friction Characteristics: A Synthesis of Highway Practice." NCHRP Synthesis 291, Transportation Research Board, National Research Council, Washington, D.C.
- Henry, J.J., and J.C. Wambold. 1992. "Use of Smooth-Treaded Test Tire in Evaluating Skid Resistance." *Transportation Research Board*, no. 1348: 35–42.
- "High Friction Surface Treatments in Pennsylvania." n.d. Pennsylvania DOT. Accessed March 8, 2021. <https://www.tesc.psu.edu/assets/docs/high-friction-surface-treatments.pdf>.
- Illinois DOT. 2014. "Special Provision for High Friction Surface Treatment (BMPR/BSE)."
- Indiana DOT. 2017. "High Friction Surface Treatment." Standard Specifications.

- Iowa DOT. 2011. "Special Provisions for High Friction Surface Treatment." Standard Specification Series 2009.
- Kandhal, P.S., F. Parker, and E.A. Bishara. 1993. "Evaluation of Alabama Limestone Aggregates for Asphalt Wearing Courses." *Transportation Research Record*, no. 1418: 12–21.
- Kandhal, P.S., and F. Parker. 1998. "Aggregate Tests Related to Asphalt Concrete Performance in Pavements." NCHRP Report 405, Transportation Research Board, National Research Council, Washington, D.C., U.S.A.
- Kassem, E., A. Awed, E.A. Masad, and D.N. Little. 2013. "Development of Predictive Model for Skid Loss of Asphalt Pavements." *Transportation Research Record: Journal of the Transportation Research Board* 2372 (1): 83–96. <https://doi.org/10.3141/2372-10>.
- Kentucky DOT. n.d. "Special Note for Polymer Concrete Overlay Systems."
- Li, S., R. Xiong, D. Yu, G. Zhao, P. Cong, and Y. Jiang. 2017. "Friction Surface Treatment Selection: Aggregate Properties, Surface Characteristics, Alternative Treatments, and Safety Effects." FHWA/IN/JTRP-2017/09, Joint Transportation Research Program Purdue University West Lafayette, IN, U.S.A. <https://doi.org/10.5703/1288284316509>.
- Mahmoud, E.M. 2005. "Development of Experimental Methods for the Evaluation of the of Aggregate Resistance to Polishing, Abrasion, and Breakage." M.Sc. Thesis, Texas A&M University, College Station, TX, U.S.A.
- Mahmoud, E., and E. Masad. 2007. "Experimental Methods for the Evaluation of Aggregate Resistance to Polishing, Abrasion, and Breakage." *Journal of Materials in Civil Engineering* 19 (11): 977–85. [https://doi.org/10.1061/\(ASCE\)0899-1561\(2007\)19:11\(977\)](https://doi.org/10.1061/(ASCE)0899-1561(2007)19:11(977)).
- Mahmoud, E., and E. Ortiz. 2014. "Implementation of AIMS in Measuring Aggregate Resistance to Polishing, Abrasion, and Breakage." FHWA-ICT-14-014, Illinois Center for Transportation, Urbana, IL, U.S.A.
- Masad, E., A. Luce, and E. Mahmoud. 2006. "Implementation of AIMS in Measuring Aggregate Resistance to Polishing, Abrasion, and Breakage." FHWA/TX-06/5-1707-03-1, Texas Transportation Institute, Texas A&M University, College Station, TX, U.S.A.
- Masad, E., A. Rezaei, and A. Chowdhury. 2011. "Field Evaluation of Asphalt Mixture Skid Resistance and Its Relationship to Aggregate Characteristics." FHWA/TX-11/0-5627-3, Texas Transportation Institute, Texas A&M University, College Station, TX, U.S.A.
- Masad, E., A. Rezaei, A. Chowdhury, and P. Harris. 2009. "Predicting Asphalt Mixture Skid Resistance Based on Aggregate Characteristics." FHWA/TX-09/0-5627-1. Texas Transportation Institute, Texas A&M University, College Station, TX, U.S.A.
- Merritt, D., M. Moravec, and M. Heitzman. 2014. "High Friction Surface Treatment Aggregate Durability Study." Pavement Evaluation 2014, Blacksburg, Virginia, U.S.A. 2014. Accessed March 10, 2021. <https://vtechworks.lib.vt.edu/bitstream/handle/10919/54620/Merritt.pdf?sequence=1&isAllowed=y>.
- Michigan DOT. 2016. "Special Provisions for Special Provision for High Friction Surface Treatment - TSF-000-S (918) -- 92-00." 12SP-800A-03.
- Milstead, R., X. Qin, B. Katz, J. Bonneson, M. Pratt, J. Miles, and P. Carlson. 2011. "Procedures for Setting Advisory Speeds on Curves." FHWA-SA-11-22, Federal Highway Administration, Office of Safety, Washington, D.C., U.S.A.
- Missouri DOT. 2015. "High Friction Surface Treatment (NJSP-15-13B)." Standard Specifications.
- Pennsylvania DOT. 2014. "High Friction Surface Treatment (HFST)." Special Provisions.
- Rezaei, A., and E. Masad. 2013. "Experimental-Based Model for Predicting the Skid Resistance of Asphalt Pavements." *International Journal of Pavement Engineering* 14 (1): 24–35. <https://doi.org/10.1080/10298436.2011.643793>.
- South Carolina DOT. 2015. "High Friction Surface Treatment." Supplemental Specification.
- South Dakota DOT. 2015. "Special Provision for High Friction Surface Treatment." *Project PH 00SW (43), PCN 05H9*.
- Tennessee DOT. 2017. "Special Provision Regarding High Friction Surface Treatments (HFST)." 406HFST.

- Texas DOT. 2004. "Special Specification 3289 High Friction Surface Treatment." 2004 Specifications.
- Vandel, A. n.d. "High Friction Surface Treatment: Winter Road Conditions." South Dakota Department of Transportation. Accessed March 8, 2021.
<https://static.tti.tamu.edu/conferences/elcsipfs19/presentations/day2/topic5/vandel.pdf>.
- Virginia DOT. 2012. "Special Provisions for High Friction Surface Treatments for Asphalt Pavements." Contact ID No. C00098916N01.
- Wambold, J.C., C.E. Antle, J. J. Henry, and Z. Rado. 1995. "International PIARC Experiment to Compare and Harmonize Texture and Skid Resistance Measurement." PIARC Report C-1, Technical Committee on Surface Characteristics, Permanent International Association of Road Congress, France.
- Wilson, B., and A. Mukhopadhyay. 2016. "Alternative Aggregates and Materials for High Friction Surface Treatments." Final Report, Project BDR74-977-05, Texas A&M Transportation Institute, College Station, Texas, U.S.A.
- Wisconsin DOT. n.d. "Asphaltic Binder Enhanced Friction Surface Treatment." *Item SPV.0180. XX*.
- Won, M.C., and C.N. Fu. 1996. "Evaluation of Laboratory Procedures for Aggregate Polish Test." *Transportation Research Record: Journal of the Transportation Research Board* 1547 (1): 23–28.
<https://doi.org/10.1177/0361198196154700104>.
- Wu, Y., F. Parker, and P.S. Kandhal. 1998. "Aggregate Toughness/Abrasion Resistance and Durability/Soundness Tests Related to Asphalt Concrete Performance in Pavements." *Transportation Research Record: Journal of the Transportation Research Board* 1638 (1): 85–93.
<https://doi.org/10.3141/1638-10>.

APPENDIX A: STATE HFST AGGREGATES SPECIFICATION

A.1 State Standards

In this appendix, the High Friction Surface Treatment (HFST) standards for 14 other states and an Enhanced Friction Surface Treatment (EFST) standard for Wisconsin were presented. In the following subsections, the requirements for the HFST and EFST aggregate toppings were comprehensively demonstrated.

A.1.1 Alabama

Alabama’s HFST specification is under special provision 12-0817, section 431. They require a Calcined Bauxite (CB) aggregate that is 100% fractured. Table A-1 presents the other requirements.

Table A-1 Physical characteristics of high friction aggregates in Alabama State.

Property		Threshold Values	Specifications
Resistance to Degradation (LAA)		20% Max. loss	AASHTO T 96
Polish Stone Value		38 Min.	AASHTO T 279
Moisture Content		0.2% Max.	AASHTO T 255
Aluminum Oxide Content		87 Min.	ASTM C25
Gradation (% Passing)	#4	100% Min.	AASHTO T 27
	#6	95% Min.	
	#16	5% Max.	

A.1.2 Alaska

Alaska’s HFST specification is in their special provisions section 405. They require a blend of CB aggregate. They also require a manufacturer’s certification of aggregate quality but have no further requirements. The aggregate gradation specification for Alaska State is summarized in Table A-2.

Table A-2 The high friction Aggregate Gradation in Alaska State.

Property		Threshold Values	Specifications
Gradation (% Passing)	#6	95% Min.	AASHTO T 27
	#16	5% Max.	

A.1.3 California

California’s HFST specification was found on page 90 of a notice to bidders and special provisions document for contract No.403704. The aggregates’ requirements are outlined in Table A-3.

Table A-3 Physical characteristics of high friction aggregates in California State.

Property		Threshold Values	Specifications
Resistance to Degradation (LAA)		10% Max. loss at 100 Revolutions	CT 211
Cleanness Value		75 Min. at Operating Range 71 Min. for Contract Compliance	CT 227
Acid Insolubility		90% Min.	ASTM D3042
Magnesium Soundness		30 % Max.	ASTM C88
Gradation (% Passing)	#6	95% Min.	AASHTO T 27
	#16	5% Max.	

A.1.4 Florida

Florida’s High Friction Surface Treatment (HFST) specification is in section 333. They require a Calcined Bauxite (CB) aggregate that meets the requirements in Table A-4.

Table A-4 Physical characteristics of high friction aggregates in Florida State.

Property		Threshold Values	Specifications
Resistance to Degradation (LAA)		10% Max. loss	AASHTO T 96
Moisture Content		0.2% Max.	AASHTO T 255
Aluminum Oxide Content		87% Min.	ASTM C25
Gradation (% Passing)	#4	100% Min.	AASHTO T 27
	#6	95% Min.	
	#16	5% Max.	

A.1.5 Illinois

Illinois’s HFST specification is titled *Special Provision for High-Friction Surface Treatment*. The requirements for CB aggregate are summarized in Table A-5.

Table A-5 Physical characteristics of high friction aggregates in Illinois State.

Property		Threshold Values	Specifications
Resistance to Degradation (LAA)		20% Max loss	AASHTO T 96
Moisture Content		0.2% Max	AASHTO T 255
Aluminum Oxide Content		87% Min	ASTM C25
Gradation (% Passing)	#4	100% Min	AASHTO T 27
	#6	95% Min	
	#16	5% Max	

A.1.6 Indiana

The conditions of Indiana’s HFST specification (617-T-213) for CB aggregate are illustrated Table A-6.

Table A-6 Physical characteristics of high friction aggregates in Indiana State.

Property		Threshold Values	Specifications
Resistance to Degradation (LAA)		10% Max loss (Grading C)	AASHTO T 96
Moisture Content		0.2% Max	AASHTO T 255
Sodium Sulfate Soundness		12% Maximum	AASHTO T 104
Aluminum Oxide Content		87% Min	ASTM C25
Hardness		8 Minimum	Mohs Scale
Polish Stone Value		38 – 44	AASHTO T 279
Gradation (% Passing)	#4	100% Min	AASHTO T 27
	#6	95% Min	
	#16	5% Max	
	#30	1% Max.	

A.1.7 Iowa

Iowa’s HFST specification is under special provision 090134. They require a CB aggregate that is 100% fractured. Table A-7 summarizes Iowa’s requirements for CB.

Table A-7 Physical characteristics of high friction aggregates in Iowa State.

Property		Threshold Values	Specifications
Resistance to Degradation (LAA)		20% Max loss	AASHTO T 96
Accelerated Polishing Value		70.0 BPN Min	ASTM E660
Gradation (% Passing)	#6	95% Min	AASHTO T 27
	#16	5% Max	

A.1.8 Michigan

Michigan’s High Friction Surface Treatment (HFST) specification is under special provision 12-800B-03. They require a Calcined Bauxite (CB) aggregate that meets the requirements in Table A-8.

Table A-8 Physical characteristics of high friction aggregates in Michigan State.

Property		Threshold Values	Specifications
Fineness Modulus		2.28–2.81	N/A
Aluminum Oxide Content		87 Min	ASTM C25
Gradation (% Passing)	#4	98% Min	AASHTO T 27
	#8	30–75%	
	#16	5% Max	
	#30	1% Max	

A.1.9 Pennsylvania

Pennsylvania’s HFST specification is under special provision 00-c9001 Item 9000-0002. They require a bauxite aggregate that meets the requirements in Table A-9.

Table A-9 Physical characteristics of high friction aggregates in Pennsylvania State.

Property		Threshold Values	Specifications
Resistance to Degradation (LAA)		20% Max	AASHTO T 96
Moisture Content		0.2 % Max	AASHTO T 255
Aluminum Oxide Content		87 Min	ASTM C25
Polish Stone Value		38 Min	AASHTO T 279
Gradation (% Passing)	#4	100% Min	AASHTO T 27
	#6	95% Max	
	#16	5% Max	

A.1.10 South Carolina

South Carolina has a supplemental specification for their HFST aggregates. They require a CB aggregate that meets the requirements in Table A-10.

A.1.11 South Dakota

South Dakota’s HFST specification was found in a notice to contractors, proposal, special provisions, contract, and contract bond for HFST project number PH 00SW (43) on page 18/97 of the PDF. The CB aggregate must meet the requirements in Table A-11.

Table A-10 Physical characteristics of high friction aggregates in South Carolina State.

Property		Threshold Values	Specifications
Resistance to Degradation (LAA)		20% Max	AASHTO T 96
Moisture Content		0.2 % Max	AASHTO T 255
Aluminum Oxide Content		87 Min	ASTM C25
Polish Stone Value		38 Min	AASHTO T 279
Gradation (% Passing)	#4	100% Min	AASHTO T 27
	#6	95% Max	
	#16	5% Max	

Table A-11 Physical characteristics of high friction aggregates in South Dakota State.

Property		Threshold Values	Specifications
Resistance to Degradation (LAA)		20% Max	AASHTO T 96
Moisture Content		0.2 % Max	AASHTO T 255
Aluminum Oxide Content		87 Min	ASTM C25
Gradation (% Passing)	#4	100% Min	AASHTO T 27
	#6	95% Max	
	#16	5% Max	

A.1.12 Tennessee

Tennessee's High Friction Surface Treatment (HFST) specification was found in special provision 406HFST. They require a Calcined Bauxite (CB) aggregate that meets the requirements in Table A-12.

Table A-12 Physical characteristics of high friction aggregates in Tennessee State.

Property		Threshold Values	Specifications
Moisture Content		0.2 % Max	AASHTO T 255
Aluminum Oxide Content		87 Min	ASTM C25
Micro-Deval (MD)		5% Max	ASTM D7428
Gradation (% Passing)	#4	100% Min	AASHTO T 27
	#6	95% Max	
	#16	5% Max	

A.1.13 Texas

The Texas HFST specification is special specification 3288. They require a CB aggregate that meets the requirements presented in Table A-13.

Table A-13 Physical characteristics of high friction aggregates in Texas State.

Property		Threshold Values	Specifications
Resistance to Degradation (LAA)		10% Max loss	ASTM C131
Acid Insolubility		90% Min	Tex-512-J
Aggregate Magnesium Soundness		30% Max	Tex-411-A
Aluminum Oxide Content		87% Min	ASTM C25
Gradation (% Passing)	#6	95% Min	AASHTO T 27
	#16	5% Max	

A.1.14 Virginia

Virginia’s High Friction Surface Treatment (HFST) specification was found in the contract with ID number C00098916N01. The required characteristics of a Calcined Bauxite (CB) aggregate are summarized in Table A-14.

Table A-14 Physical characteristics of high friction aggregates in Virginia State.

Property		Threshold Values	Specifications
Resistance to Degradation (LAA)		10% Max loss	AASHTO T 96
Micro-Deval (MD)		5% Max loss	AASHTO T 327
Gradation (% Passing)	#6	95% Min	AASHTO T 27
	#16	5% Max	

A.1.15 Wisconsin

Wisconsin is the only state found to have an Enhanced Friction Surface Treatment (EFST) standard, instead of an HFST standard. The standard is SPV.0180. XX. They require either a natural aggregate or synthetic aggregate that has a history of good performance in surface treatments, and it must meet the requirements in Table A-15.

Table A-15 Physical characteristics of high friction aggregates in Wisconsin State.

Property		Threshold Values	Specifications
Resistance to Degradation (LAA)		10% Max loss at 100 revolutions 25% Max loss at 500 revolutions	AASHTO T 96
Moisture Content		0.2% Max	AASHTO T 255
Water-Alcohol Freeze Thaw Soundness		9% Max loss	AASHTO T 103
Fine Aggregate Angularity		45% Min Method A	AASHTO T 304
Micro-Deval (MD)		15% Max loss	ASTM D7428
Gradation (% Passing)	#4	100% Min	AASHTO T 27
	#6	95% Min	
	#16	5% Max	
	#30	1% Max	

APPENDIX B: SKID PERFORMANCE MODELING

This appendix presented regression models which correlated the friction coefficients [e.g., International Friction Index (IFI) and Skid Number (SN)] with Aggregate Image Measurement System (AIMS) Texture (TX) and Gradient Angularity (GA) indices of aggregates used in the Hot Mix Asphalt (HMA) or surface treatments (e.g., seal coats).

B.1 Skid Resistance Prediction Models Based on Aggregate Image Measurement System Results

B.1.1 Skid Resistance Prediction Models for Hot Mix Asphalt

Kassem et al. (Kassem et al. 2013) conducted a study on limited numbers of aggregates (soft limestone, intermediate hardness limestone, and hard sandstone) to investigate the impacts of aggregate source and gradation on the skid resistance levels. It was found that the IFI reflected the skid resistance of the pavement (Kassem et al. 2013). Therefore, a regression model was developed to correlate the IFI with COF values measured by DFT at 20 km/hr. (DFT_{20}) and Mean Profile Depth (MPD) values, as demonstrated in Equation B.1 (Wambold et al. 1995). The sandstone had the highest IFI value (Kassem et al. 2013). The mixtures with finer gradations (Type C and Type F) showed lower IFI values than mixtures with the coarser gradations (SMA and PFC) (Kassem et al. 2013):

$$IFI = 0.081 + 0.732 DFT_{20} \left(\frac{-40}{S_p} \right) \quad \text{Equation B.1}$$

where,

S_p is the speed constant parameter ($S_p = 14.2 + 89.7 \times MPD$), and MPD is the mean profile depth.

The Mean Texture Depth (MTD) values obtained from the sand batch test were used to estimate the MPD values using Equation B.2:

$$MTD = 0.947 MPD + 0.069 \quad \text{Equation B.2}$$

The researchers (Kassem et al. 2013) discussed a skid resistance prediction model explored in other studies (Masad et al. 2009; Masad, Luce, and Mahmoud 2006; Kassem et al. 2013; E. Mahmoud and Masad 2007; Masad, Rezaei, and Chowdhury 2011), which is illustrated in Equation B.3. The regression coefficients (a_{mix} , b_{mix} , and c_{mix}) in Equation B.3 were correlated with the aggregate TX, aggregate GA, and Weibull distribution parameters that described the AGs, as illustrated in Equation B.4 through Equation B.6:

$$IFI(N) = a_{mix} + b_{mix} \times e^{(-c_{mix} \times N)} \quad \text{Equation B.3}$$

$$a_{mix} = \frac{47.493 + \lambda}{307.071 - 0.003 (AMD)^2} \quad \text{Equation B.4}$$

$$a_{mix} + b_{mix} = 0.308 \times \ln \left(\frac{1.438 \times (a_{TX} + b_{TX}) + 46.893 \times \lambda + 333.491 \times \kappa}{2.420 \times (a_{GA} + b_{GA})} \right) + 1.008 \quad \text{Equation B.5}$$

$$c_{mix} = 0.052 + 2.284 \times 10^{-14} \times e^{\left(\frac{0.523}{c_{TX}} \right)} + 2.008 \times 10^{-47} \times e^{\left(\frac{1.708}{c_{GA}} \right)} \quad \text{Equation B.6}$$

where,

a_{mix} is the terminal International Friction Index (IFI),
 $(a_{mix} + b_{mix})$ is the initial IFI,
 c_{mix} is the rate of change in IFI,
 N is the number of polishing cycles in the laboratory, using the NCAT Three-Wheel Polishing Device (TWPD), in thousands (e.g., $N=10$ for 10,000 polishing cycles),
 AMD is the aggregate texture, measured by the Aggregate Image Measurement System (AIMS), after 105-minutes polishing time in the Micro-Deval (MD) device,
 λ and κ are scale and shape parameters of the Weibull distribution, respectively,
 a_{TX} , b_{TX} , and c_{TX} are texture index constants determined by Equation B.8,
 a_{TX} is the terminal texture index,
 $(a_{TX} + b_{TX})$ is the initial texture index,
 c_{TX} is the rate of texture change,
 a_{GA} , b_{GA} , and c_{GA} are angularity index constants determined following Equation B.9,
 a_{GA} is the terminal angularity index,
 $(a_{GA} + b_{GA})$ is the initial angularity index, and
 c_{GA} is the rate of angularity change.

The Weibull distribution parameters were obtained by fitting Equation B.7 (Masad et al. 2009; Masad, Luce, and Mahmoud 2006; Kassem et al. 2013; Masad, Rezaei, and Chowdhury 2011), and they changed according to the aggregates' gradations because they affected the pavement microstructures and skid resistances (E. Mahmoud and Masad 2007):

$$F(x, \lambda, \kappa) = 1 - e^{-\left(\frac{x}{\lambda}\right)^\kappa} \quad \text{Equation B.7}$$

where,

F is the cumulative percentage passing, and
 x is the aggregate size in mm.

The regression constants (a_{TX} , b_{TX} , and c_{TX}) and (a_{GA} , b_{GA} , and c_{GA}) were obtained from Equation B.8 and Equation B.9, respectively. Equation B.8 shows the change in the aggregates' Texture (TX) with the MD polishing time. Furthermore, Equation B.9 illustrates the relationship between the aggregates' Gradient Angularity (GA) and the MD polishing time. The regression constants were obtained by fitting three TX and GA measurements with AIMS: before the MD and after the MD polishing times of 105 and 180 minutes (Kassem et al. 2013; E. M. Mahmoud 2005; Masad, Luce, and Mahmoud 2006; E. Mahmoud and Masad 2007):

$$TX(t) = a_{TX} + b_{TX} \times e^{(-c_{TX} \times t)} \quad \text{Equation B.8}$$

$$GA(t) = a_{GA} + b_{GA} \times e^{(-c_{GA} \times t)} \quad \text{Equation B.9}$$

After that, the measured Skid Number measured at 50 mi/hr. by a skid trailer with smooth tires [SN(50)] was correlated with the IFI and speed constant, as presented in Equation B.10 (Rezaei and Masad 2013). Table B-1 illustrates the recommended SN threshold values after five years of service (Chowdhury et al. 2016):

$$SN(50) = 1.41 + 143.19 \times (IFI - 0.045) \times e^{\left(-\frac{20}{Sp}\right)} \quad \text{Equation B.10}$$

Table B-1 SN threshold values after 5 years of service (Chowdhury et al. 2016).

Aggregate Class	Skid Number (SN) Threshold Value
High	≥ 30
Medium	21–30
Low	< 21

The Mean Profile Depth (MPD) was also correlated with the Weibull distribution parameters (λ and κ), as expressed in Equation B.11. Moreover, a relationship between the number of NCAT Three-Wheel Polishing Device (TWPD) cycles and traffic data is presented in Equation B.12:

$$MPD = 0.139\lambda + 0.086\kappa - \frac{0.041}{\kappa^4} \quad \text{Equation B.11}$$

$$N = TMF \times 10^{\left(\frac{1}{A+B \times c_{mix} + \left(\frac{C}{c_{mix}}\right)}\right)} \quad \text{Equation B.12}$$

where,

A , B , and C are regression coefficients ($A = -0.452$, $B = -58.95$, and $C = 5.834 \times 10^{-6}$), TMF is the traffic multiplication factor ($TMF = \frac{AADT \text{ (for outer lane)} \times \text{years in service} \times 365}{1000}$), and $AADT$ is the Average Annual Daily Traffic.

Eventually, the International Friction Index (IFI) prediction model is expressed as displayed in Equation B.13:

$$IFI = a_{mix} + b_{mix} \times \exp\left(-c_{mix} \times TMF \times 10^{\left(\frac{1}{A+B \times c_{mix} + \left(\frac{C}{c_{mix}}\right)}\right)}\right) \quad \text{Equation B.13}$$

The skid resistance prediction model was developed by Kassem et al. (Kassem et al. 2013), and it was validated and revised based on a wide range of aggregates used in Texas for the Hot Mix Asphalt (HMA), which were collected from 56 different sources (Chowdhury et al. 2016; Aldagari et al. 2020). Different field test sections were evaluated: 35 HMA test sections and 35 seal coat test sections. The fitting parameters of the IFI prediction model, which were expressed in Equation B.3, were predicted from Equation B.14 through Equation B.16:

$$a_{mix} = \frac{49.3144 + \lambda}{351.289 - 0.00193 (AMD)^2} \quad \text{Equation B.14}$$

$$(a_{mix} + b_{mix}) = 0.33 \times \ln\left(\frac{1.43757 \times (a_{TX} + b_{TX}) + 46.8933 \times \lambda + 333.491 \times \kappa}{2.42031 \times (a_{GA} + b_{GA})}\right) + 1.00801 \quad \text{Equation B.15}$$

$$c_{mix} = 0.018 + 1.654 \times C_{TX} + 1.346 \times C_{GA} \quad \text{Equation B.16}$$

Moreover, they investigated 16 aggregate sources and applied regression analyses to obtain the Texture (TX) and Gradient Angularity (GA) coefficients from only two points, Before Micro-Deval polishing

(BMD) and After 105-minutes of Micro-Deval polishing time (AMD 105), instead of three points, as explained earlier in Equation B.8 and Equation B.9 (Chowdhury et al. 2016; Aldagari et al. 2020). The TX index's coefficients were estimated by Equation B.17 through Equation B.19. The Gradient Angularity (GA) index's coefficients were estimated by Equation B.20 through Equation B.22:

$$a_{TX} = 0.864 \times AMD + 14.985 \quad \text{Equation B.17}$$

$$(a_{TX} + b_{TX}) = 0.999 \times BMD + 0.438 \quad \text{Equation B.18}$$

$$c_{TX} = \frac{0.492 + TL}{59.506 - (7.106 \times ARI)} \quad \text{Equation B.19}$$

$$a_{GA} = 1.237 \times AMD - 699.759 \quad \text{Equation B.20}$$

$$(a_{GA} + b_{GA}) = 0.999 \times BMD + 2.646 \quad \text{Equation B.21}$$

$$c_{GA} = \frac{1.891 + AL}{111.658 - (1.081 \times ARI)} \quad \text{Equation B.22}$$

where,

TL is the texture loss index ($TL = \frac{BMD - AMD}{AMD}$),

ARI is the aggregate roughness index ($ARI = \frac{AMD/BMD}{1 - (AMD/BMD)^2}$), and

AL is the angularity loss index ($AL = \frac{BMD - AMD}{AMD}$).

Furthermore, the relationship between the Skid Number measured at 50 mi/hr by a skid trailer with smooth tires [SN(50)] and International Friction Index (IFI) was developed as presented in Equation B.23:

$$SN(50) = 4.81 + 140.32 \times (IFI - 0.045) \times e^{\left(-\frac{20}{Sp}\right)} \quad \text{Equation B.23}$$

Eventually, the Mean Profile Depth (MPD) regression model and the Traffic Multiplication Factor (TMF) parameter were revised and optimized, as expressed in Equation B.24 and Equation B.25. Moreover, Table B-2 illustrates the four categorization of traffic level based on the TMF:

$$MPD = (\lambda/34.180) - (0.398/\kappa) + \kappa^{0.416} - 0.003N \quad \text{Equation B.24}$$

$$TMF = \frac{\text{Days between Construction and Field Testing} \times \text{Adjusted Traffic}}{1000} \quad \&$$

$$\text{Adjusted Traffic} = \frac{AADT \times (100 - \%T) \times Dlf_{AADT}}{100} + \frac{AADT \times (\%T) \times Dlf_T}{100} \quad \text{Equation B.25}$$

where,

$\%T$ is the percentage of trucks,

Dlf_{AADT} is the design lane factor for Average Annual Daily Traffic (see Table B-3), and

Dlf_T is the design lane factor for trucks (see Table B-3).

Table B-2 Traffic groups based on TMF for HMA (Chowdhury et al. 2016).

Level	Traffic Multiplication Factor (TMF)
Low	0 – 15,000
Medium	15,000 – 40,000
High	40,000 – 90,000
Very High	> 90,000

Table B-3 Design lane factors of AADT and trucks (Chowdhury et al. 2016).

Number of Lanes per Each Direction	Rural Highway				Urban Highway			
	Undivided		Divided		Undivided		Divided	
	Dlf_{AADT}	Dlf_T	Dlf_{AADT}	Dlf_T	Dlf_{AADT}	Dlf_T	Dlf_{AADT}	Dlf_T
1	0.50	0.50	N/A	N/A	0.50	0.50	N/A	N/A
2	0.40	0.45	0.80	0.90	0.30	0.40	0.70	0.90
3	0.30	0.40	0.40	0.50	0.25	0.35	0.40	0.50
4	-	-	-	-	N/A	N/A	0.30	0.40

B.1.2 Skid Resistance Prediction Model for Seal Coats

To develop a skid resistance prediction model for the seal coats, the researchers (Chowdhury et al. 2016; Aldagari et al. 2020) followed the same methodology for the Hot Mix Asphalt (HMA) model. The regression coefficients of Equation B.3 were obtained by using the characteristics of the seal coats' materials, as presented in Equation B.26 through Equation B.28. Equation B.17 through Equation B.22 were optimized and calibrated based on 19 aggregate sources, as presented in Equation B.29 through Equation B.34 (Chowdhury et al. 2016; Aldagari et al. 2020):

$$a_{mix} = \frac{40.493 + \lambda}{330 - 0.0011 (AMD)^2} \quad \text{Equation B.26}$$

$$a_{mix} + b_{mix} = 0.4 \times \ln \left(\frac{1.43757 \times (a_{TX} + b_{TX}) + 46.8933 \times \lambda + 3343.491 \times \kappa}{2.02031 \times (a_{GA} + b_{GA})} \right) \quad \text{Equation B.27}$$

$$c_{mix} = 2.654 \times C_{TX} + 1.5 \times C_{GA} \quad \text{Equation B.28}$$

$$a_{TX} = 1.011 \times AMD - 17.918 \quad \text{Equation B.29}$$

$$(a_{TX} + b_{TX}) = BMD + 0.134 \quad \text{Equation B.30}$$

$$C_{TX} = \frac{1.555 + TL}{126.995 - (18.174 \times ARI)} \quad \text{Equation B.31}$$

$$a_{GA} = 1.232 \times AMD - 648.34 \quad \text{Equation B.32}$$

$$(a_{GA} + b_{GA}) = 0.994 \times BMD + 21.084 \quad \text{Equation B.33}$$

$$C_{GA} = \frac{1.292 + AL}{-9.77 + (58.155 \times ARI)} \quad \text{Equation B.34}$$

Eventually, the Mean Profile Depth (MPD) regression model was revised and optimized, as expressed in Equation B.35, and the values of Dlf_f and Dlf_{AADT} are demonstrated in Table B-3:

$$MPD = (\lambda/5.403) + (3.491/\kappa) + \kappa^{0.104} + N^{-0.47} - 2.594 \quad \text{Equation B.35}$$

The traffic level was categorized into four groups based on the TMF, as illustrated in Table B-4.

Table B-4 Traffic groups based on TMF for seal coats (Chowdhury et al. 2016).

Level	Traffic Multiplication Factor (TMF)
Low	0 – 5,000
Medium	5,000 – 20,000
High	20,000 – 40,000
Very High	> 40,000

B.2 Skid Number Prediction Model Based on Dynamic Friction Test Results

In this section, the COF values measured by DFT at 40 km/hr (DFT_{40})—at different polishing cycles—was used to predict the Skid Number measured at 40 mi/hr by a skid trailer with Ribbed tires (SN40R). The initial SN40R was calculated at zero polishing cycles, and the terminal SN40R was calculated at 140k polishing cycles. The prediction model presented in Equation B.36 was developed by Heitzman et al. (Heitzman, Turner, and Greer 2015), and it was used in this study to compare the different aggregates used in the High Friction Surface Treatment (HFST). This model was based on laboratory friction measurements using DFT_{40} and SN40R in the field. The friction limits differed from one state to another. Table B-5 presents the friction limits for states based on the SN40R values (John J. Henry 2000). Equation B.36 explains the relationship between the SN40R and the COF using DFT_{40} :

$$SN40R = 92.3 \times DFT_{40} - 13.9 \quad \text{Equation B.36}$$

where,

$SN40R$ is the predicted skid number measured in the field using a skid trailer with ribbed tires at 40 mi/hr, and
 DFT_{40} if the COF values measured by DFT at 40 km/hr in the lab.

Table B-5 Friction Limits for states based on SN40R (John J. Henry 2000).

State	SN40R
Illinois	> 30
Kentucky	> 28
New York	> 32
South Carolina	> 41
Texas	> 30
Utah	> 30–35
Washington	> 30
Wyoming	> 35
Puerto Rico	> 40
Maine	> 35
Wisconsin	> 38

B.3 Skid Number Prediction Model Based on British Pendulum Test Results

The British Pendulum (BP) results for aggregates were used to predict the Skid Number measured at 40 mi/hr by a skid trailer with Ribbed tires (SN40R). The relationship between the British Pendulum Number (BPN) and the SN40R is presented in Equation B.37 (John Jewett Henry and Wambold 1992):

$$SN40R = 0.83(BPN) - 10.5 \qquad \text{Equation B.37}$$

where,

SN40R is the Skid Number measured at 40 mi/hr by a skid trailer with Ribbed tires, and
BPN is the British pendulum number.

APPENDIX C: PHYSICAL PROPERTIES, DURABILITY, AND PERFORMANCE TESTING

C.1 Physical Properties Testing

C.1.1 Procedures of Estimating the Uncompacted Void Content Percentages of Fine Aggregates

1. Calibrate the test cylinder following ASTM C1252 – 17,
2. Obtain the required amount of materials,
3. Place funnel and cylinder as shown in Figure C-1,
4. Use a finger to block the opening of the funnel,
5. Pour the sample into the funnel,
6. Level the material in the funnel using a spatula,
7. Remove the finger and allow the sample to fall freely into the test cylinder,
8. Strike off excess heaped fine aggregates at the top surface of the test cylinder,
9. Tap the cylinder lightly but avoid significant compaction,
10. Record the weight of the cylinder and fine aggregates, and
11. Record the weight of the empty cylinder.



Figure C-1 Funnel and cylindrical measure.

C.2 Durability Testing

C.2.1 Los Angeles Abrasion Test Conditions

Table C-1 Charge weight and the number of revolutions for the LAA test.

Grading	Number of Spheres	Weight of Charge (g)	Number of Revolutions
A	12	5000 ± 25	500
B	11	4584 ± 25	500
C	8	3330 ± 20	500
D	6	2500 ± 15	500
E	12	5000 ± 25	1000
F	12	5000 ± 25	1000
G	12	5000 ± 25	1000

Table C-2 Grading of test samples used in LAA test.

Passing	Retained on	Grading A	Grading B	Grading C	Grading D
1 1/2" (37.5 mm) ^a	1" (25.0 mm)	1250 ± 25 ^b			
1" (25.0 mm)	3/4" (19.0 mm)	1250 ± 25			
3/4" (19.0 mm)	1/2" (12.5 mm)	1250 ± 10	2500 ± 10		
1/2" (12.5 mm)	3/8" (9.5 mm)	1250 ± 10	2500 ± 10		
3/8" (9.5 mm)	1/4" (6.3 mm)			2500 ± 10	
1/4" (6.3 mm)	#4 (4.75 mm)			2500 ± 10	
#4 (4.75 mm)	#8 (2.36 mm)				5000 ± 10
Total Mass		5000 ± 10	5000 ± 10	5000 ± 10	5000 ± 10

^a Sieve Size (Square Openings).

^b Mass of indicated sizes (g).

C.3 Performance Testing

C.3.1 Accelerated Friction Testing

C.3.1.1 Preparation of Hot Mix Asphalt Test Slabs

1. Assemble the compaction mold,
2. Prepare approximately 50 lb. to 55 lb. of loose asphalt mixtures at a temperature of 320 °F,
3. Place the thermal paper at the bottom of the compaction mold,
4. Place the loose asphalt mixtures into the mold and spread the material evenly,
5. Place the thermal paper at the top of the compaction mold,
6. Place the compaction metal cover at the top of the compaction mold,
7. Place the plate compactor on the top of the compaction mold and compact the mix for approximately 10 minutes,
8. Remove the metal plate,
9. Leave the compacted slabs overnight in the compaction mold to cool before they are removed from the mold to avoid damage or deformation, and
10. Disassemble the compaction mold and remove the prepared slab after 24 hours.

C.3.1.2 Installation of High Friction Surface Treatment Application on Hot Mix Asphalt Slab

1. Clean the surface of the Hot Mix Asphalt (HMA) slab. It is recommended to use air to avoid causing damage to the surface,
2. Using an electric mixer with a Jiffy blade, mix the two-component epoxy for 3 to 5 minutes, and avoid generating air bubbles,
3. Pour the mixed epoxy at the center of the asphalt slab,
4. Spread the epoxy with a spatula on the surface,
5. Achieve an epoxy film thickness between 55 to 65 mils. Measure the thickness with a wet film thickness gauge,
6. Place the aggregate evenly over the mix (an amount of 3 to 5 kg of materials is recommended),
7. Leave the prepared surface to cure overnight (24 hours before testing), and
8. Sweep the surface with a broom to remove excess materials.

C.3.1.3 Procedures of Sand Patch Test

1. Clean the surface with a brush, avoid removing aggregates and causing surface damage,
2. Fill the cylinder with a known volume (80 ml) of dry materials (i.e., clean silica sand) and tap the cylinder base several times,
3. Pour the materials into the center surface of the sample test area,
4. Distribute the materials in a circular patch with the spreader tool, and

5. Measure the diameter of the circular area covered by the materials and calculate the mean diameter.

C.3.1.4 Three-Wheel Polishing Machine and Dynamic Friction Tester

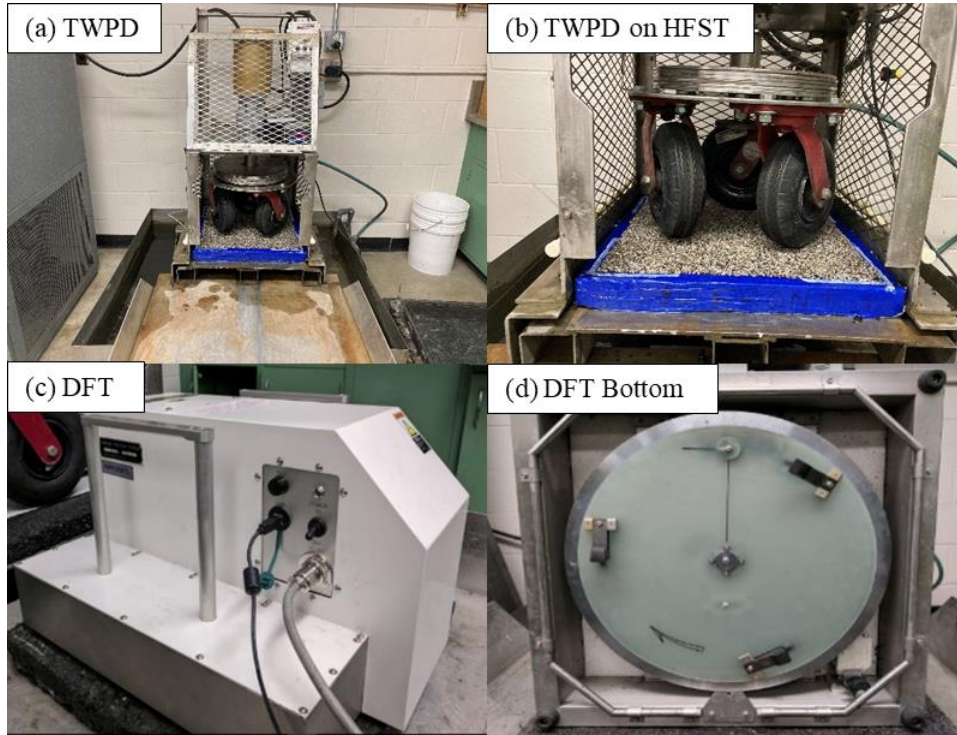


Figure C-2 Three-wheel polishing device and DFT.

C.3.2 Measuring Aggregate Coupons' Surface Frictional Properties Using the British Pendulum

C.3.2.1 Preparing Aggregate Coupons

A ready-mix plaster with a weight of 12g was added and spread on the bottom of the metal molds, and the aggregates were embedded into the plaster so that the plaster prevented the epoxy binder from flowing into the gaps between the aggregates' particles (see Figure C-3). Different plaster weights were tried; it was determined that 12g worked well for the (#6 - #8) sized aggregates and the (#4 - #6) sized aggregates. Additional plaster was painted onto the sides of the molds using a small brush to completely cover the surface and keep the epoxy from adhering to the metal molds. Other mold release agents (e.g., car wax and PAM™ cooking spray) were tried first. The car wax did not keep the epoxy from adhering to the molds, and the PAM™ spray reacted with the epoxy, thereby creating a thin layer of weak epoxy. In the end, the plaster was not a perfect solution and there were still issues with the epoxy sticking to the metal molds in places where the plaster did not entirely cover the mold. For this reason, the researchers created silicone molds, instead of metal ones. The metal mold was cast in plaster (see Figure C-4a), and it was then used to cast a silicone mold. The first silicone mold, presented in Figure C-5a, was used to create an epoxy cast (see Figure C-4b) that was used to make additional silicone molds. This was necessary because the plaster was weak in places and the silicone was absorbed by the outermost layer, resulting in issues during the demolding process. The advantages of the silicone molds were that removal of the specimens was easier, resulting in quicker production times. This also meant that aggregate was not being broken away from the coupons during the demolding process. There was no noticeable difference between the coupons made with silicone molds and the ones made with metal molds. There was no

noticeable wear on the initial mold or any of the other silicone molds at the end of this project. Figure C-6 illustrates the prepared aggregate coupons.



Figure C-3 Plaster used in metal molds.

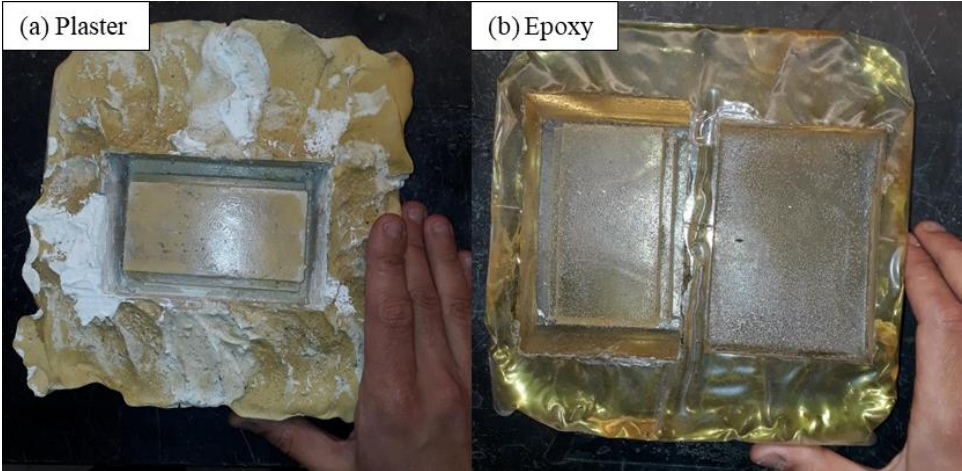


Figure C-4 Plaster and epoxy cast.

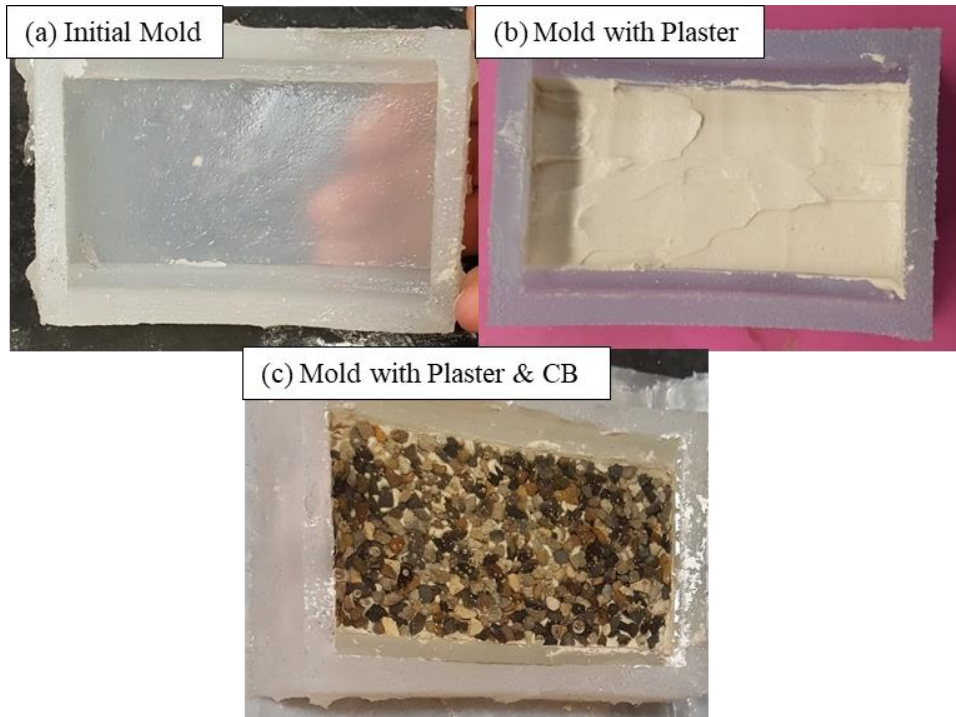


Figure C-5 Silicone molds.



Figure C-6 Prepared aggregate coupons.

C.3.2.2 British Pendulum Tester and the British Wheel

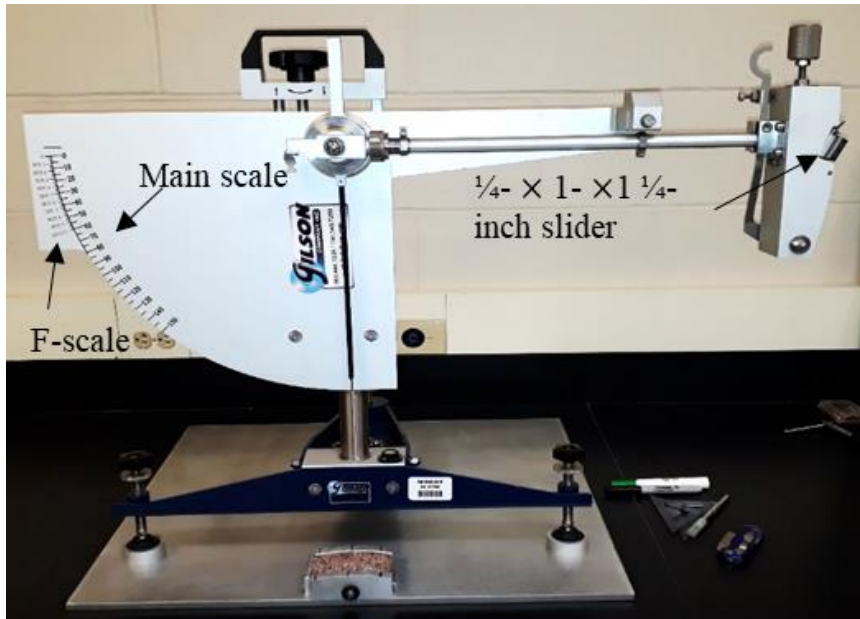


Figure C-7 British pendulum tester.

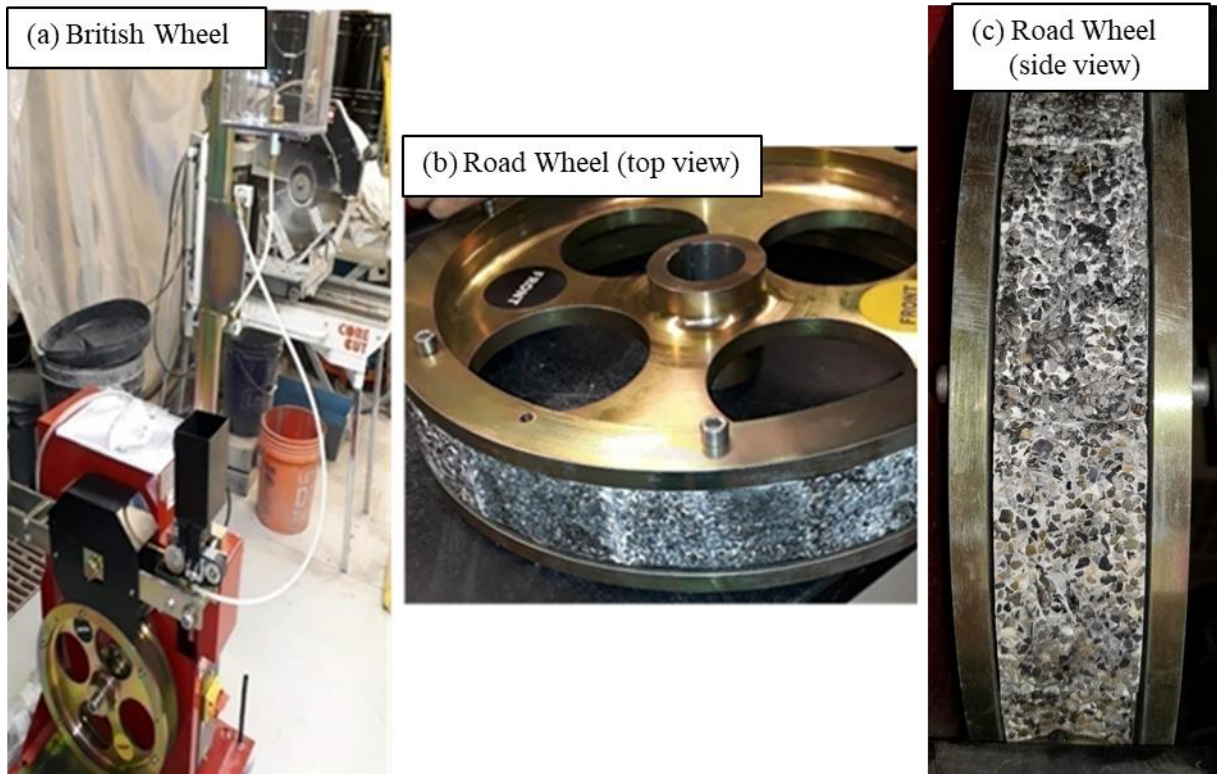


Figure C-8 The British wheel and the road wheel with aggregate coupons (before polishing).

APPENDIX D: LIFE CYCLE COST ANALYSIS CALCULATION PROCESS

The researchers developed a LCC simple program using Excel to conduct Life Cycle Cost Analysis (LCCA) for the High Friction Surface Treatment (HFST) application using Aggregate Image Measurement System (AIMS), Dynamic Friction Tester (DFT), or British Pendulum (BP) results. This program was used to predict the Skid Number (SN) and the Net Present Value (NPV) for HFST applications. The major input data were categorized into material and project specifics. The LCC program results were the SN and NPV. More details about these data and results are explained in the following sections.

D.1 Input Data

The input data used in the LCC program were categorized into two categories: the first category was the material specifics, and the second category was the project specifics.

D.1.1 Material Specifics

The material specifics depended on the HFST aggregates' results (AIMS, DFT, or BP) and other specifics as follows:

D.1.1.1 Aggregate Image Measurement System Results

The AIMS results included the Texture (TX) and Gradient Angularity (GA) indices for Before Micro-Deval polishing (BMD), After 105-minutes of Micro-Deval polishing time (AMD 105), After 180-minutes of Micro-Deval polishing time (AMD 180). The terminal TX index (a_{TX}), initial TX index ($a_{TX} + b_{TX}$), and rate of TX change (c_{TX}) were calculated by fitting the AIMS TX indices for BMD, AMD 105, and AMD 180 at zero, 105-, and 180-minutes Micro-Deval (MD) polishing times. Equation B.8 was used for curve fitting that was conducted using Excel. The terminal GA index (a_{GA}), initial GA index ($a_{GA} + b_{GA}$), and rate of GA change (c_{GA}) were calculated by fitting the AIMS GA indices for BMD, AMD 105, and AMD 180 at zero, 105-, and 180-minutes MD polishing times. The curve fitting was conducted using Equation B.9 and Excel, as outlined in Appendix B. For more details, note Figure D-1.

D.1.1.2 Dynamic Friction Test Results

The DFT results were the Coefficient of Friction (COF) values measured at 40 km/hr and three polishing cycles (0, 70k, and 140k cycles). The COF values at zero polishing cycles were considered initial values, and the COF values at 140k polishing cycles represented the terminal values.

D.1.1.3 British Pendulum Test Results

The BP results came from the British Pendulum Number (BPN) values before and after polishing in the British wheel. The BPN was measured by the BP.

D.1.1.4 Other Specifics

Aside from the material specifics, the following specifics were taken into considerations:

- Aggregates' costs in \$/ton,
- Aggregates' shipping costs in \$/mi,
- The distance in miles from the origin (aggregates' source) to destination (Columbia City, MO, U.S.A.),
- Aggregates' number of tons per load (tons/load),
- Applied rate of aggregate in ton/yd²,
- Epoxy binder's costs in \$/gallon,
- Epoxy binder's shipping costs in \$/gallon,

- Epoxy binder's applied rate in gallon/yd², and
- Construction, labor, equipment,etc. costs in \$/yd².

D.1.2 Project Specifics

The second data input category was project specifics that included the following:

- Average Annual Daily Traffic (AADT) per each section in veh/day,
- Percentage of trucks (%T),
- Highway classification (rural or urban) and divided or undivided highway,
- Number of lanes in each direction,
- Lane width in ft,
- HFST length in mi,
- Cost of removing HFST in \$/yd²,
- The recommended terminal Skid Number (SN) value, and
- Interest rate and inflation rate in %.

More details about the project specifics are deemed in Figure D-2.

D.2 Skid Performance Prediction Results

Performance prediction models were used to predict the SN values, as discussed in Appendix B and Section 7.3 in Chapter 7. Then, the rehabilitation decision was taken based on the rehabilitation matrix. Table 7-1 presents the rehabilitation matrix used in the LCC program.

D.3 Output Data

The output data of the LCC program was the Net Present Values (NPVs), as exemplified in Figure 7-1. The best HFST application was selected based on the lowest NPV. The LCC program output data, based on AIMS results, was depicted in Figure D-3.

	Calcined Bauxite	Alternative 1: Meramec River Agg.	Alternative 2: Earthworks	Alternative 3: Rhyolite	Alternative 4: Flint Chat	Alternative 5: Potosi Dolomite	Alternative 6: Steel Slag
b- Project Specifics:							
→ AADT per each section (veh/day),	5800	5800	5800	5800	5800	5800	5800
→ Percentage of trucks (%),	10	10	10	10	10	10	10
→ Highway classification (Rural or Urban),	Rural	Rural	Rural	Rural	Rural	Rural	Rural
→ Divided or Undivided highway,	Divided	Divided	Divided	Divided	Divided	Divided	Divided
→ Number of lanes per each direction,	2	2	2	2	2	2	2
→ Lane width (ft),	12	12	12	12	12	12	12
→ Length of HFST (mile),	1	1	1	1	1	1	1
→ Cost of HFST removing (\$/yd ²),	10	10	10	10	10	10	10
→ Recommended Terminal SN(50) value,	21	21	21	21	21	21	21
→ Interest rate (%), and	4	4	4	4	4	4	4
→ Inflation rate (%).	3	3	3	3	3	3	3

Figure D-2 LCC program input data (project specifics).

	Calcined Bauxite	Alternative 1: Meramec River Agg.	Alternative 2: Earthworks	Alternative 3: Rhyolite	Alternative 4: Flint Chat	Alternative 5: Potosi Dolomite	Alternative 6: Steel Slag
Outputs:							
→ Predicted SN(50) after 5 years,	43.47	44.03	30.06	24.07	52.32	28.53	16.13
→ Aggregate class based on SN(50) after 5 years, and	High	High	High	Medium	High	Medium	Low
→ NPV (\$), and	126,725.15	98,379.50	115,828.46	116,223.24	104,763.62	100,304.06	259,295.53
→ Best alternative.	Alternative 1: Meramec River Agg.						

Figure D-3 LCC program output data based on AIMS.